Development and Diagnostic Application of a Novel Quantitative Test
for Determination and Characterization of Autoantibodies against
Insulin-like Growth Factor 1 Receptor

Inaugural-Dissertation
to obtain the academic degree

Doctor rerum naturalium (Dr. rer. nat.)

submitted to the Department of Biology, Chemistry and Pharmacy
of Freie Universität Berlin

by
TIM WELSINK
from Düsseldorf

2014

Entwicklung und diagnostische Anwendung eines neuen
Nachweisverfahrens zur Bestimmung und Charakterisierung von
Autoantikörpern gegen den Insulin-like Growth Factor 1 Rezeptor

Dissertation zur Erlangung des akademischen Grades des
Doktors der Naturwissenschaften (Dr. rer. nat.)

eingereicht im Fachbereich Biologie, Chemie, Pharmazie
der Freien Universität Berlin

vorgelegt von

TIM WELSINK
aus Düsseldorf

2014

This dissertation was prepared from 2010 to 2014 at the Institute for Experimental Endocrinology at Charité - Universitätsmedizin Berlin and has been supervised by Prof. Dr. Lutz Schomburg.

Professor Dr. Markus Wahl has been the supervisor at the Institute for Chemistry and Biochemistry at Freie Universität Berlin.

Angefertigt wurde diese Dissertation in den Jahren 2010 bis 2014 am Institut für Experimentelle Endokrinologie der Charité - Universitätsmedizin Berlin unter der Leitung von Prof. Dr. Lutz Schomburg.

Betreut wurde diese Dissertation am Institut für Chemie und Biochemie der Freien Universität Berlin von Prof. Dr. Markus Wahl.

1. Gutachter (first referee):   Prof. Dr. Lutz Schomburg

2. Gutachter (second referee):   Prof. Dr. Markus Wahl

Disputation am (disputation date)   13. April 2015

Summary / Zusammenfassung

Summary

Autoantibodies (aAb) are characteristic for autoimmune diseases. Specific aAb are often found both in diseased and apparently healthy individuals and may precede pathological symptoms. The contribution of thyrotropin receptor (TSHR) stimulating aAb to the progression of Graves´ Orbitopathy (GO) is widely accepted. The coexistence of stimulating insulin-like growth factor 1 receptor (IGF1R) aAb in GO patients was hypothesized and tested in the present study. As no method for routine testing was available, a suitable non-radioactive test was established to evaluate IGF1R-aAb in human sera and test the hypothesis.

As a first step, an IGF1R-aAb precipitation assay for detection and reliable quantification of these aAb was developed. This work package included the genetic engineering and expression of the recombinant antigen, its purification and characterization, the definition of a standardized operating procedure, and the adaptation of the assay format for future routine use. Assay development also includes the generation and purification of monoclonal antibodies (mAb) to the IGF1R, needed for standardization and supplementary characterization of the assay. A central part of this work focuses on the clinical, biological and molecular role of IGF1R-aAb. To this end, aAb were purified from human sera and characterized *in vitro*. The IGF1R-aAb inhibit signal transduction via the IGF1R directly and acted as antagonists of IGF1-induced proliferation of MCF7 breast cancer cells in culture An analysis of IGF1R protein domains indicates that IGF1R-aAb in human sera are polyclonal and often recognize conformational epitopes. As IGF1R aAb were detected with a prevalence of approx. 10% in human subjects, and immunoglobulins are known to contain two antigen binding sites, a second more direct and convenient assay type was developed for routine diagnostic use.

A cohort of GO patients were analyzed yielding a prevalence of 10% positive IGF1R-aAb carriers, but not different from the prevalence in healthy controls. Moreover, IGF1R-aAb were not stimulating the IGF1R. Hence, the initial hypothesis that IGF1R-Ab contribute to GO pathogenesis needs to be rejected as it was not supported by the data. Nevertheless, this study demonstrates a high prevalence of aAb against the IGF1R in pathological samples and apparently healthy subjects as well, which might be of clinical importance given the central role of IGF1 in growth, metabolism and disease. In cooperation with a fellow PhD student who established an analogous assay for the structurally-related insulin receptor (IR), an analysis of the specificity of the IGF1R-aAb was performed. We realized that roughly 50% of IGF1R-aAb positive samples cross-reacted with the IR, highlighting their potential clinical importance for a specific form of diabetes mellitus, i.e., autoimmune

type B insulin resistance. Further studies with samples from well characterized samples, respective pre- and diabetic patients, and controls are needed to clarify this notion.

Collectively, two novel analytical assays for the identification and quantification of IGF1R-aAb were successful established and characterized. With these tools, the prominent hypothesis on the causal importance of stimulating IGF1R-aAb for the development and course of GO was tested and rejected. However, the high prevalence of IGF1R-aAb in diseased and healthy donors, the antagonistic nature, and the cross-reactivity of these aAb to the IR, indicate their potential relevance in certain forms of insulin resistance, metabolism or growth deficiencies, which needs to be clarified in future studies.

Zusammenfassung

Autoantikörper (aAb) sind charakteristisch für Autoimmunkrankheiten. Spezifische aAb werden häufig in erkrankten, aber häufig auch in gesunden Personen gefunden, wobei sie pathologischen Symptomen vorangehen oder diese kausal begründen können. Die Beteiligung von stimulierenden Thyrotropin-Rezeptor (TSHR) aAb im Krankheitsverlauf von Graves´ Orbitopathie (GO) ist weitreichend anerkannt. Als Hypothese wurde auch von vielen Experten akzeptiert, dass stimulierende aAb gegen den Insulin-ähnlichen Wachstumsfaktor 1 Rezeptor (IGF1R) in Patienten mit GO auftreten und diese aAb den Exophthalmus verursachen. Im Rahmen dieser Arbeit wurde diese Hypothese experimentell überprüft. Da derzeit aber kein Verfahren für den routinemäßigen Nachweis von IGF1R-aAb verfügbar ist, wurde ein geeignetes, nicht-radioaktives Nachweisverfahren entwickelt, um IGF1R-aAb in humanen Seren von GO Patienten und Kontrollen zu bestimmen und die aufgestellte Hypothese zu testen.

Der erste Teil der Arbeit umfasst die Entwicklung eines IGF1R-aAb Präzipitationsassays für den Nachweis und die verlässliche Quantifizierung dieser aAb. Hierfür musste eine genetische Herstellung und Expression des rekombinanten Antigens, sowie dessen Aufreinigung und Charakterisierung erfolgen. Abgeschlossen wurde dieses Arbeitspaket mit der Entwicklung und Definition eines standardisierten Protokolls zur Darstellung dieser zentralen Assaykomponente und die Adaptierung des Assayformats für eine routinemäßige Anwendung. Die Entwicklung des Nachweisverfahrens beinhaltete zudem die Generierung und Aufreinigung monoklonaler Antikörper (mAb) zum Antigen IGF1R, die für eine Standardisierung und die erweiterte Charakterisierung des Assays erforderlich sind. Der zweite und zentrale Teil dieser Arbeit beinhaltet die Charakterisierung der klinischen, biologischen und molekularen Bedeutung der IGF1R-aAb. Hierfür wurden aAb aus humanen Seren isoliert und *in vitro* charakterisiert. Es wurde eine direkte Inhibierung der Signaltransduktion über den IGF1R durch die IGF1R-aAb nachgewiesen. Zusätzlich konnte die direkte Wirkung von IGF1R-aAb als Antagonisten zur IGF1-induzierten Zellproliferation von MCF7 Brustkrebszellen in der Zellkultur gezeigt werden. Zur weiteren

Charakterisierung wurde eine Feinanalyse mit rekombinanten Proteindomänen des IGF1R durchgeführt. Es zeigte sich, dass die IGF1R-aAb in humanen Seren polyklonal vorliegen und auch Konformationsepitope des Antigens erkennen. Da IGF1R-aAb mit einer Prävalenz von ca. 10% in humanen Testpersonen vorkommen und bekannt ist, dass Immunoglobuline zwei Antigen-Bindestellen besitzen, sollte zusätzlich ein weiteres Assaysystem für die routinemäßige und schnellere Diagnostikanwendung entwickelt werden.

Der entwickelte IGF1R-aAb Präzipitationsassay wurde als Methode zur Bestimmung von IGF1R-aAb in einer Kohorte pathologischer GO Patienten angewendet. Es wurde wiederum eine Prävalenz von 10% positiver IGF1R-aAb Träger nachgewiesen, welche sich somit nicht von der Prävalenz bei gesunden Menschen unterschied. Des Weiteren wurde festgestellt, dass diese IGF1R-aAb nicht stimulierend sondern antagonisierend auf den IGF1R wirken. Die Hypothese, dass IGF1R-aAb entscheidend zur Pathogenese von GO beitragen, wird somit von diesen Ergebnissen nicht gestützt und muss dementsprechend verworfen werden. Gleichwohl wurde in weiteren Vermessungen die relativ hohe Prävalenz von aAb gegen den IGF1R bestätigt, was hinsichtlich der zentralen Rolle von IGF1 für Wachstum, Metabolismus und Onkologie auf eine potentiell bedeutende klinische Relevanz der IGF1R-aAb hindeutet. In Kooperation mit einem Kollegen, der ein analog funktionierendes Nachweissystem für den strukturell ähnlichen Insulinrezeptor (IR) etabliert hatte, gelang ein detaillierter Vergleich der Kreuzreaktivität dieser aAb und die Identifizierung immunopositiver Probanden mit sowohl IGF1R- als auch IR-aAb. Hierbei konnten wir eine Kreuzreaktion bei ca. 50% der positiven Seren feststellen. Für eine grundlegende Einordnung dieser Ergebnisse und der pathologischen Relevanz der aAb ist die Vermessung weiterer Humanstudien mit Proben gut charakterisierter Probanden notwendig.

Im Rahmen dieser Arbeit wurden somit zwei neue analytische Nachweisverfahren zur Identifizierung und Quantifizierung von IGF1R-aAb entwickelt, etabliert und charakterisiert. Die weit verbreitete Annahme, dass stimulierende IGF1R-aAb als Mitursache von Graves´ Orbitopathie angesehen werden müssen, konnte in dieser Arbeit widerlegt werden. Die festgestellte relativ hohe Prävalenz von IGF1R-aAb in Patienten und scheinbar gesunden Kontrollprobanden, deren antagonistische Wirkung am IGF1R, und die Kreuzreaktivität zum IR, sprechen für eine pathophysiologische Relevanz der IGF1R-aAb in der klinischen Diagnostik. Die in dieser Arbeit neu etablierten Assays können in Zukunft geeignet sein, um eine bessere Einordnung und Diagnostik bestimmter Formen von Insulinresistenz, sowie Wachstums- und Stoffwechselstörungen vorzunehmen. Gegebenenfalls werden sie sich auch als sinnvolle Methode bei stratifizierenden Verfahren in der Therapie erweisen.

1 Table of Content

2 Introduction

2.1 Autoantibodies

Immunoglobulins (Ig) are known as being part of the organism's protecting immune system defeating pathogens. This view changed when the existence of IgG targeting structures of the own human organism were described as an abnormality in the essential protective system [1]. Their existence was suggested by having auto-reactive clones in the immune system, which were directed against permanently available self-structures, being contrary to the appearing concept of immune tolerance. Presence of these specific Ig's leading to auto-reactivity could only be explained by the existence of so called "forbidden clones", which produced the undesired teammates [2]. Shortly after the first report on the presence of autoantibodies in serum of healthy individuals [3], auto-reactive autoantibodies were identified in nearly all vertebrate species [4]. The acceptance and relevance of autoantibodies contributed to the modern understanding of the adaptive immunity as a shapeable and adaptive system operating over the individuals' whole lifetime.

2.1.1 History – past to present

More than 100 years ago, at an epidemic boom of syphilis, the disease was noticed by former society as one of the most displeasing and painful sufferings at that time. Thus autoantibodies became first tangible hint at the point, when Wassermann, Neisser and Bruck presented a badly needed simple and accurate laboratory test [5]. They assumed that infected persons suffering from syphilis carry specific antibodies present in their blood or cerebrospinal fluid, which react when brought in contact with their specific antigen, and form a complex in a complement-fixation response. First results were highly promising, because serum from syphilitic patients reacted with syphilitic liver extract and healthy serum did not. But it was later revealed that the presented test was not specific for syphilis. Wassermann worked with syphilitic liver extract which should represent the antigen. Serum antibodies reacted with an unknown antigen present in both normal liver and other tissues like the heart. It turned out that the phospholipid cardiolipin served as antigen in the liver extracts [6]. However, cardiolipin is still used as one of the first diagnosis parameter in syphilis, which had shown over the years to be a reliable first evidence. The antigen cardiolipin as endogenous compound meets the criteria for an autoantigen and the corresponding antibody as autoantibody, even if the insights into Wassermann's test are still unclear. The observed phenomenon may represent an example of molecular mimicry between spirochaete and a cellular component, or may be due to release of intracellular antigen following tissue inflammation and injury. Today

Treponema pallidum had been defined as the pathogen causing syphilis. If the pathogen had not been identified as origin, syphilis might today represent a classic example of a systemic autoimmune disease with a related multi-organ autoantibody [7]. While in the midst of the 20th century prevalence of syphilis decreased considerably, the Wassermann serologic test showed up with a huge majority of positive reactions, not as a consequence of syphilis, but as a result of others disorders. The most famous group of the false positives from Wassermann's test for syphilis was lupus [8]. This observation came along with a new serological fluorescent antibody test against anti nuclear antibodies (ANAs) for lupus [9, 10]. After introducing the term of "antiphospholipid syndrome" later, tests for antiphospholipid antibodies like lupus-antikoagulans (LA), cardiolipin-, beta-2-glycoprotein-, or phosphatidylserin antibodies have become the most common laboratory procedures, leaving behind their forerunner, the serologic test for syphilis [7]. As already mentioned, one of the most focused autoimmune diseases of the last century was lupus. Lupus erythematosus is an autoimmune disease that can affect multiple organ systems (systemic lupus erythematosus, SLE) or a single system such as the skin. The exact cause is unknown but genetic factors, ethnic origin, environmental factors, and medications may all be involved in its development. The development of SLE is a complex immune process that is brought about dysregulation of B- and T-lymphocytes, followed by the production of auto-antibodies, and the formation of immune complexes leading to cell death and suffering [11, 12].

The presence of autoantibodies (aAb) may represent an early warning of impending disease, even in clinically normal persons. This hypothesis is underlined by a study, in which autoantibodies were shown in pediatric patients with chronic thyroiditis together with their siblings and parents. There was a significantly greater incidence of thyroid autoantibodies in siblings and parents of the adolescent patients compared to controls [13]. In a study of patients in the preclinical phase of rheumatoid arthritis it was found, that autoantibodies to the IgM rheumatic factor and to cyclic citrullinated peptide (CCP) were detectable in serum samples up to 14 years before the actual onset of the disease [14]. Thus autoantibody formation may often develop years before the first symptoms of autoimmune diseases occur.

2.1.2 Definition and induction

Autoantibodies as immunoglobulins are the results of the immune response, activated by a physiological component of the own organism. The response may be triggered as a result of bacterial or viral infection [15, 16], chemical exposure [17], and medical treatment [18] or trauma [19]. Further evidence came up, that genetic factors and environmental factors could increase the incidence and severity of autoimmune diseases [20].

2.1.3 Relevance of autoantibodies in endocrinology

Autoantibodies may cause systemic autoimmune diseases. The thyroid-stimulating hormone receptor (TSHR) is a major autoantigen in autoimmune thyroid diseases, which represent a major health issue predominantly affecting females. TSHR autoantibodies are functionally heterogeneous and can be classified into thyroid stimulating (TSAb) and thyroid blocking (TBAb) antibodies. TSAb interact with TSHR, activate it and represent the pathogenic principle causing hyperthyroidism in Basedow's (Graves') disease [21, 22]. TBAb bind TSHR without receptor activation, prevent its interaction with TSH and cause hypothyroidism in some patients with Hashimoto's disease [23]. The TSHR plays a central role in the function and growth of thyrocytes. TSHR is a member of the family of G protein-coupled, seven-transmembrane receptors, and the TSHR ectodomain is sufficient for high-affinity binding of TSH [24]. TSH stimulation leads to an activation of the cAMP cascade, which is the major signal transduction pathway of the TSHR *in vivo* and has been shown to activate thyrocyte function (thyroid hormone production) and growth (mitogenesis) with some species differences (reviewed in [25]).

Graves' hyperthyroidism is a common autoimmune disorder, affecting primarily women, with an incidence of approximately 4 per 10,000 every year [26]. During lifetime, approximately 1% of the population is affected. The hyperthyroidism is directly caused by autoantibodies to the TSHR that mimic the stimulatory effects of TSH [25, 27]. None of the currently available therapeutic options can cure Graves' disease. Furthermore, the consequence of 131-Iodine-induced thyroid ablation (a widely used therapy) is frequently hypothyroidism, requiring life-long T4 replacement in conjunction with monitoring thyroid function. The clinical features of Graves' disease include weight loss, hyperkinesis, tachycardia, diffuse goiter, increased levels of serum T4 and/or T3, and suppressed TSH. Other common manifestations are heat intolerance and anxiety and, in women, oligomenorrhea. The immunological hallmark of Graves' disease (as already mentioned) is the presence of TSAb, that stimulate thyroid hormone production [28]. In addition to TSHR autoantibodies, approximately 75% of Graves' patients have autoantibodies to thyroid peroxidase (TPO) and, depending on the assay, 25–55% have autoantibodies to thyroglobulin (Tg) [29]. These autoantibodies are more prevalent in Hashimoto's thyroiditis [30]. Besides, also false positives from Wassermann test finally came down with Hashimoto's thyroiditis [31].

Returning to Graves' disease – the influence of TSAb which interact with TSHR and pathogenically cause hyperthyroidism remains undisputed [21]. Complementary one of the main symptoms in Graves' disease is Graves' orbitopathy (GO, or Graves' ophthalmopathy, or endocrine orbitopathy called EO, or thyroid-associated ophthalmopathy, called TAO), which develops in approximately half of the Graves'

disease patients, and characterizes a significant disease aspect [32]. Symptoms mostly include swelling of orbital muscles and connective tissue, limited eye movement, ocular pain, double vision and inflamed eyes. During the course of GO, balance of production of the extracellular matrix in the retro-orbital space is instable, which leads to increased volume requirements within the bony eye cavity by proliferation of orbital adipocytes and fibroblasts. Increased intraorbital pressure and compression of ocular muscles and the optic nerve result [33]. Because expression of TSHR on pre-adipocytes and orbital fibroblasts is comparatively low, although increasing during adipocyte differentiation, it is unlikely that TSAb necessarily cause GO. However, an association of TSAb with GO disease development is well established [34].

Some studies implicated involvement of the insulin-like growth factor 1 (IGF1) axis in GO [35-37]. Production of glycosaminoglycans from retroocular tissue fibroblasts is stimulated by IGF1 [38] and IGF1R is considerably higher expressed in retroorbital fibroblasts in GO patients compared to controls [34]. The frequency of IGF1R expressing B cells from affected twins is increased relative to healthy controls, which indicates the presence of IGF1R on B cells as an acquired but not genetically-determined disease parameter [39, 40]. The observation that hyaluronan production is induced by antibodies from GD patients in orbital fibroblasts suggests an activation of IGF1R apparently by antibodies [41]. Further IGF1R and TSHR colocalize and physically interact in TSHR-positive fibroblasts [34]. Thus a key indication for contribution of IGF1R regulation or the presence of anti-IGF1R antibodies on the molecular level seems supposable, influencing the potential functional complex of IGF1R and TSHR in thyroid and orbital tissue or IGF1R itself. Many of the previously mentioned effects can be mediated by the IGF1R [42], but an implication of anti-IGF1R antibodies in development of GO has just been speculated so far and never been directly shown [43, 44].

2.1.4 Autoantibodies to the IGF1R

First indication for the prevalence of IGF1R autoantibodies came together in the year 1988 with the development of a new assay for detection of existing IGF1R autoantibodies in human sera [45]. In short, purified human placental IGF1R was labeled with radioactive 125-Iodine and used to precipitate IGF1R antibodies from human serum. After washing, relative radioactive counts were measured. In this study 141 sera of patients with rheumatic diseases and metabolic related disease, like different forms of diabetes mellitus or insulin resistance, were analyzed. Around 7% of those patient sera were able to immunoprecipitate the IGF1R. Seven of the 11 positive sera failed to inhibit IGF1 binding to human placental membranes, while remaining 4 sera inhibited IGF1 binding. The authors examined that immunoprecipitation was comparable with sera and IgG prepared

from these sera. A year later, the previously described assay was used to study autoantibodies binding radioactive 125-Iodine labeled human insulin receptor [46]. Antibodies in sera from 10 of 104 diabetic patients were found to precipitate the IR. 9 of these sera failed to inhibit insulin binding to cultured rat hepatocytes, thus the authors described a similar pattern in hormone binding as mentioned for IGF1 inhibiting capacity of autoantibody positive sera before [45]. Even in a more recent study about the prevalence of IR-aAb in young adults with documented insulin resistance syndrome (IRS), an antiquated β-emitter radioactive detection system was used [47]. To this end, 20,000 cpm of 35S-labeled IR as antigen was incubated in each antibody analysis, with serum sample and antibody-bound 35S-IR was precipitated. In this study, 25% of patients with type B IRS were tested positive on IR-aAb. Returning to components of the IGF-system as autoantigen, interestingly, a possible correlation between autoantibodies against the IGF1R ligand IGF1 as antigen in patients with type 1 diabetes was suggested [48]. This assumption was based on the high structural homology between IGF1 and proinsulin [49]. Additionally, IGF1 suppressed the development of type 1 diabetes in non-obese diabetic (NOD) mice [50], which led to the assumption that IGF1 could serve as a therapeutic autoantigen. Other than expected, Maruyama and co-workers were unable to demonstrate the existence of anti-IGF1 antibodies in type 1 diabetes patients [48], but they did not discuss the IGF1R serving as a promising autoantigen. An additional hint for the significance of IGF1R as an autoantigen was the observation, that antibodies of a patient with insulin resistance and acanthosis nigricans have been shown to inhibit the binding of both insulin and IGF1 to their respective receptors [51].

2.2 The insulin-like growth factor system

The insulin-like growth factors (IGFs) are polypeptides with high sequence similarity to insulin. IGFs are part of a complex system often referred to as the somatotrope or IGF axis, or growth hormone (GH) – IGF axis.

2.2.1 The IGF system – an overview

The IGF system is functionally conserved in mammals (reviewed in: [52, 53]). Overlooking the IGF system, it includes the ligands IGF1 and IGF2, how these were made available as free hormones and which were then able to interact with their receptors (Figure 2.1). Within serum the vast majority of both hormones are bound to IGF-binding proteins (IGFBPs). Those release IGF1 or IGF2 only, if degraded by IGFBP-proteases. The resulting free IGF1 binds to the IGF1R, induces an autophosphorylation step and phosphorylation of intracellular substrates by the receptor, which leads to signal transduction into the cell. Free IGF2 binds as ligand to the IGF1R and the IGF2R as well. The function of IGF2R is still insufficiently understood, it might serve as a scavenger

receptor, cleaning the serum from circulating IGF2. The IGF2R is also known as the mannose 6-phosphate receptor implicated in intracellular trafficking of lysosomal proteins [54-56].
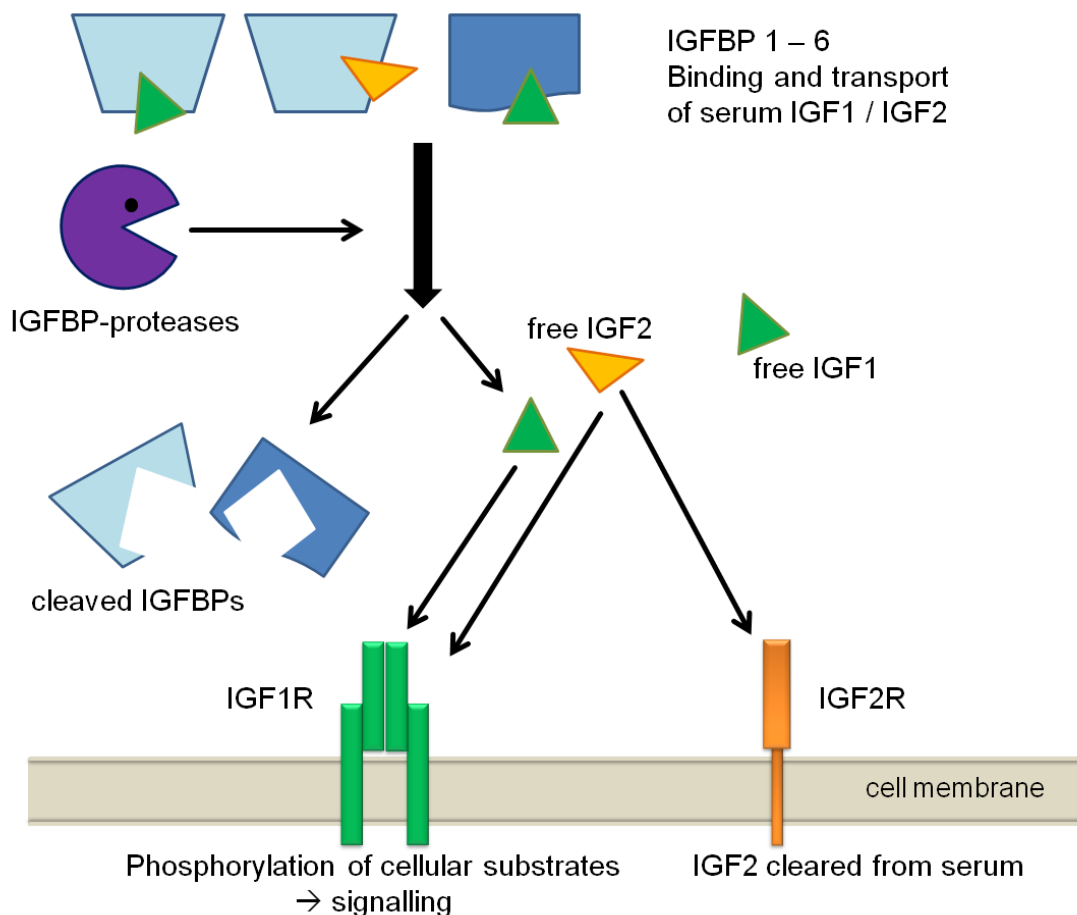
Figure 2.1: *Schematic representation of the insulin-like growth factor (IGF) system. In serum most IGF1 (green triangles) and IGF2 (yellow triangles) is bound to IGFBPs. These are released as free hormones from their binding partners by simple on- and off-reactions or when IGFBP-proteases cleave the IGFBPs. Free IGF1 binds to IGF1R (green bars) and initiates the IGF1R`s intracellular signaling cascade. IGF2 can bind to IGF1R or the IGF2R (yellow bar). While no purpose of bound IGF2 to IGF2R was found so far, a function as scavenger receptor for free serum IGF2 was suggested. Black arrows conventionalize an action or translocation of an indicated component.*

Biological features and actions of previously introduced IGF system components are summarized in Table 2.1.

Table 2.1: *Biological features and actions of components in the IGF system.*

Components	Nature	Role
IGF1	70 amino acid polypeptide hormone	Postnatal growth, anti-apoptosis, mitogenesis, proliferation, migration and differentiation [57-60]
IGF2	67 amino acid polypeptide hormone	Fetal and embryonic growth [52]
IGF1R	Heterotetrameric glycoprotein in $\alpha_2\beta_2$-formation, tyrosine kinase ~320 kDa	Mediates the effect of growth factors including IGF1 and IGF2; induction of MAPK and PI3-Kinase/ Akt pathway [61, 62]
IGF2R	Monomeric glycoprotein, ~300 kDa	Binds to IGF2 and mannose-6-phosphate, inhibits action of IGF2 by sequestering [63]
IGF1R / IR hybrid receptor	Dimer from consisting of $\alpha_1\beta_1$-IGF1R and $\alpha_1\beta_1$-IR [64]	Binds mainly IGF1 [65]
IGFBP	7 isoforms with different specificity and ligand preferences	Bind and transport more than 90% of circulating IGFs [66]
IGFBP proteases	Several types (serine protease, metalloproteinases, cathepsins and specific proteinases) [67, 68]	Causes proteolysis of IGFBP-IGF complex to free IGF [69]

2.2.2 The ligands IGF1 and IGF2

Both IGF1 and IGF2 were identified as "sulphation factors" in the midst of the last century by recognizing their capability to stimulate sulphate incorporation into cartilage *in vitro* [70]. Later on, the non-suppressable insulin-like activity (NSILA) of two soluble serum factors was described, which led to the name "NSILA I and II" [71]. These labels were substituted by "somatomedin" referring to their inducement by GH and mediating its effects [72]. After isolation of the two peptides from human serum they were named "insulin-like growth factor 1 and 2" due to their structural similarity to proinsulin [73]. The largest amount of IGF1 is produced in the liver following stimulation with growth hormone (GH), which is the mainly supporter for postnatal growth [57]. In short, IGF1 is the mediator of anabolic and mitogenic activity of GH [74]. Similar to IGF1, IGF2 is mainly synthesized in the liver, both IGF1 and IGF2 act on a variety of mammalian cells in an endocrine, paracrine and autocrine fashion to regulate cell proliferation, apoptosis, transformation and differentiation, while both are essential for normal human growth and development [75]. Generally IGF1 was shown to having a large impact on regulation of physiological and pathological conditions in cancer development by influencing cell differentiation and preventing apoptosis [76]. Recent studies show the involvement of IGF2 in brain tumors in infancy [77] and breast cancer [78]. Adult serum contains a higher concentration of IGF2 than IGF1, but IGF1 plays the more important role in postnatal

growth, while IGF2 acts mainly in embryonic and fetal life [79]. More than 90% of the IGFs are bound to IGFBPs and only 1% of IGF circulates in the free form [80]. IGF1 is a basic single chain peptide with 70 amino acids retaining its structure by 3 disulfide bridges [81]. IGF2 is a slightly acidic peptide with 67 amino acids, while amino acid similarity between IGF1 and IGF2 is around 60%. The homology of both prohormones to proinsulin is around 40% [52, 80] . The IGF1 and IGF2 prohormones contain a C-terminal E-peptide, which is cleaved in the Golgi apparatus during secretion [82].

2.2.3   IGFBPs and IGFBP-proteases

Turnover of IGF1 is regulated by the degree ofIGF1 being bound to IGFBPs and by specific proteases directed to IGFBPs, IGF1 itself or the complex of IGFBP / IGF1 (Figure 2.1) [83]. IGFBPs are a family of at least 7 homologous proteins (IGFBP 1–7), all of which are found in serum and can act as a carrier for IGFs. They interact with IGFs with affinities from 2-100 times higher than with IGF1R, but do not interact with insulin [84, 85]. The large majority of serum IGFs is bound by IGFBP3 or IGFBP5 and is coupled with a protein named the acid labile subunit (ALS) to a ternary complex [86, 87]. IGFBPs are degraded by several specific and non-specific proteases including quite a few types (e.g. serine proteases, cathepsins, various matrix metalloproteinases) [67, 68]. The degradation of the binding proteins results in an increasing availability of circulating free IGF. In contrast to their role as chaperones for IGF1, some of the IGFBPs appear to act in the absence of IGF1 and bind extracellular matrix components. IGFBP3 can inhibit cell growth in an IGF-independent fashion [88] and it was shown that IGFBP3 directly reduces phosphorylation activity of tyrosine kinase in MCF-7 cells. Consequently the binding protein influences IGF1 signaling directly and IGF1-independent pathways thereby affecting tyrosine phosphorylation efficiency of the IGF1R [89]. Concluding the functions and significance of IGFPs for the IGF1-system, IGFBPs do serve as carriers, mediators and reservoirs of IGFs to limit IGF access to their biologically designated reaction spot as their receptors. Moreover, at least some IGFBPs were postulated to act in the absence of bound IGF1 via extracellular matrix components [83].

2.2.4   IGF1-receptor

The actions of IGFs are primarily mediated by their type 1 and type 2 receptors (IGF1R and IGF2R), which are both glycoproteins and found in the cell membrane. IGF1R was distinguished from IR in 1975 [90] and is expressed by almost all cell types during embryogenesis, widely expressed on normal tissue but little detectable in the liver [91]. IGF1R represents a 1337 amino acid containing type 2 tyrosine kinase receptor and shares a 60% homology at the amino acid sequence level with the IR [92]. The receptor is synthesized as a straight-lined precursor polypeptide of 1367 amino acids in length

(Figure 2.2, A), containing a 30 amino acid signal peptide cleaved post-transcriptionally. The signal peptide is followed by the α-subunit (aa 1-706), including two successive homologous globular L1 and L2 domains, separated by a cysteine rich region (aa 148-302) [93], followed by three fibronectin domains [94]. The α- and β-subunits (aa 711-1337) are connected by a disulfide bond and are separated by a proteolytic cleavage site (aa 707-710). The 24-residue containing hydrophobic transmembrane domain (aa 906-929) is located on the β-subunit as well as the C-terminal intracellular tyrosine kinase domain (aa 973-1229) [92]. The precursor protein is glycosylated, folded and dimerizes with guidance of lectins before the transport to the Golgi apparatus [95]. Next, mature IGF1R is formed following proteolytic division into the α- and β-subunits at the furin-protease cleavage site. The final structure shows a tetramer out of two dimers, each containing an entirely extracellular α-subunit and a transmembrane spanning β-subunit (Figure 2.2, B). The β-subunit is passing through the membrane, but mainly located in the cytoplasm. The formation of the mature receptor depicts an $\alpha_2\beta_2$-confirmation, its subunits connected by disulfide bonds [96], thus describing a heterotetrameric receptor. Functionally this structure results in two extracellular α-subunits to bind their ligand and two intracellular β-subunits containing the cytoplasmic tyrosine kinase domain. Ligand binding at the α-subunits triggers a conformation change in the β-subunits and induces the tyrosine kinase domain to autophosphorylation. Major phosphorylation sites are tyrosine residues located at position 1131, 1135 and 1136 [97], which are found identical to those in the IR. In total a mature IGF1R dimer holds a molecular mass of more than 300 kDa, with ~80 kDa for the α-subunits and ~71 kDa for the β-subunits [98, 99].

A

B
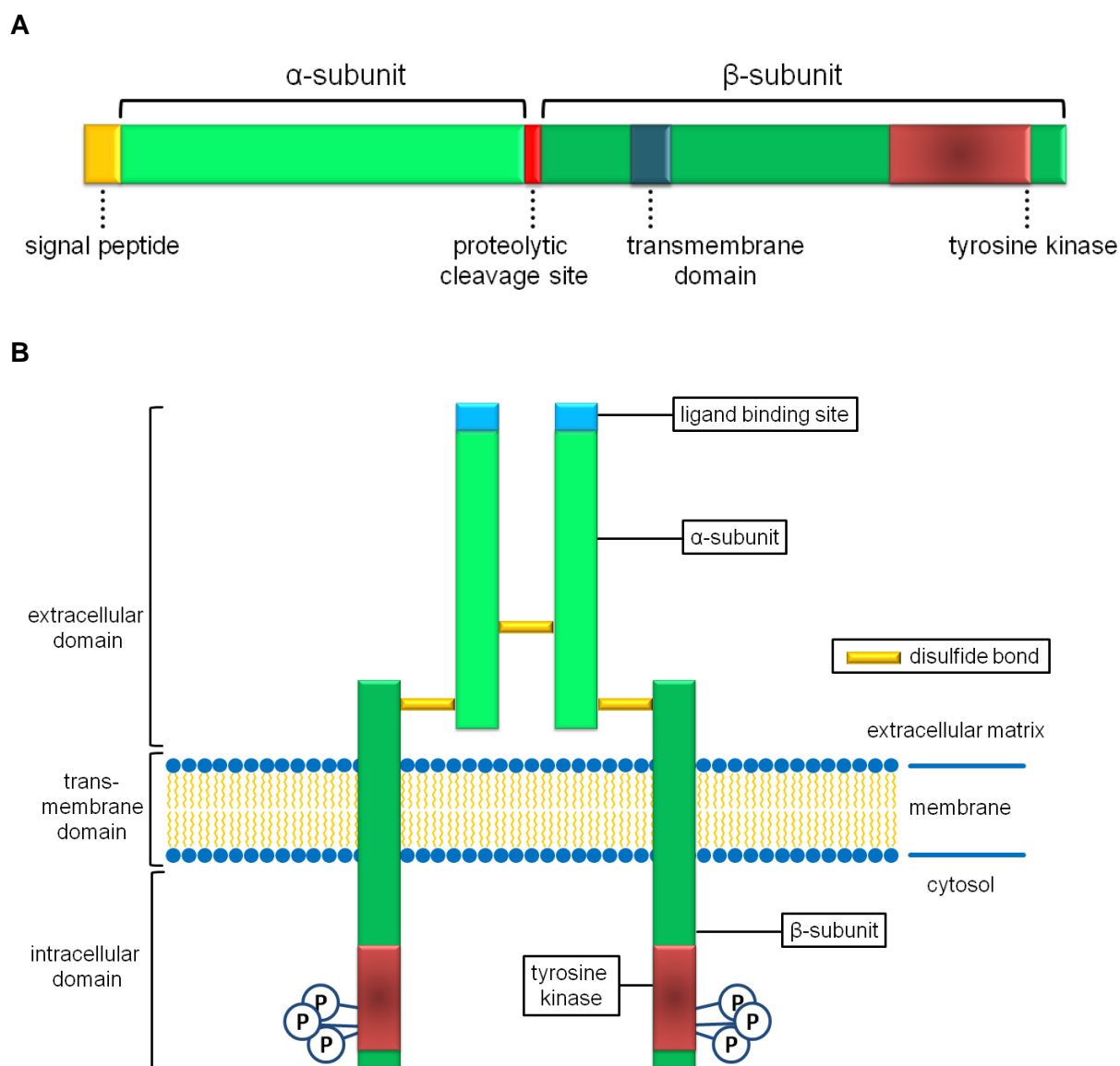
Figure 2.2: *Schematic presentation of the IGF1R. (A) Bar diagram representing the IGF1R precursor protein, 1367 amino acids in length. The signal peptide is cleaved post-transcriptionally and followed by the α-subunit, which is connected with the β-subunit by a proteolytic cleavage site. The β-subunit includes the transmembrane domain along with the intracellular tyrosine kinase domain. Subunits are cleaved after glycosylation and dimerization with a second precursor peptide to form the mature heterotetramer. (B) The mature IGF1R represents a heterotetrameric structure in a α$_2$β$_2$-formation with a molecular mass higher than 300 kDa. The α- and β-subunits are connected with each other by a disulfide bond; similarly, both subunits are linked by a disulfide bone between their α-subunits. The α-subunit is located fully extracellular and contains the ligand binding site at the N-terminus. The β-subunit contains a short extracellular section, the transmembrane region and the tyrosine kinase domain, which is activated by ligand induced conformational changes and initiates autophosphorylation of tyrosine residues. The elements are presented schematically and not necessarily at scale.*

In contrast to the widely known insulin receptor, which primarily mediates metabolic regulations, the IGF1R mediates different growth-promoting functions. It controls cell growth, mitogenesis, anti-apoptosis, cell differentiation and proliferation. IGF1R plays an important role in cell transformation, cancer growth and metastasis [66].

2.2.5 IGF2-receptor

Insulin-like growth factor 2 receptor (IGF2R) or "type 2 IGF1R" was found to be identical to the "cation-independent mannose-6-phosphate (M6P) receptor (MPR)" [100, 101] and binds IGF2 with the highest affinity. Binding to IGF1 is unlikely and it fails to bind insulin at all. IGF2R is around 300 kDa in size and represents a single membrane spanning domain-containing type I transmembrane protein with a large extracellular domain and a short cytoplasmic tail [63]. The extracellular domain consists of a repetitive structure with 15 continuous repeats of 147 amino acid length (Figure 2.3). The repeats show a sequence homology of 14 – 38% [102], while two distinct M6P-binding sites were located in repeats 3 and 9 [103] at which a mannose-6-phosphate is added in the Golgi system. IGF2R is a multifunctional protein receptor that binds IGF2 at the cell surface at repetitive segment 11 [104]. IGF2R has no tyrosine kinase activity, seems to exist as a dimer in the membrane, but it behaves as a monomer in detergent solutions [105, 106]. There is no data available for the role of IGF2R in signal transduction, thus IGF2R is thought to function as a clearance receptor for IGF2 and regulating the extracellular levels of its ligand [63]. A supposed additional mechanism is clearance of IGF2 through receptor-mediated endocytosis followed by IGF2 degradation in lysosomes [107]. Leading to reduced bioactivity of IGF2 by confiscating it away from the IGF1R, the IGF2R has probably talent as a tumor suppressor gene [108].
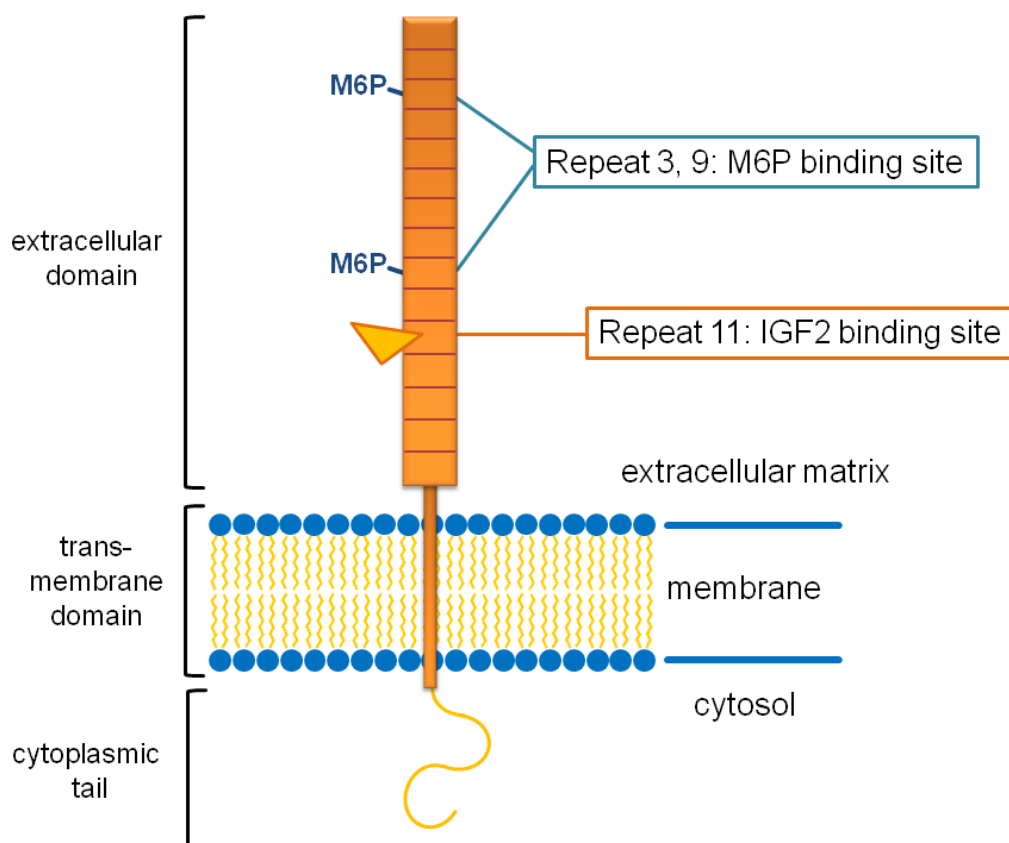
Figure 2.3: *Schematic representation of the IGF2R. The IGF2R or cation-independent mannose-6-phosphate (M6P) receptor represents a single membrane spanning type I transmembrane protein with a large extracellular domain and a short cytoplasmic tail. The extracellular domain consists of 15 continuous repeats with a high sequence similarity. Binding site for IGF2 is located at repeat 11 and repeats 3 and 9 bind M6P. No data suggest IGF2R for a role in signal transduction, which intends a probable function for a clearance receptor.*

2.2.6 IGF1 and IGF2 binding to their receptors

IGF1 and IGF2 bind as ligand to their designated receptors with highest affinity, but both bind moreover to other receptors with reduced affinity, including structural similar receptors, like the insulin receptor (IR). Because of structural homology, particularly in the intracellular tyrosine kinase domain, IGF1R- and IR-proreceptors are able to form heterodimeric receptors post-transcriptionally, prior to cleavage to generate two extracellular α-subunits and two β-subunit containing a short extracellular, the transmembrane and a tyrosine kinase domain, one pair originating from each receptor type [65]. Thus the IGF1 hormone binds as ligand to the IGF1R, IGF2R, IR and IGF1R/IR-heteroreceptors with different affinities (Figure 2.4). Both IGF1 and IGF2 bind the IGF1R with high affinities, while IGF2 is the only ligand for the IGF2R [109]. IGF1 binds to IR only at very high doses, IGF1 has a 100-fold higher affinity to IGF1R compared to IR [52]. IGF2

binds to IR only in fetal development until the IGF1R is expressed sufficiently [110]. IGF1 is the preferred ligand for IGF1R/IR-hybrid receptors compared to insulin [52, 111].
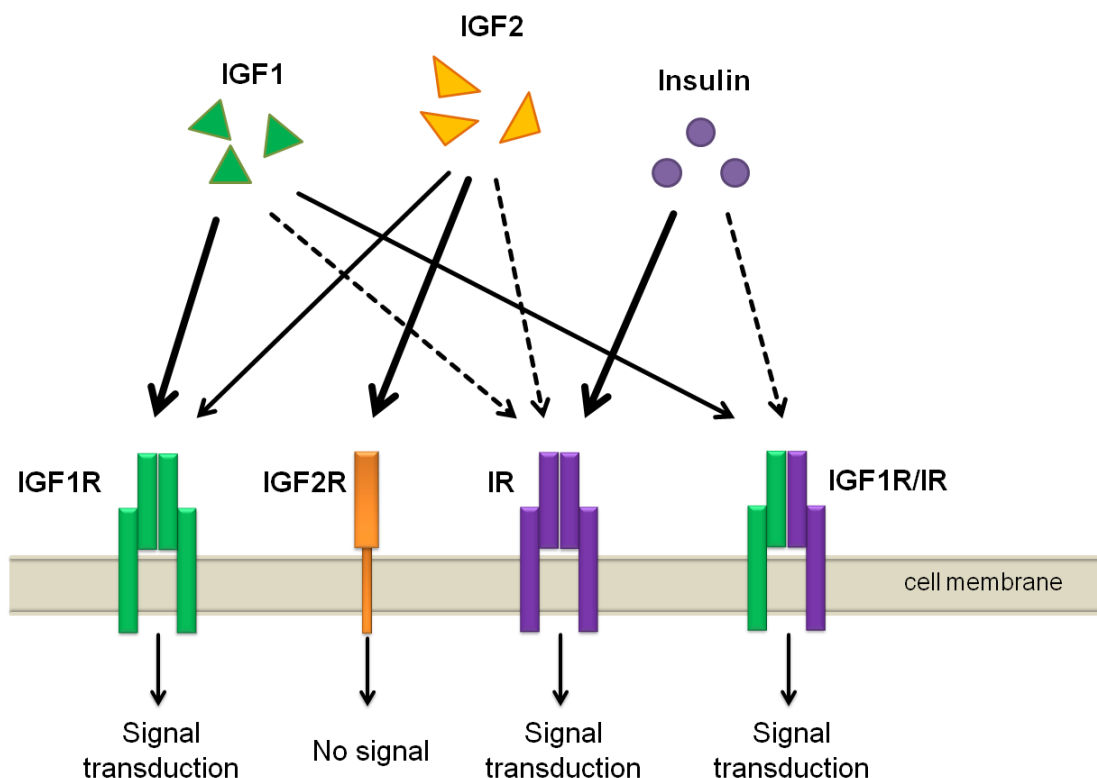
Figure 2.4: *Schematic depiction of interaction among ligands and receptors of the insulin-IGF family. Insulin and IGF1R share structurally a high homology and act as tyrosine kinases. Both can build IGF1R/IR-hybrid receptors containing one α- and β-subunit from each type. IGF2R structure differs substantially and the downstream signal is unclear. IGF2R might work primarily as clearance receptor for IGF2. IGF1 binds to the IGF1R, to IGF1R/IR-hybrid receptors with clearly reduced affinity and binds weakly to IR. IGF2 binds to its own and IGF1R and binds to IR only in early fetal development. Insulin binds to its own receptor with high affinity and IGF1/IR-hetero receptors at a high concentration only. The relative affinities of ligands are indicated by the width of the arrows, dotted lines represent weak binding. Modified from [111].*

2.2.7   Signal transduction by the IGF1R

Initiation of signal transduction starts with ligand binding at the extracellular α-subunits of IGF1R, which triggers a confirmation change in the intracellular β-subunits, containing the cytoplasmic tyrosine kinase domain, and induces autophosphorylation at β-subunits major phosphorylation sites [97, 112]. Activation of the receptor leads to subsequent activation of at least two signaling pathways. One time activated by phosphorylation, the IGF1R employs and activates signaling adapter proteins like IRS-1, IRS-2 (IRS: insulin receptor substrate) and SHC (Src homology domain-containing protein), which initiates multiple signal cascades [61, 62]. The first pathway stimulated following IGF1R activation is the phosphoinositol 3-kinase (PI3K)-Akt signaling pathway, inhibiting apoptosis and to ensure

cell survival [113]. Studies suggested a recruitment of IRS-1 primarily required for effecting mitogenesis, whereas IRS-2 might have a key function in cellular motility reply [114]. Initiated by phosphorylated IRS-1, a complex formation with the regulatory subunit of PI3K takes place, which leads to stimulated PI3K activity and increased levels of phosphatidylinositol 3,4,5-triphosphate (PIP$_3$). As a result, AKT is co-localized at the membrane, where AKT phosphorylation is executed and thereby activated by PDK1 and the mTORC2 complex [115]. Activation of AKT causes anti-apoptotic effects by inhibiting phosphorylation of pro-apoptosis factors like BAD and transcription factors of the FOXO family. Additionally, activation causes expression of anti-apoptotic proteins like BCL-1, BCL-XL and nuclear factor kappa-B (NF-κB) [116]. Activated AKT also triggers the activity of the mTORC1 complex and by that influences glucose metabolism by regulation of GSK-3β activity and regulating cell growth by a sequence of adjacent intermediate signaling actions [117]. The second pathway initiated by IGF1R activated SHC, consists of RAS, RAF and extracellular-signal-regulated kinase (ERK) / mitogen-activated protein kinase (MAPK) activation, from there leading to proliferation and tumor growth, and transduction of mitogenic signals through ELK1 activation in the nucleus [53, 75].

The importance of the IGF1R on physiology and development was undoubted since knocking out the IGF1R gene in mice resulted in neonatal lethality [118]. An always high rated topic is the contribution of the IGF1-system and the IGF1R-axis to cancer, cancer development and cancer treatment. The IGF1R was found to be overexpressed in many tumor types [119]. Despite the IGF1R being not unique for driving tumor cell proliferation, it is definitively required for cellular transformation by most oncogenes and mediates the combination of proliferation and survival required for anchorage –independent growth [120]. However, undergoing these processes permit cells to survive the detachment necessary for metastasis formation and to form macroscopic tumors [113, 121]. In the clinical view, studies suggest that overexpression of IGF1R might persuade tumor formation and metastasis [122, 123].

The involvement of the IGF-system, and the IGF1R in particular, in cancer cell growth and cell survival, led to today's interest of cancer research for the system as target for a potential therapeutic intervention. One reason is simply because of the observation that reduced circulating IGF1 levels in animal models result in major decrease in cancer development and growth, whereas rising IGF1 levels lead to enhanced tumor growth [124]. One of the first approaches was inhibition of the ligand-receptor interaction by an antibody to the IGF1R [125], followed by various developments of IGF1R-inhibitors based on human monoclonal antibodies, placed on different stages of pharmaceutical trials [126]. A formerly encouraging clinical trial, in which treatment of metastatic breast cancer with a monoclonal antibody that blocks IGF1R was combined with hormonal therapy, was

finally discontinued, when a clear survival benefit was observed in the placebo group [127]. Other examples of studies, in which IGF1R inhibition failed to have clinical profits, showed unsatisfactory results in the treatment of lung cancer or Ewing's sarcoma [128, 129]. Thus the approach of antibody targeting of a single receptor might be too simple for such a complex system, because the IGF-pathway is more complex than a single receptor interacting with a single ligand. After blocking one signaling system, a linked alternative pathway can be addressed to compensate the lost signal [130]. This scenario might occur in IGF1R-resistance, where for example, inhibition of IGF1R might induce exceeding insulin secretion, leading to an increased signaling by the IR pathway [126]. Non-antibody based approaches were also successful, thus ligand binding could be enabled by an D-amino acid analog of IGF1 [131] or the tyrosine kinase activity was repressed by a "small molecule" [132, 133]. Further, downstream signaling inhibition could provide a useful pharmaceutical biomarker, also presenting information before and after treatment about medical response [134].
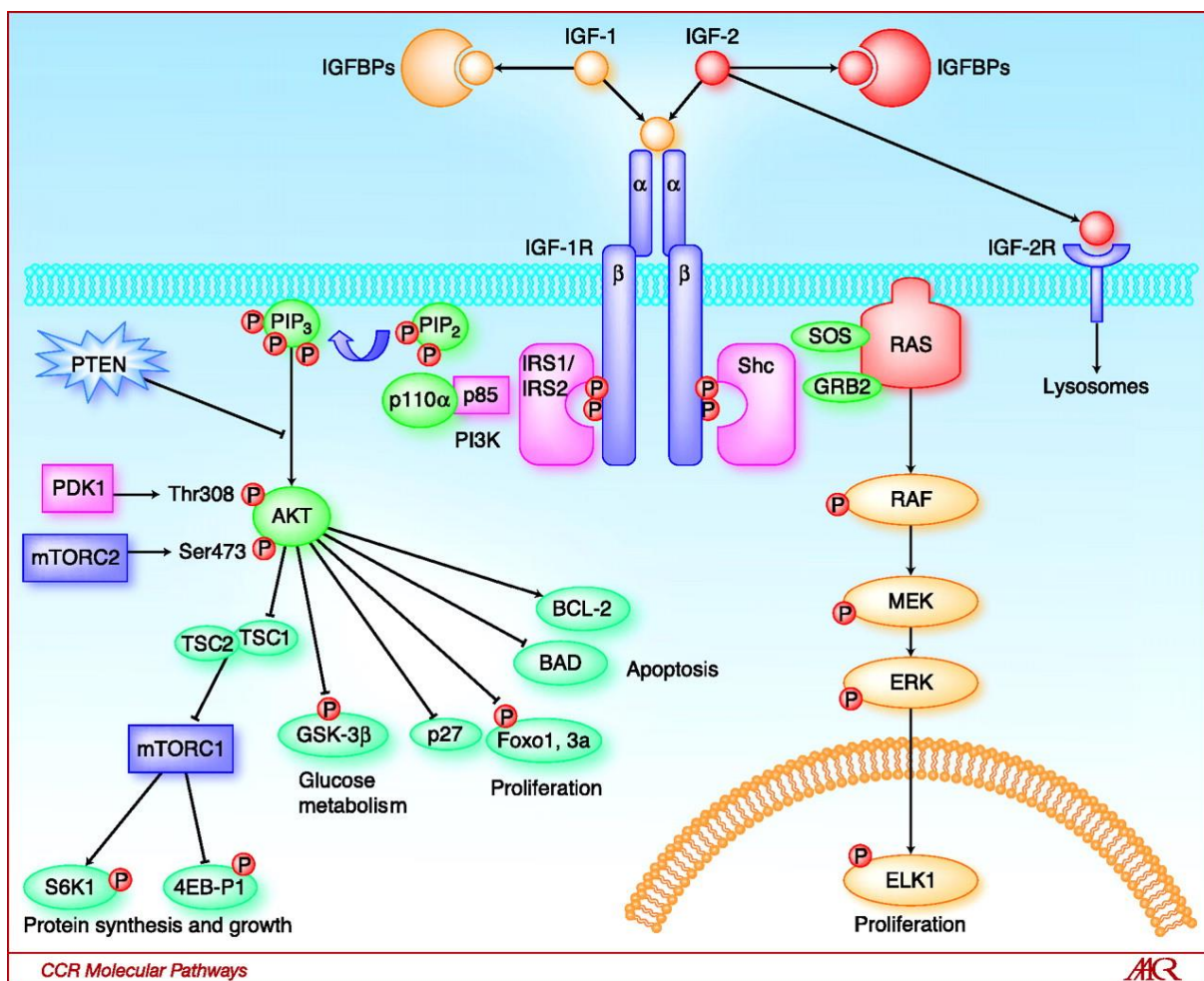
Figure 2.5: *Key components of the IGF1R pathway.* *The ligands IGF1 and IGF2 are both capable of binding to and stimulating the catalytic activity of the IGF1R. Bioavailability of IGF1 is modulated by a family of IGFBPs, whereas bioavailability of IGF2 is modulated both by the IGFBPs*

and by binding to the IGF2R, an event that leads to receptor-mediated internalization and degradation of IGF2 in lysosomes. Upon binding by either IGF1 or IGF2, the IGF1R undergoes receptor cross-linking and autophosphorylation, leading to the creation of multiple docking sites for the adaptor proteins IRS-1, IRS-2, and SHC. IRS-1 and IRS-2 binding results in activation of the class I phosphatidylinositol 3' kinase, whose catalytic activity is the conversion of PIP2 to the second messenger PIP3. This event recruits the AKT family of kinases to the plasma membrane, where they can be phosphorylated and activated by PDK1 and the mTOR-containing complex mTORC2. Activated AKT then mediates a host of cell signalling events, including disinhibition of the mTORC1 complex and increased protein synthesis and cell growth, increased conversion of glucose to glycogen via inhibition of GSK-3β, and increased proliferation and survival by activation or inhibition of key effectors such as the FOXO transcription factors, p27, BAD, and BCL-2. In contrast, SHC binding to activated IGF1R results in stimulation of the RAS/MAP kinase pathway, which also leads to increased cell proliferation. Transferred from [135].

2.3 Potential role of IGF1R-Ab in endocrine diseases

The potential role of IGF1 in regulation of immune function was already discussed by professionals in the scientific field [44]. The impacts of autoantibodies to the TSHR causing hyperthyroidism in Graves' disease directly by mimicking the stimulatory effects of TSH were widely specified above. A first hint for a relation between thyroid function and IGF1 was discovered, when the response of a rat thyroid epithelial cell line to TSH significantly increased after adding insulin or IGF1 to the culture medium [136-138]. It was further shown in a mouse study, that overexpression of IGF1 and IGF1R in thyroids of mice increases weight and volume of the thyroid gland [139]. Hints on the overlap also exist on the molecular level of TSH and IGF1 triggered signaling. Thus, several signaling events downstream of TSHR flow into the PI3-kinase pathway and the following Akt/mTOR pathway [140, 141], which is also included into the pathway elicited by IGF1 binding at the IGF1R regulating growth and proliferation effects.

Interestingly, a co-localization of TSHR and IGF1R in orbital fibroblast and human thyroid epithelial cells in culture was suggested [34]. In the same study, an interruption of the IGF1R signaling pathway was observed using a monoclonal antibody against the α-subunit of IGF1R, which also reduced the activation of ERK by TSH. These information indicate a closer connection of these both receptors in GO, as supposed before.

Autoimmunity against IGF1R is not only specific for Graves' disease, but also observed in rheumatoid arthritis. Thus IGF1 plays an important role in articular connective tissue, like cartilage, in both, regular physiological conditions and in diseases related with those tissues, like rheumatoid arthritis [142].

A participation of the GH/IGF1-pathway in the pathogenesis of Crohn's disease has yet to be consolidated, but it was shown, that GH was able to lower disease level and improve course of the disease [143].

There exist several indications, that autoantibodies against the IGF1R could influence diabetes mellitus (DM). Type 1 DM unites, as common autoimmune disease, a set of genetic and environmental factors [144]. A study showed that alteration of β-cell mass was not viable after mutation of the IGF1R, which led to non-functionality. These observations reveal a requirement of IGF1R-mediated signaling for retention of insulin secretion [145]. Defects in IGF1R and IGF2R expression in the embryonic pancreas of a type 2 diabetes rat model showed decreased β-cell mass and supported hyperglycemia [146]. This effect might be explained by the central roles of IGF1 and IGF2 on β-islet cell development and function and their triggering thereof by the IGF1R [147, 148]. Further studies underlined IGF1-supported β-islet growth mediated by IRS-1 [149], and mice showed, when IGF1 was overexpressed in β-cells, a reduced incidence of diabetes and an increased amount of intact islet cells [150]. A knockout of IGF1R in β-cells led to increased blood insulin levels and glucose intolerance [151], by activating the Akt-signaling, which leads to enhanced proliferation and resistance to apoptosis [152]. After applying IGF1 to patients with type 1 or type 2 diabetes, insulin sensitivity was increased and glycemic control was enhanced [153]. All these evidence could indicate a pathophysiological contribution of IGF1R to diabetes mellitus.

It might be obvious, that the IGF1R, due to its involvement in the GH/IGF1-axis, plays a substantial role in pre- and postnatal growth in general. Partial IGF1R-deletions were shown in a mutation analysis to being responsible for around 3% growth defects in children, born small for gestational age [154]. At a copy number variation analysis in children, born small for gestational age, in two cases further gene deletions for the total IGF1R gene were found. Both children increased their height during GH-treatment [155]. In a study regarding tiny dog breeds, 9 of 13 dogs were carrying a highly conserved arginine to histidine mutation in the IGF1R gene [156]. These studies underscore the central importance of the IGF1-pathway in controlling height and thus, aAb versus the IGF1R might be involved in growth and development resulting in a clinical phenotype, like growth deficiency, body composition defects, increased tumor sensitivity and impaired carbohydrate metabolism.

3 Aim of this study

Autoantibodies (aAb) are characteristic for autoimmune diseases, but may also be found in apparently healthy individuals and affect disease predisposition and precede pathological symptoms. As a direct player of the GH/IGF1-axis, aAb directed against the IGF1R might have a major effect on growth, metabolism and cancer. A direct pathological role of IGF1R-aAb has been suggested for Graves' orbitopathy (GO), the major sight-threatening side-effect of Graves' disease.

The aim of this work is to test this hypothesis experimentally, i.e., that individuals form aAb against the IGF1R, which modulate receptor action positively or negatively, and thus affect GO risk and disease severity. To this end, an assay system has to be established and specificity and sensitivity optimized with reliable assay characteristics and high reproducibility. At present, there is no such test available for routine testing. Until now, the aAb in focus have been detected and quantified by mainly radioactive, immunochemical or time-consuming inconvenient ELISA-based approaches. The formerly used methods were restricted by the use of radioactivity, connected with high costs and significant health risks, and relied on a high level of expertise of the operator. The quantitative analysis of a large sample collective has been severely limited by these aspects. Thus, the new test system, which needs to be developed, should not include radioactive components, enable reliable and reproducible values for autoantigen-specific antibodies against the IGF1R and should be able to allow a straightforward, fast and accurate analysis. As every test system has its own restrictions and limitation, a second assay system for detecting IGF1R-aAb with an alternative technique would be another aspect during the experimental testing of the working hypothesis.

Hence, a method involving the immunoprecipitation of IGF1R-luciferase fusion proteins by the autoantibodies will constitute one possible assay system, which may allow a reliable quantification of the autoantibody-receptor immune complexes. In addition, a new sandwich-based bridge-assay method – similar to a conventional ELISA technique – could be established as the second method of choice, which allows a more direct testing suitable for routine diagnostics.

Finally, a biochemical characterization of the autoantibodies should be attempted including the aspects of immunoglobulin heterogeneity, specificity, biological function and pathological relevance.

4 Materials and methods

Commonly used chemicals in this study were purchased from Roth (Karlsruhe), Sigma (München) or Merck (Darmstadt).

In the following tables labware and instruments (Table 4.1) and commercially available systems (Table 4.2), are listed.

Table 4.1: *Labware and Instruments.*

Labware / Instrument	Manufacturer
Analytical Balances TE64, TE601	Sartorius, Göttingen
Centrifuge 5415R, 5810R	Eppendorf, Wesseling-Berzdorf
Centrifuge RC5C Plus (Rotor: SS-34)	Thermo Scientific, Langenselbold
DNA Engine Thermal Cycler	Bio-Rad, München
Electrophoresis Power Supplies EV232, EV202, E802	Consort, Turnhout, Belgium
Gel Documentation System Gel Doc 2000	Biorad, München
Horizontal Electrophoresis Systems PerfectBlue Mini S, M, L	Peqlab, Erlangen
Imaging Plates BAS-IP MS 2325, 2340	Fujifilm, Düsseldorf
Imaging Plates Cassettes BAS 2325, 2340	Fujifilm, Düsseldorf
Incubator Innovens Category 1	Jouan, Unterhaching
Incubator Shaker Innova 44	New Brunswick Scientific, Nürtingen
Inoculation Loops 10 µl	VWR, Darmstadt
L-shape Bacteriology Loops	VWR, Darmstadt
Multi-Channel Pipette Research Pro	Eppendorf, Wesseling-Berzdorf
MultiTempIII Thermostatic Circulator	Amersham Biosciences, Freiburg
Neubauer cell counting chamber (Hemocytometer)	Roth, Karlsruhe
Pipetboy acu	Integra Biosciences, Fernwald
Pipetman P10, P20, P200, P1000	Gilson, Bad Camberg
PolyScreen PVDF Transfer Membrane	PerkinElmer, Waltham, Massachusetts USA
Reagent and Centrifuge Tubes 15, 50 ml	Sarstedt, Nümbrecht
Refrigerated Incubator Shaker C24KC	New Brunswick Scientific, Nürtingen
Safe-Lock Tubes 1.5 ml, 2.0 ml	Eppendorf, Wesseling-Berzdorf
Semi-dry Electroblotter SEDEC M	Peqlab, Erlangen
Serological Pipets 2 ml, 5 ml, 10 ml, 25 ml	Corning, Wiesbaden
Shaking Water Bath 1083	GFL, Burgwedel
Spectrophotometer NanoDrop ND-1000	Peqlab, Erlangen
Sterile fiters (0.2 µm pore size)	Whatman, Dassel
Thermomixer comfort	Eppendorf, Wesseling-Berzdorf
Thermo-Tubes 0.2 ml	Abigene, Hamburg
Ultrospec 10 photometer	Amersham Biosciences
Ventilation Cap Tubes 13 ml	Sarstedt, Nümbrecht
Vertical Electrophoresis Systems PerfectBlue Twin S, L	Peqlab, Erlangen
Vortex-Genie 2	Scientific Industries, Bohemia, USA

Table 4.2: *Commercial available systems.*

System	Application	Manufacturer
NucleoSpin Plasmid QuickPure	Plasmid isolation (small-scale)	Macherey-Nagel, Düren
PageBlue Protein Staining Solution	Protein staining	Fermentas, St. Leon-Rot
Qiagen PCR purification kit	DNA purification	Qiagen, Hilden
QiaQuick Gel extraction kit (50)	DNA purification	Qiagen, Hilden
Sample Loading Buffer	Protein sample loading buffer	Fermentas, St. Leon-Rot
Western Lightning Chemiluminescence Reagent	Western blot detection	Perkin Elmer, Weiterstadt

4.1 Assay development

4.1.1 Buffers

During the development, realization and performing of assays, it was useful and obvious to revert to an approved set of buffers. To these will be referred to in the present study (Table 4.3).

Table 4.3: *Commonly used buffers.*

Name	Specification
Extract binding buffer	20 mM HEPES pH 7.5, 50 mM NaCl, 10% Glycerol, 10 mg/ml BSA
Extraction buffer	20 mM HEPES pH 7.5, 50 mM NaCl, 10% Glycerol, 2% Triton-X-100
Ligand binding buffer	50 mM Tris pH 7.5, 50 mM NaCl, 10% Glycerol, 50 mg/ml BSA, 5% Triton-X-100
Luciferase substrate buffer	25 mM Glycilyl-Glycin, 7.5 mM $MgSO_4$, 2 mM EGTA, 7.5 mM KPO_4, pH 7.8 with NaOH, then added to 5 mM DTT, 1 mM ATP, 0.1 mM Luciferin
Sample buffer	20 mM HEPES pH 7.5, 50 mM NaCl, 10% Glycerol, 10 mg/ml BSA
Washing buffer 1	50 mM Tris pH 7.5, 50 mM NaCl, 10% glycerol
Washing buffer 2	20 mM HEPES pH 7.5, 100 mM NaCl, 0.1% Triton-X-100
Washing buffer ICI, 50x concentrate	400 mM Tris, 3 M NaCl, 1% Tween 20, 0.001% Antifoam, pH 7.5

4.1.2 Recombinant proteins

Recombinant proteins were expressed in different expression systems. At one hand stable cell lines were generated, mostly used for expression of membrane integrated proteins like the full length receptors or truncations thereof, which included still membrane bound domains (description of the method see 0). While expressed, the recombinant receptor gets enriched on the cell surface. Cell pellets were collected for further processing and to yield the recombinant receptor for usage (see 4.3.11). On the other

hand a transient expression system was used for expression of a truncated receptor without membrane domain. To this end, the baculovirus expression system, based on insect cells, was used. After generation of the bacmid, carrying the DNA encoding for desired recombinant protein, a virus was generated, which was used to infect insect cells and the resulting recombinant protein was subsequently secreted into the cell culture media (description of the method see 4.3.10). The cell culture supernatant contained the recombinant protein and was used for further purposes.

All protein fusions generated contained the desired recombinant receptor at the N-terminal position and the attached protein at the C-terminal site. Recombinant proteins purchased by a commercial supplier are also listed in Table 4.4.

Table 4.4: *Recombinant proteins used in this study.*

Name	Expression system	Recombinant protein
IGF1		commercial available IGF1 (life technologies)
IGF1R (ED)-2B5	Baculovirus H5	extracellular domain (aa 1-927) of IGF1R 2B5-tag fusion
IGF1R (-TK)-2B5	HEK293, stable	truncated (aa 1-998) IGF1R 2B5-tag fusion
IGF1R (-TK)-PGA	HEK293, stable	truncated (aa 1-998) IGF1R PGA-tag fusion
IGF1R-Luc	HEK293, stable	IGF1R luciferase fusion
IGF1R-PGA	HEK293, stable	IGF1R PGA-tag fusion
IGF2R-Luc	HEK293, stable	IGF2R luciferase fusion
Insulin		commercial available Insulin (life technologies)
IR(-TK)-2B5	HEK293, stable	truncated (aa 1-1022) IR 2B5-tag fusion
IR-Luc	HEK293, stable	IR luciferase fusion

4.1.3 Lyophilization

Antibodies were lyophilized to star shaped high capacity plastic tubes (BRAHMS Diagnostica, Hennigsdorf) with a total volume of 5 ml and a working volume of 200 µl. Antibody solution was prepared in a concentration of 2 µg/ml in coating buffer (50 mM NaPP, pH 7.4). 200 µl antibody solution was added to every tube, which equals an amount of 0.4 µg antibody per tube. Tubes were let sit for 20 h at RT, before liquid has been completely removed again. 1 ml saturation solution (50 mM HEPES pH 7.5, 5 mg/ml BSA, 0.1% Triton-X-100, 3% Karion) was incubated for 2 h at RT decanted and was allowed to rinse out for 30 min. Tubes were lyophilized for 24 h (Gefriertrocknungsanlage Beta 1-8 LD; Christ, Osterode). Lyohilizer settings with 20 min warm up, 21 h drying at -55°C and 0.040 mbar, 3 h final drying and 20 min final warm up were proceeded.

A similar protocol was chosen to lyophilize coated tube bound receptors. To this end, different amounts of IGF1R extract were bound by the fused peptide tag (PGA- or 2B5-tag) to anti-peptide tag antibody (anti-PGA or anti-2B5) coated tubes at 4°C in a total volume of 200 µl coating buffer (50 mM HEPES pH 7.5, 5 mg/ml BSA) per tube over night at 4°C. As control served HEK293 wild type extracts under same conditions. Tubes were washed twice with 1 ml blocking buffer (50 mM HEPES pH 7.5, 5 mg/ml BSA, 3% Karion), each washing step with 2 times knocking off the tubes on paper towels. Tubes were let sit on the top for 20 min followed by the lyophilization for 2 h at -55°C and 0.040 mbar.

4.1.4 Immunoprecipitation of IGF1R using human sera

100 µl of the IGF1R-PGA cell extract was incubated with 50 µl of patients' serum overnight at 4°C. Protein G-immune complexes were formed by incubation with 50 µl of protein G-sepharose beads (50% suspension in PBS) for 4 h at 4°C. Complexes were pelleted by centrifugation and washed six times with PBS. Immunoprecipitates were resuspended in 75 µl of SDS sample buffer and stripped by incubation at 95°C for 5 min. Eluted proteins were subjected to electrophoresis in 10% SDS PAGE and transferred to nitrocellulose membranes. Membranes were probed overnight at 4°C with anti PGA14 antibody to detect IGF1R-PGA. Bands were visualized using enhanced chemiluminescence Western blotting detection kit (Pierce, Rockford, UK).

4.1.5 Determination of IGF1R binding capacity

The relative capacity for hormone binding of the recombinant IGF1R was evaluated. Analyzes were performed with HEK293 cell extracts stably expressing IGF1R, which contained an PGA- or 2B5-peptide tag at the C-terminus. The tubes used were precoated and lyophilized with 200 µl anti-2B5 peptide antibodies or anti-PGA peptide antibodies, respectively, in a concentration of 2 µg/ml. Lyophilization took place in 200 µl working volume in high capacity (star shaped bottom) tubes, seizing a volume of 5 ml (ICI, Berlin), which served as capture antibody for the tagged IGF1R. A predefined amount of peptide tagged IGF1R was added in 200 µl extract binding buffer, depending on the experimental design. In this step peptide-tagged IGF1R were immobilized to the surface of the coated tubes when incubated over night at 4°C. Tubes were washed 5 times with 1 ml washing buffer 1, with knocking off following each washing step. IGF1 was labeled by acridinium NHS ester according to the manufacturer's instructions (Cayman) yielding a preparation of acridinium ester-labeled IGF1 (10^8 RLU/µg IGF1).

0.2. µl acridinium-labeled hormone was added per tube in 50 µl ligand binding buffer and incubated for 2 h at RT shaking or at 4°C not shaking over night. A competition sample

with non-labeled hormone was prepared for methodical verification of the experiment. This sample included 10 µg /ml unlabeled IGF1, which was added to the mix containing the labeled IGF1. Labeled and unlabeled IGF1 competed for the receptors hormone binding sites and subsequently unlabeled IGF1 replaced labeled IGF1, because the unlabeled hormone was available in high excess. Where appropriate, control samples carrying HEK293 wild type extract were added.

4.1.6   Screening of anti IGF1R-Ab in hybridoma cell culture supernatant

The presence of anti IGF1R-Ab in hybridoma cell culture supernatant was screened by binding potential antibodies from the supernatant to immobilized anti-mouse antibodies and specific binding to IGF1R antigen in one assay in plate format. Surface activated luminescence compatible multi titer 96-well plates (Greiner, Frickenhausen) were coated with 0.2 µg rabbit anti-mouse coating antibody (Rockland, Gilbertsville, USA) in 100 µl coating buffer (50 mM Na-phosphate, pH 7.4) and incubated over night at 4°C. Plates were washed 2 times with 300 µl ddH$_2$O and 100 µl hybridoma cell culture supernatant was added. As background control conditioned hybridoma medium was used. As positive control 0.5 µg/ml commercial anti-IGF1R-Ab (Millipore, Billerica, USA) was added on each plate in double determination. Following over night incubation at 4°C and 2 washing steps with 300 µl ddH$_2$O, 100 µl IGF1R-Luc cell extract diluted 1:10 in extract binding buffer was added. Plates were incubated for 2 h at RT and washed 5 times with 300 µl washing buffer (ICI, Berlin) containing 5% glycerol using a plate washer with a refill of 300 µl following last aspiration step. Plates were drained by gravity flow and luminescence was measured for 2 s with a plate luminometer (Mithras plate luminometer, Berthold, Bad Wildbad) using 100 µl luciferase substrate buffer.

4.1.7   Bridge assay in tube format

The bridge assay format was designed as fast and highly specific assay, in which the antibody links (or "bridges") two autoantigen molecules. Experiments were performed in tubes coated with anti-2B5 peptide monoclonal antibodies, whereat those have been lyophilized to high capacity (star shaped bottom) tubes, seizing a volume of 5 ml (ICI, Berlin) and have been coated as described previously (4.1.3). These immobilized anti-2B5 peptide antibodies were used as capture antibody for the recombinantly expressed antigen IGF1R, which was constructed as fusion protein, connected to a sequence specific 2B5-peptide tag. By this step, the

IGF1R-2B5 tagged antigen was immobilized to the 2B5-antibody-coated tube in an 1 to 20 dilution of the extract in extract binding buffer, which means 10 µl extract in 200 µl working volume in the assay tubes. This step was followed by incubation over night at 4°C and washing 2 times using 1 ml washing buffer 1 at each, while every single washing step was completed by knocking off the tube rack two times on paper towels (the described process hereafter referred to as "washing"). Sample or serum containing antibodies to the IGF1R were added in favored concentration diluted in sample buffer and incubated over night at 4°C. After tubes were washed again 2 times with washing buffer 1, extract containing IGF1R-Luc fusion protein was added in an dilution of 1 to 10 in 200 µl working volume and incubated over night at 4°C. By this, the second variable chain region of the antigen specific antibody was able to bind to IGF1R-Luc simultaneously. After 5 times repeated washing with 1 ml washing buffer 2, luciferase activity was determined using a plate luminometer (Mithras plate luminometer, Berthold, Bad Wildbad) by measuring light emission for 10 s with 300 µl luciferase substrate buffer.

4.1.8 Bridge assay in microtiter plate

Experiments were performed using a 96-well white luminescence compatible plate (Greiner, Frickenhausen). The wells were coated with 0.2 µg anti-2B5 peptide monoclonal antibody per well as described previously (section 4.1.6) on a working volume of 100 µl per well. The consecutive washing procedure included washing with 1x 200 µl and 2x 250 µl ddH$_2$O per well, while every single washing step was completed by knocking off plate two times on paper towels (the described process hereafter referred to as "washing"). 100 µl IGF1R-2B5 containing extract in extract binding buffer was immobilized per well over night at 4°C, followed by washing using washing buffer 1. Antibody samples were added in favored concentration diluted in sample buffer and incubated over night at 4°C. Plates were washed again with washing buffer 1. Then 100 µl IGF1R-Luc extract in extract binding buffer was added per well. After incubation over night at 4°C, washing was performed with 3 additional washing steps using washing buffer 2. 75 µl washing buffer 1 was added per well to prevent drying, plate luminescence signal was read out with a plate luminometer (Mithras plate luminometer, Berthold, Bad Wildbad) for 2 s using 75 µl luciferase substrate buffer in a 2-fold concentration.

4.1.9 Calculation of coefficients of variation (CV)

IGF1R autoantibodies in 4 serum samples were determined in 5 replicates using the IGF1R-luciferase precipitation assay in 4 independent assay sets. The %-CV for each sample was calculated by finding the standard deviation of 5 replicates, dividing that by the replicates mean, and multiplying by 100. The average of the individual CVs is reported as the intra-assay CV. The replicates mean for each sample was calculated and then used to evaluate the overall mean, standard deviation, and %-CV for each sample in all assays. The average of all samples %-CV is reported as the inter-assay CV [157].

4.2 Molecular biology

A list of the oligonucleotides and commercially available antibodies used in this study is provided below. Primers were purchased from BioTeZ (Berlin) or Life Technologies (Darmstadt).

Table 4.5: *Olinucleotides used in this study. Sequence is noted from 5' in 3' direction.*

Name	Sequence
3'IGF1R-(full-length)-PGA-EcoRI	ACGGAATTCTCATGTTCCTGCTCCTGGTTGCTGATTCTCTGAAAGCT CACTGCTGCCAAGGCAGGTCGAAGACTGGGGCAGCGG
3'E1-IGF1R-EcoRI	ACGGAATTCGCCCTCAAACCTGTAGGTGTTGGG
3'E2-IGF1R-EcoRI	ACGGAATTCGATGATGCGATTCTTCGACGTGGT
3'E3-IGF1R-EcoRI	ACGGAATTCCCTTTCAGGTCTGGGCACGAAGAT
3'E4-IGF1R-EcoRI	ACGGAATTCGATGATCAGATGGATGAAGTTTTC
3'IGF1R(ED)-HindIII-2B5	ATCAAGCTTAATCTCGGTTCTCTGGGTGACCCTGCCTATGCTGACCT TTGGCCTGGACATAGAAGAACAC
3'IGF1R(full-length)-EcoRI	ACGGAATTCGCAGGTCGAAGACTGGGGCAGCGG
3'IGF1R(-TK)-EcoRI-2B5	TATGAATTCTAATCTCGGTTCTCTGGGTGACCCTTGCCTATGCTGAC CCTTCTCCCGAGCCACCTCCCACTC
3'IGF1R(-TK)-EcoRI-PGA	ACGGAATTCTTATGTTCCTGCTCCTGGTTGCTGATTCTCTGAAAGCT CACTGCTGCCAAGCTTCTCCCGAGCCACCTCCCACTC
3'IGF2R-MfeI	ATACAATTGGATGTGTAAGAGGTCCTCGTCGCT
5'E1-IGF1R-NotI	ACGGCGGCCGCATGGAAATCTGCGGGCCAGGCATCGAC
5'E2-IGF1R-NotI	ACGGCGGCCGCATGTGCCCGCCCAACACCTACAGGTTT
5'E3-IGF1R-NotI	ACGGCGGCCGCATGTCCACCACCACGTCGAAGAATCGC
5'E4-IGF1R-NotI	ACGGCGGCCGCATGAAGCGGAGAGATGTCATGCAAGTG
5'IGF1R-BamHI	ATCGGATCCACCCATGAAGTCTGGCTCCGGA
5'IGF1R-NotI	ACGGCGGCCGCATGAAGTCTGGCTCCGGAGGAGGG
5'IGF2R-NotI	ATAGCGGCCGCCATGGGGGCCGCCGCCGGCCGGAGC
5'TSHR-EcoRV	CGCGATATCATGAGGCCGGCGGACTTGCTGCAG
Firefly3'-BamHI	GCGGAATTCGTCACCGACGCCAAAAACATAAAG
Firefly5'-EcoRI	GCGGAATTCGTCACCGACGCCAAAAACATAAAG

Table 4.6: *Commercially available antibodies used in this study.*

Antibody	Origin	Working dilution	Provider
anti-IGF1R (Tyr1165/Tyr1166)	rabbit	1:10000	Novus Biologicals, Edinburgh, UK
anti-IGF1R α-subunit cl. 24-57	monoclonal	diverse	Millipore, Billerica, USA
anti-mouse-IgG	rabbit	2 mg/ml	Rockland, Gilbertsville, USA
α-mouse-HRP-conjugated	sheep	1:5000	Roche Applied Science, Mannheim, Germany
α-rabbit-HRP-conjugated	goat	1:5000	Dako, Hamburg, Germany

4.2.1 Media and growth conditions of prokaryotic cells

Bacterial strains were grown in LB (-Lennox) broth at 37°C, 220 rpm or on LB agar plates at 37°C throughout this study. SOC medium was used to recover transformants after heat-shock prior to plating. Antibiotics (where appropriate) were used at the following concentrations: 100 µg/ml ampicillin or 50 µg/ml kanamycin.

Table 4.7: *Composition of media used for bacteria culture.*

LB (-Lennox):	1% (w/v) tryptone, 0.5% (w/v) yeast extract, 85.6 mM sodium chloride
LB agar:	as above, but supplemented with 1.2% (w/v) agar
SOC:	2% (w/v) tryptone, 0.5% (w/v) yeast extract, 85.6 mM sodium chloride, 2.5 mM potassium chloride, 10 mM magnesium chloride, 20 mM glucose

4.2.2 Bacterial strains and plasmids

Throughout this study chemically competent *Escherichia coli DH5α* (Life Technologies, Darmstadt) were used for heat-shock transformation and propagation of plasmids. For recombinant bacmid preparation chemically competent *E.coli DH10Bac* (Life Technologies) were used.

Construction of plasmids encoding for luciferase fusion proteins were initiated by integrating the firefly luciferase into pIRESneo vector. The DNA sequence encoding amino acids 2-551 for firefly luciferase was amplified by PCR from pSP-luc+NF using primers "Firefly5'-EcoRI" and "Firefly3'-BamHI". pIRESneo plasmid was digested with appropriate restriction endonucleases, the fragment was removed and replaced with the similarly digested PCR fragment giving pIRESneo-luc plasmid. To integrate DNA sequence encoding the full-length human IGF1R (1368 aa) in pIRESneo-luc plasmid, cDNA was amplified by PCR using primers "5'IGF1R-NotI" and "3'IGF1R(full-length)-EcoRI". pIRESneo-luc plasmid was digested with appropriate restriction endonucleases, the fragment was removed and replaced with the similarly digested PCR fragment giving rise to pIRESneo-IGF1R-luc plasmid encoding the IGF1R-luc fusion protein. Fragments of the IGF1R fused to luciferase were generated by the same principle. pIRESneo-IGF1R-luc plasmid was used as PCR template. Epitope 1, representing amino acids 31 – 273 of the

receptor, was amplified using primers "5'E1-IGF1R-NotI" and "3'E1-IGF1R-EcoRI". Epitope 2, representing amino acids 264 – 506 of the receptor, was amplified using primers "5'E2-IGF1R-NotI" and "3'E2-IGF1R-EcoRI". Epitope 3, representing amino acids 497 – 737 of the receptor, was amplified using primers "5'E3-IGF1R-NotI" and "3'E3-IGF1R-EcoRI". Epitope 4, representing amino acids 738 – 938 of the receptor, was amplified using primers "5'E4-IGF1R-NotI" and "3'E4-IGF1R-EcoRI".

Fusion proteins carrying a peptide tag were constructed by genetically adding the tag to the C-terminus of the receptor or its truncated version. To this end, the 3'-primer, which was used to amplify the receptor, contained the DNA sequence for the peptide tag. For the PGA tag, a 16-residue epitope recognized by PGA14 antibodies [158] was added. For the 2B5 peptide tag, a 12-residue epitope recognized by 2B5 antibodies was included. The 2B5-tag originates from epitope analysis of Selenoprotein P (SePP), and the anti-2B5-antibody was developed to bind most efficiently to the tag (Hybsier, S. *et al.*, unpublished).

For construction of the pIRESneo-IGF1R-PGA14 vector encoding the full length IGF1R fused to PGA14 peptide tag, the pIRESneo-IGF1R-luc plasmid was used as template for PCR amplification by using the primers "5'IGF1R-NotI" and "3'IGF1R-(full-length)-PGA-EcoRI". The amplified PCR product was inserted with appropriate restriction endonucleases into pIRESneo plasmid. For construction of the pIRESneo-IGF1R(-TK)-PGA14 vector, the pIRESneo-IGF1R-PGA14 plasmid was used as template for PCR amplification by using the primers "5'IGF1R-NotI" and "3'IGF1R(-TK)-EcoRI-PGA". This PCR product contained the DNA sequence encoding the first 998 amino acids of the IGF1R, misses the tyrosine kinase domain, and is fused to the PGA14 peptide tag as well. For construction of the pIRESneo-IGF1R(-TK)-2B5 vector, the pIRESneo-IGF1R(-TK)-PGA14 plasmid was used as template for PCR amplification by using the primers "5'IGF1R-NotI" and "3'IGF1R(-TK)-EcoRI-2B5". This PCR product was integrated by the appropriate restriction enzymes into pIRESneo vector and contained the DNA sequence encoding for the first 998 amino acids of the IGF1R, misses the tyrosine kinase domain, and is fused to the 2B5 peptide tag as well. The extracellular domain including amino acids 1 to 927 of IGF1R was integrated in the pFastBac1 vector by restriction endonuclease digestion after amplifying the sequence from pIRESneo-IGF1R(-TK)-PGA14 using primers "5'IGF1R-BamHI" and "3'IGF1R(ED)-HindIII-2B5", yielding the plasmid pFastBac1-IGF1R(ED)-2B5.

For generation of pIRESneo-IGF2R-luc plasmid, the full length IGF2R cDNA sequence was amplified with PCR using primers "5'IGF2R-NotI" and "3'IGF2R-MfeI". The resulting fragment was integrated by the appropriate restriction enzymes into pIRESneo-luc vector. Expression plasmids were verified by sequencing (MWG, Erlangen).

Plasmids used throughout this study are listed in Table 4.8. If not annotated otherwise, these plasmids have been generated in this work.

Table 4.8: *Plasmids used in this study.*

Name	Description	Comment
pFastBac1	backbone for insect expression	Life Technologies (Darmstadt)
pFastBac1-IGF1R(ED)-2B5	extracellular domain IGF1R	
pIRESneo	backbone for mammalian expression	Clonetech (Mountain View, CA, USA)
pIRESneo-IGF1R(-TK)-2B5	truncated IGF1R with 2B5-tag	Δ tyrosine kinase domain
pIRESneo-IGF1R(-TK)-PGA14	truncated IGF1R with PGA-tag	Δ tyrosine kinase domain
pIRESneo-IGF1R-luc	full-length IGF1R with luciferase	
pIRESneo-IGF1R-luc-E1	fragment IGF1R – aa 31 – 273	
pIRESneo-IGF1R-luc-E2	fragment IGF1R – aa 264 – 506	
pIRESneo-IGF1R-luc-E3	fragment IGF1R – aa 497 – 737	
pIRESneo-IGF1R-luc-E4	fragment IGF1R – aa 738 – 938	
pIRESneo-IGF1R-PGA14	full-length IGF1R with PGA-tag	
pIRESneo-IGF2R-luc	full-length IGF2R with luciferase	
pIRESneo-IR(-TK)-2B5	truncated IR with 2B5-tag	from C. Schwiebert and Dr. W.B. Minich, unpublished
pIRESneo-IR-luc	full-length IR with luciferase	
pIRESneo-luc	inserted firefly luciferase	basis for further constructs
pSP-luc+NF	template for amplification of firefly luciferase	Promega (Mannheim)

4.2.3   Polymerase chain reaction

The polymerase chain reaction (PCR) was used to selectively amplify a piece of DNA by *in vitro* enzymatic replication [159]. For plasmid construction and chromosomal integration Phusion DNA polymerase (Fermentas, now Thermo Fisher Scientific) was used. This polymerase possesses a 3'→5' exonuclease proof-reading activity. Thus it is possible to create DNA with high fidelity.

PCRs were performed using a Mastercycler gradient (Eppendorf). Composition of the program was dependent on the size of the sequence that should be amplified, so a respectively required time of elongation was chosen. The annealing temperature was determined experimentally for each primer pair and was selected from experience around 3 degrees below primer melting temperature. The composition and the PCR program for a typically amplification reaction with the Phusion polymerase is described in Table 4.9.

Table 4.9: *Composition of a typical Phusion PCR reaction and corresponding PCR program.*

Volume [µl]	Solution		Temperature in °C	Time
10	5x HF or GC buffer		98	30 sec
1	dNTPs [10 mM each]		98	10 sec
0.5	Sense Primer [100 µM]		50 – 60	30 – 45 sec
0.5	Antisense Primer [100 µM]		72	30 sec per kb
variable	Template DNA [10-100 ng]		30 – 35 cycles beginning with step 2	
1	*Phusion* DNA Polymerase [1 U/µl]		72	10 min
add to 50µl	ddH$_2$O		4	for ever

To determine whether inserts in constructed plasmids were located correctly, one possibility is to perform a colony PCR. This allows the screening of a large number of bacterial clones for the presence of a particular DNA sequence. Selected colonies of bacteria were picked with a sterile pipette tip from an agar plate and transferred into a PCR reaction mix. Bacterial cells were destroyed during the initial denaturation step of 95°C. For colony PCR *Taq* DNA polymerase (Fermentas) was used, since a high fidelity was not necessary. PCR is conducted with primers for the specific sequence.

4.2.4   Purification of PCR products

For purification of obtained PCR products the QIAquick PCR Purification Kit (Qiagen) was used according to the manufacturer's protocol. In brief, 1 volume of sample was mixed with 5 volumes of buffer PBI and directly loaded onto the QIAquick spin column. The DNA bound to the silica membrane of the column and was eluted with 30 µl elution buffer after washing. DNA fragments below 65 bp of size as well as primers and primer dimers are not retained on the column and thereby efficiently removed during loading and washing prior to elution.

4.2.5   Agarose gel electrophoresis

For separation of DNA molecules 1-2.5% (w/v) agarose - TAE gels were used (1x TAE: 40 mM Tris-acetate; 1 mM EDTA (pH 8.0)). Chosen concentration of agarose was dependent on the size of DNA fragments to be separated. For DNA fragments larger than 500 kb 1% gels were used, for fragment smaller than 500 kb higher percentage gels were used. For visualization of the DNA 1% ethidium bromide was added to the liquid agarose solution. Solidified gels were submerged in 1x TAE and DNA samples were supplemented with 6x Orange G loading dye (Fermentas) before loading.

For sizing the DNA fragments 5 µl of a 1 kb ladder (GeneRuler, Fermentas) were additionally loaded onto the gel. DNA fragments were separated for about 1 h at 100 V. The ethidium bromide stained DNA was visualized using an UV-transilluminator (λex=312 nm).

4.2.6 Gel extraction and purification of DNA fragments

For extraction of separated DNA fragments by agarose gel electrophoresis the QIAquick Gel Extraction Kit (Qiagen) was used according to the manufacturer's protocol. This technique is more convenient to separate specific PCR products from unwanted side products and to isolate specific DNA fragments after restriction digestion. In brief, DNA fragments were visualized in the agarose gel using a UV-transilluminator (λex=312 nm), excised with a scalpel and transferred into a clean micro centrifuge tube. For each 100 mg of agarose gel 300 µl buffer QG (Qiagen) was added and incubated at 50 °C for 10 min until gel slices were dissolved. The solution was loaded onto the QIAquick spin column. DNA bound to the silica membrane of the column was eluted with 30 µl elution buffer after washing.

4.2.7 Restriction enzyme digest

For preparative restriction digestion the insert DNA fragment was usually excised out of a PCR-amplified DNA product. Suitable restriction sites were included in the primers used to amplify the fragment. Purified plasmid DNA was also digested to use either the excised fragment as insert or to use the residual plasmid as backbone.

Restriction digestion was conducted in a total volume of 10-50 µl depending on concentration and amount of DNA. A typical reaction included 500 ng to 1 µg DNA in presence of 1 unit from each restriction enzyme. Restriction enzymes were obtained from Fermentas and New England Biolabs (NEB). Appropriate digestion buffer and potential additives were added as specified by the restriction enzyme used. When multi-enzyme digestions were performed, the digestion buffer offering highest activity for all enzymes applied in that particular reaction was chosen. Digestions were incubated at 37°C for 1-12 hours. For separation of digestion products, agarose gel electrophoresis and purification by gel extraction was performed.

Analytical restriction enzyme digest was used to check the correct integration of an insert into a plasmid. To this end, 1 to 5 µl of plasmid DNA obtained from mini prep plasmid purification were digested in a total reaction volume of 10 µl. One or more restriction enzymes were chosen for digestion to yield DNA fragments with construct specifics length. Appropriate reaction buffers were used and reactions were incubated at 37°C for 15 minutes to 2 hours. For separation of digestion products, agarose gel electrophoresis was performed.

4.2.8 Ligation of DNA fragments

For ligation reaction T4 DNA ligase was used (NEB). The ligase catalyzes the ATP dependent formation of a phosphodiester bond between a 5' phosphate and 3' hydroxyl terminus in double stranded DNA with cohesive or blunt ends.

For ligation of insert and plasmid DNA an at least five fold molar excess of insert compared to vector DNA was used in presence of 400 units of T4 DNA ligase in appropriate buffer. Ligation reactions were usually incubated for one hour at room temperature or over night at 16°C. Ligation samples were subsequently used to transform chemically competent *E.coli* via heat-shock as described beneath.

4.2.9 SDS-polyacrylamide gelelectrophoresis analysis (SDS-PAGE)

For protein separation sodium dodecyl sulfate (SDS)-polyacrylamide gel electrophoresis (SDS-PAGE) was performed [160]. The anionic detergent SDS denatures proteins and applies a negative charge to each protein in proportion to its mass. When subjected to gel electrophoresis the distance of migration through the gel correlates directly to the size of the protein.

Whole-cell protein fractions for SDS-PAGE and Western blot analysis were prepared from standard cell cultures by harvesting cells in appropriate density by centrifugation (2 min, 16000 g, 4°C) after scraping in PBS. Supernatant was discarded and cell pellet was resuspended in 1x sample loading buffer (1x SLB, Fermentas) and heated 5 min at 95°C for denaturation.

When proteins were separated, intended for following Western blot analysis, samples were usually separated by 12% SDS-PAGE into Electrophoresis System Mini (Biorad), according to the manufacturer's instructions.

Table 4.10: *Composition of a 12% SDS-PAGE gel and SDS-PAGE running buffer.*

Separation gel (12%):	3.75 ml separation gel buffer (1 M Tris-HCl [pH 8.8])
	3 ml Acrylamide mix (37.5 : 1 Acrylamide/Bisacrylamide)
	3.25 ml H_2O, 100 µl 10% SDS, 7.5 µl Temed, 75 µl APS
Stacking gel:	1.25 ml stacking gel buffer (1 M Tris-HCl [pH 6.8])
	1 ml Acrylamide mix (37.5 : 1 Acrylamide/Bisacrylamide)
	7 ml H_2O, 100 µl 10% SDS, 15 µl Temed, 150 µl APS
Running buffer (1 x):	25 mM Tris, 192 mM Glycine, 0.1 % SDS

4.2.10 Western blot analysis

For Western blotting nitrocellulose membranes (Whatman) were used and preincubated in transfer buffer (5 min; 25 mM Tris, 192 mM Glycine, 20% Methanol, pH 8.3). Gels were blotted for 2 h at 2 mA/cm^2 and 4°C in a semi-dry electroblotter (Peqlab), onto the PVDF membranes in transfer buffer. After blotting membranes were blocked for 1 h in 10% dry milk in TBST$_{20}$ (TBST$_{20}$: 20 mM Tris, 150 mM NaCl, 0.1% Tween 20) at room temperature or over night at 4°C. Blocking was followed by incubation with the primary antibody for 1 h at room temperature under agitation. Membranes were washed 3 x 10 min in TBST$_{20}$ and incubated with the secondary antibody for 1 h at room temperature and washed again 3 x 10 min in TBST$_{20}$. Blots were developed using Western Lightning Reagent (Perkin Elmer)

and signals detected with a Biorad Chemidoc MP camera and band intensities were quantified were appropriate using Image Lad software (Biorad, München).

All antibodies used in this study are listed in Table 4.6. When the antibody was directly conjugated to horse-radish peroxidase (HRP), no incubation with a secondary antibody was required.

4.2.11 Capillary gel electrophoresis

For analysis of monoclonal antibody the chip based technology for capillary gel electrophoresis of Agilent Technologies (Santa Clara, CA, USA) was used. The conversion of the electrophoresis process to chip format reduced the separation time of proteins and the required reagent or sample volume. For antibody quality analyses a "Protein 230 Chip" was used, which allowed separation of proteins up to a molecular weight of 230 kDa. One of those chips accommodated 10 spaces, whereof 1 was used for the external standard marker with known molecular weight fragments and 9 were available for samples. The chip was prepared by inserting a polymer mixed with a fluorescing dye. To this end, 25 µl dye concentrate was pipetted into a tube containing 650 µl gel matrix, mixed immediately and centrifuged for 15 s. The solution was processed by centrifugation for 15 min at 2500 g via a spin filter tube and stored at 4 °C. The chip was placed in the "chip-priming-station" and dye-matrix solution was filled by syringe in the wells following manufacturer's instructions. Remaining gel-dye mix was removed from well surface. Antibody samples were prepared by mixing 4 µl antibody in PBS with 2 µl reducing loading dye (loading dye containing 35 mM DTT) and mixed immediately and centrifuged down. Sample-dye mixture and the ladder were heated for 5 min to 95-100°C and centrifuged again. Then 84 µl deionized water was added to every sample. 6 µl sample or ladder was inserted into the corresponding well, when less than 10 samples were analyzed, remaining wells were filled with a replica-solution. The chip was shaken for 60 s on a vortex (Ikamap) at 1000 rpm, adapted onto a cartridge with electrode pins fitting exactly in each well of the chip. Analyzes were started via "Bioanalyzer Software" (Agilent Technologies) as described in the manual. Protein /SDS molecules were separated by molecular weight electrophoretically in a currency gradient while passing through the net like polymer matrix. This resulted in a quicker movement of small fragments than larger ones and time of migration was correlated to size. The fluorescent labeled molecule, included in the loading dye, intercalate into protein/SDS micelles. Thus fragments were detected by laser initiated fluorescence. Data were converted into density plots resulting in gel-like pictures. Size information was provided automatically in a digital format by comparing internal marker fragments in each sample (240, 7.0 and 4.5 kDa) to an external standard with known molecular weight fragments, loaded onto the same chip.

4.2.12 Transformation

For transformation of plasmid DNA in *E.coli*, CaCl$_2$ competent bacteria from strain *DH5α* (Life Technologies) were used. Typically 5 µl DNA either from ligation reactions or plasmids was added to 50 µl competent bacteria and chilled on ice for at least 15 minutes. Afterwards cells were heated to 42 °C for 45 sec and cooled on ice immediately for 2 min. 300 µl SOC media was added and transformed bacteria were grown for 1h at 37°C, 220 rpm in a shaking incubator. After recovery cells were spread on LB-agar plates with appropriate antibiotics and grown over night at 37°C.

4.2.13 Preparation of chemically competent *E.coli* cells

50 ml LB-media was inoculated with around 10 colonies of freshly spread and overnight grown appropriate *E.coli* strain and incubated for 14 to 18 hours at 37°C. Subsequently 100 ml LB-media was inoculated with 1 ml over night culture and cultivated until a OD$_{600}$ of 0.5 to 0.6 was reached. The flask was cooled down quickly on ice for 10 minutes, followed by a centrifugation (10 min, 2500 x g, 4°C). The resulting pellet was resuspended slightly in ice-cold transformation buffer 1 (100 mM RbCl, 50 mM MnCl$_2$, 30 mM Potassiumacetate, 10 mM CaCl$_2$, 15% Glycerol, pH 5.8) and incubated on ice for 90 minutes. After centrifugation (10 min, 2500 x g, 4°C) pellet was resuspended in 4 ml ice-cold transformation buffer 2 (10 mM MOPS, 10 mM RbCl, 75 mM CaCl$_2$, 15% Glycerol, pH 6.8 with KOH). Finally cells were aliquoted to 100 µl in sterile 1.5 ml reaction tubes and directly frozen in liquid nitrogen and stored at -80°C.

Transfection efficiency was determined by a transformation with 1 µl pUC18 plasmid DNA with a stock concentration of 0.1 ng/µl. Transformation was carried out as described in 4.2.11. 5 µl of transformed cells were diluted in 100 µl LB-media and plated on a LB-agar plate containing 100 µg/ml ampicillin as selection antibiotic and incubated overnight at 37°C. 50 colonies on the plate equal a transfection efficiency of 1 x 10^8 cfu/µg DNA.

4.2.14 Preparation of recombinant bacmid DNA

The Baculovirus expression system in insect cells relies on the generation of recombinant baculovirus by site-specific transposition in *E.coli*. A recombinant donor plasmid was generated carrying the sequence for the extracellular domain of the IGF1R connected to a C-terminal 2B5 peptide, named pFastBac1-IGF1R(ED)-2B5. The vector was transformed in DH10Bac competent *E.coli*. This strain contained a parental bacmid with a *lacZ*-mini-*att*Tn7 fusion, which allows the integration of the recombinant plasmid DNA via its Tn7 transposition sites, harboring the sequence of the recombinant protein and a gentamicin resistance gene as well. Transposition occurred between the Tn7 elements of the pFastBac1 vector and the Tn7 transposition cassette of the parental plasmid in the presence of the transposition proteins provided by a helper plasmid. After successful

transposition, the expression cassette disrupted the *lacZ* gene and easy visualization of positive colonies was possible by X-gal blue/white screening. The new expression bacmid was carried by the white colonies. Subsequent to verification of positive clones by colony PCR, a mini-prep of high molecular weight DNA was performed (PureLink HiPure Plasmid DNA Miniprep Kit, Life Technologies) as described in the manual and led to a recombinant plasmid carrying the expression cassette with the IGF1R(ED)-2B5 DNA sequence.

4.2.15 X-gal blue/white selection

For identifying positive clones with integrated expression cassette in the pFastBac1 vector, X-gal blue/white selection was used. When an insert had been inserted into the MCS successfully, the β-galactosidase gene (*lacZ*) was disrupted. Thus X-gal could not be hydrolyzed and no intensively stained blue product was generated. For selection, transformations were spread on previously prepared LB-agar plates containing appropriate antibiotics, X-gal and IPTG. To this end, LB-agar plates with suitable antibiotics were spread evenly with 50 µl 20 mg/ml X-gal solution in DMF and 25 µl 100 mM IPTG. Plates were incubated at 37°C for at least 20 minutes to allow the organic toxic solvent to evaporate before plating out the transformation. White colonies contained plasmids with an insert in the plasmids MCS, blue colonies should not contain any inserts as their reading frames were not interrupted.

4.2.16 Isolation of human immunoglobulins

Human serum (1 ml) was diluted with PBS (1 ml) and incubated overnight at 4°C with 0.2 ml of protein G-sepharose known to preferentially bind and purify immunoglobulins (Ig) of the IgG class. Complexes were pelleted and washed ten times with 1 ml PBS. Bound Ig were eluted with 200 µl 25 mM citric acid (pH 3.0), and pH was adjusted to 7.0 using 1 M Hepes-NaOH, pH 8.0. Eluted Ig were concentrated to 100 µl (~ 10 mg/ml) using Speedvac at room temperature. Protein was transferred into DMEM/F12 using gel filtration on sephadex G25.

4.2.17 Mouse antibody isotyping

Isotyping of purified antibodies from hybridoma cell culture supernatant was performed by "Mouse monoclonal isotyping kit" (AbD Serotec, Düsseldorf, Germany). The assay principle was based on anti-mouse kappa fragment and anti-mouse lambda fragment antibodies coupled onto colored micro particles on a test stripe. Those were equally reactive to any mouse monoclonal antibody regardless of its isotype. Bands of goat anti-mouse antibodies were immobilized on the strip corresponding to each of the common mouse antibody isotypes (IgG1, IgG2a, IgG2b, IgG3, IgM, and IgA) and to the kappa and lambda light chains. By using these two components, a mouse monoclonal antibody could be screened for isotype by simply diluting the antibody sample to a concentration of 1.0

µg/ml in PBS (pH 7.4) containing 1% w/v BSA, pipetting the diluted sample into the development tube, where it formed a complex with the antibody coated micro particles, and inserting the strip. This complex flowed through the strip until it was bound by the immobilized goat anti-mouse antibody specific for the monoclonal's isotype and its light chain. In approximately 5-10 minutes, the micro particle complexes aggregate as two blue bands in the two sections corresponding to the monoclonal antibodies isotype and its light chain characteristics, respectively.

4.3 Cell culture

4.3.1 Eukaryotic cell lines

Table with strains and corresponding stable expressed protein.

4.11: *Cell lines used in this study.*

Name	Trivial name in this study	Description
High Five	High Five	Insect cell line for protein expression with baculovirus system
Human Embryonic Kidney 293 cells	HEK293	Standard human lab cell line for recombinant protein expression
MCF-7	MCF-7	Breast-cancer cell line; standard cell line for analyses of effects on cell growth and/or proliferation
Sf9	Sf9	Insect cell line for protein expression and generation of baculoviruses

4.12: *Genetically modified stable HEK293 cell lines for recombinant protein expression used in this study.*

Name	Recombinant protein	Stable integrated plasmid
IGF1R(-TK)-2B5	IGF1R, deleted tyrosine kinase domain, 2B5-tag	pIRESneo-IGF1R(-TK)-2B5
IGF1R(-TK)-PGA	IGF1R, deleted tyrosine kinase domain, PGA-tag	pIRESneo-IGF1R(-TK)-PGA
IGF1R-Luc	IGF1R luciferase-fusion	pIRESneo-IGF1R-luc
IGF1R-luc-E1	fragment IGF1R – aa 31 – 273	pIRESneo-IGF1R-luc-E1
IGF1R-luc-E2	fragment IGF1R – aa 264 – 506	pIRESneo-IGF1R-luc-E2
IGF1R-luc-E3	fragment IGF1R – aa 497 – 737	pIRESneo-IGF1R-luc-E3
IGF1R-luc-E4	fragment IGF1R – aa 738 – 938	pIRESneo-IGF1R-luc-E4
IGF1R-PGA	IGF1R full-length, PGA-tag	pIRESneo-IGF1R-PGA14
IGF2R-Luc	IGF2R luciferase-fusion	pIRESneo-IGF2R-luc
IR-2B5	IR, deleted tyrosine kinase domain, 2B5-tag	pIRESneo-IR(-TK)-2B5
IR-Luc	IR luciferase-fusion	pIRESneo-IR-luc

The procedure of cell line generation is described in more detail in section 4.3.7. The register does not include insect cell lines yielded after baculovirus infection or bacmid transfection, because viral or bacterial gene fragments were only inserted transiently for ensuring the desired gene expression.

4.3.2 Media and growth conditions of eukaryotic cells

HEK293 cells were cultivated in a humidified incubator at 37°C with 5% CO_2. Insect cells were cultivated in a not humidified incubator at 27°C without CO_2 regulation. Cell culture media were completed with appropriate supplements for cultivation. All centrifugation steps of cell in culture were carried out at 65 to 200 x g.

Table 4.13: *Cell culture media and supplements.*

Medium / Supplement	Description	Supplier
ISF1	culture and production medium for adherent and suspension HEK293 cells	PAA
RPMI 1640	culture medium for HEK293 suspension cells	PAA
Express Five SFM	culture and production medium for High Five insect cells	Life Techn.
Sf900 II SFM	culture medium for Sf9 insect cells	Life Techn.
Glutamin	supplement for cell culture media	diverse
FBS	supplement for cell culture media	diverse
G418	selection antibiotic for cells carrying a neomycin resistance gene	diverse
Penicillin / Streptomycin	antibiotic to prevent bacterial contamination in cell culture	diverse
Grace's Insect Cell Medium	Transfection medium for insect cells	Life Techn.
DMEM / Ham´s F12 (1:1)	culture medium for adherent HEK293 cells	Biochrom

4.3.3 Culture of adherent cells

Cells were routinely cultivated adherent on cell culture T-flasks or well plates with appropriate surface area in a humidified incubator at 37°C with 5% CO_2. Usually used medium for culture of adherent cells was DMEM / Ham´s F12 supplemented with 2 mM Glutamine, 10% FCS and 1% Penicillin / Streptomycin. Where needed Geneticin (G418) was used as selection antibiotic in a concentration range from 0.2 to 0.8 mg/ml, originating from a 20 mg/ml stock solution. Confluent cultures were split every 2 to 3 days. To this end, cells were washed with PBS (no Mg^{2+}, no Ca^{2+}; Life Technologies) and dissociated using trypsin / EDTA solution (0.05% / 0.75 mM, in PBS, without $Ca^{2+}$and Mg^{2+}; PAA, Cölbe) by a 2 to 5 minute incubation step. Reaction was stopped by adding FCS-containing medium and a suitable dilution of cell suspension was prepared. Cell counts and viability were routinely determined by trypan blue exclusion method [161] in a Hemocytometer (Neubauer cell counting chamber, Roth).

4.3.4 Adaptation to suspension culture

A promising strategy to improve yield to volume ratio in a reliable and practicable system, volumetric upscale of the culture is the system of choice. An adherent cell clone in culture, stably expressing recombinant proteins, has to be adapted to suspension culture before up-scaling. Thus, a specialized medium composition was required. To assure a suitable suspension culture with ideally single cell suspension, FCS had to be depreciated, because it promotes cell-to-surface and cell-to-cell adhesion. There are two possibilities to do so. On the one hand a direct medium change could be performed, on the other hand a sequential adaptation with successively reduction of FCS containing medium could be prepared. A second issue are Calcium ions as they stabilize cell-to-cell adhesion, thus necessitating another medium matrix. Media for culture of suspension cells are commercially available, and a proprietary self-developed in-house medium of the cooperation partner InVivo Biotech Services (Hennigsdorf) was used in this study, which is based on RMPI1640. When adapted sequentially, adherent cells were expanded to a T-150 cell culture flask until a viability of >90% was ensured. For the first adaption step, the conditioned standard culture medium of a T-150 flask with 50% confluence of adherent cells was decanted. Subsequently a medium mixture of 75% standard culture medium and 25% medium for suspension cells, where cells should have been adapted to, was added to 100 ml. Cells were grown in this medium mixture until an acceptable growth rate with a good viability was ensured. After 2 to 3 passages the next adaptation step was performed with a confluence around 50% using a medium mixture of 50% standard culture medium and 50% adaptation medium. Next adaptation step follows as described before but with a medium mixture of 25% standard culture medium and 75% adaptation medium. Most cells detached from the bottom of the flask in this adaptation step and grew in suspension. Finally the adaptation step with using 100% serum free medium for suspension culture follows. Adaptation was completed when cells show a regular growth rate with a viability >90% under serum-free conditions.

To speed up the adaptation process, a direct adaptation was performed. To this end a nearly confluent T-150 flask with adherent cells with a viability >90% was trypsinized and the cell pellet was resuspended directly into serum-free medium for suspension culture and cells were refilled in the flask. Growth rate was usually impaired for several passages associated with a dropped viability below 40% when cells were transferred directly to serum free medium. Adaptation was completed when cells showed a regular growth rate with a viability >90%.

4.3.5 Large scale recombinant protein production

After cells have been adapted successfully to serum-free media and suspension culture, an appropriate volume of cell suspension was used to inoculate a 1 liter super spinner flask (Sartorius, Göttingen) with bubble-free gas entry via a tube-like Accurel membrane (Sartorius), wound around the vertical magnet styrer, which is connected to the spinner's top lid. Two T-150 flasks with 150 ml cell suspension each were used to inoculate a spinner with 1 liter capacity to 600 ml filling volume. The spinner was filled successively with serum-free medium for suspension cells to its filling volume. When cell density reached 2 to 3 x 10^6 cells per ml, 800 ml cell suspension was harvested and the spinner was filled up to 1 liter again. When cell culture with a 2 liter spinner was performed, inoculation amount of cell culture was risen to four T-150 flasks with 150 ml cell suspension each, in an inoculation volume of 1.0 to 1.2 liter. Cultivation process was upscaled analogous to the 1.0 liter spinner system.

4.3.6 Hybridoma cell culture and upscale for antibody production

Hybridoma cells were cultivated in RPMI 1640 medium, including 10% FCS and 400 µg/ml G418. Cryo conserved clones obtained from Unicus were revitalized in T-25 flasks in the same medium with supplements for a time period of 7 to 10 days. During the following cultivation, medium was switched constantly to ISF1 with the same supplements. Culture volume was expanded up to three T-150 flasks, in which FCS concentration was decreased continuously during the routine cell-splitting procedures. Cells detached from the plastic surface and went into suspension. Culture volume was increased to 150 - 200 ml in every T-150 flask. Next, a 2.0 L superspinner system was inoculated with at least two T-150 flasks (depending on cell density). When a 1.0 L superspinner was used, inoculation volume was cut in half. Culture was performed for 10 – 14 days in batch format, followed by harvest of the cell culture supernatant using a centrifuge at >3000 g for 10 minutes.

4.3.7 Generation of stable cell lines

HEK293 cells were grown in DMEM / Ham´s F12 supplemented with10% fetal bovine serum and transfected with the appropriate pIRESneo plasmids using FuGENE6 reagent (Promega) according to the manufacturer's instructions. The pIRESneo plasmid carried the neomycin phosphotransferase (NPT II) gene. The antibiotic G418 exerts selective pressure on the whole expression cassette; thus, a high dose of antibiotic will select only cells expressing a high level of the gene of interest [162]. This selective pressure also ensures that the expression of the gene of interest will be stable over time in culture. Forty-eight hours after transfection, selection of stable transfectants was started by adding 0.8 mg/mL G418. Remaining cells were separated by limited dilution in two 12-well plates

7 to 14 days following addition of selection antibiotic. Stable clones were transferred to appropriate culture size vessels while expanding the culture volumes and cryo conservations were stocked. Clones expressing high levels of recombinant protein were selected and expanded for protein production. Stable HEK293-IGF1R-Luc cell clones were functionally analyzed by measuring total luciferase activity, stable HEK293-IGF1R peptide-tagged cell clones were functionally analyzed for binding of labeled IGF1. To ensure a truly stable expression of the integrated gene, re-clones of the selected stable clones may be prepared. In this case, a cell culture of the chosen clone was limited diluted in two 12-well plates, separate clones were picked and expanded and analyzed as described before.

4.3.8 Cryo conservation and revitalization

Eukaryotic cells were deep-frozen to save the stable gene expressing cell lines on the one hand and to replenish the stock of cells to be worked with on the other hand. During the freezing procedure, cells were exposed to an enriched osmotic pressure of the extracellular liquid, because ice crystals built up first outside the cells. In case too much water stayed inside the cell, ice crystals destroy its structure mechanically. To minimize this effect, cells were mixed with DMSO as anti-freezing agent which narrows the freezing point. When entering the cell, DMSO leads to a slightly dehydration and decreases the osmotic pressure on the cell wall.

Usually adherent growing cells with a vitality of at least 80% were used, which were in the exponential growing phase. Prior to conservation cells were detached with trypsin / EDTA treatment (see 4.3.2) and cell density was determined. Following centrifugation, cells were resuspended in pre-cooled freezing medium (2-8°C) containing 50% culture medium, 40% FCS and 10% DMSO to reach a cell density of 10^6 to 10^7 cells per ml. Equilibration time of DMSO into the cells should not exceed 15 minutes, because it shows cytotoxic effects especially at room temperature. Cell suspension was distributed in cryo vials, suitable for storage in liquid nitrogen. Cells were frosted in a 2-8°C pre-cooled thermo-container filled with isopropanol, which ensures a constant defrosting rate of -1°C per minute when stored at <-60°C. Cryo vials were stored short term at -80°C. For long term storage vials were transferred to liquid nitrogen earliest 48 hours after being put at -80°C. Storage took place in liquid nitrogen at -196°C or in its gas phase at -156°C.

For revitalization of cells from cryo vials a suitable culture vessel was chosen depending on number of cells available in the cryo vial and proliferation rate of the cell line. The cryo vial was quickly removed from the freezer or liquid nitrogen tank and incubated in a 37°C water bath until it was defrosted except for a small chunk of ice. The vials content was transferred into a 10 ml aliquot of a pre-cooled (2-8°C) aliquot of an appropriate culture

medium. This diluted cell suspension was centrifuged at 100 x g for 5 to 10 minutes. The supernatant was decanted and the resulting pellet was resuspended in pre-warmed culture medium and finally transferred into the chosen culture vessel.

4.3.9 Generation of recombinant baculovirus particles

Sf9 insect cells were transfected with isolated recombinant bacmid DNA (0) containing the expression cassette with the IGF1R(ED)-2B5 DNA sequence. To this end, a culture of Sf9 cells was expanded accordingly. Cells had a viability greater than 95% and were growing in the logarithmic phase with a density of 1.5×10^6 to 2.5×10^6 cells/ml before proceeding to transfection. Seeding proceeded by placing 6×10^5 cells in 2 ml un-supplemented Grace's insect cell medium into 6-well cavities. Cells were allowed to attach for 15 minutes at room temperature in the hood. Per well 8 µl Cellfectin transfection reagent was diluted in 100 µl un-supplemented Grace's insect cell medium. 1 µl of appropriate baculovirus DNA was also diluted in 100 µl un-supplemented Grace's insect cell medium. Dilutions of transfection reagent and DNA were combined, mixed gently and incubated for 30 minutes at room temperature. The mixture was added dropwise into the well with arranged cells and incubated for 4 hours at 27°C. Transfection mixture was removed and replaced by 2 ml of fully supplemented growth medium. 48 to 72 hours post transfection, cells typically display characteristics of virally infected cells. Cell growth appeared to stop and cells detached from the bottom as well and first signs of cell lysis appeared.

For preparation of the P1 viral stock, the culture medium containing the virus was collected when signs of late stage viral infection appeared, but after at least 72 hours post transfection. The medium was cleared by centrifugation to remove cells and large debris. The clarified supernatant was named to be the "P1 viral stock" and was stored at 4°C. The P1 baculoviral stock was amplified by infecting a 10 ml suspension culture at 2×10^6 cells/ml of Sf9 cells with 0.5 ml of P1 stock to prepare a high titer P2 viral stock. Cells had a viability greater than 95% and were growing in the logarithmic phase. Medium was collected 48 hours post infection and the clarified supernatant was named to be the "P2 viral stock" and was stored at 4°C.

4.3.10 Infection and transient gene expression with baculovirus

High Five insect cells were cultivated in serum free Express Five SFM medium. The culture to be infected was at mid-logarithmic phase of growth at a cell density of 1×10^6 to 2×10^6 c/ml. Suspension cultures of 100 ml were infected with recombinant baculovirus particles contained in 0.5 ml from viral stock P2 (4.3.9), which included the expression cassette with the IGF1R(ED)-2B5 DNA sequence in its viral DNA. Infected cells were cultivated for additional 3 days and conditioned medium, containing the secreted recombinant IGF1R(ED)-2B5 protein, was collected by centrifugation and stored at -80°C.

4.3.11 Preparation of cell extract

In order to work with the recombinant receptors *in vitro,* an extraction of the stably expressed membrane bound proteins or of their genetically modified variants was needed. To this end, cell pellets originating from culture of cell lines stably expressing the desired recombinant receptor of fragment were collected and stored at -80°C. In the case of luciferase receptor fusions, 1 gram pellet was resuspended with 10 ml extraction buffer. When peptide tagged receptors were extracted, 3 ml of extraction buffer was used per gram pellet weight. During the whole procedure samples and reagents were kept on ice, and centrifugation steps were carried out at 4°C. Pellet suspensions were homogenized by pipetting up and down and by mechanical mixing. 20% Triton-X-100 was added to 2% final concentration and incubated for 15 minutes. The suspension was pushed through a syringe with a 25g x 1" needle for three times, followed by a centrifugation step for 15 minutes at no less than 3000 x g. The supernatant was distributed in adequate volumes and stored at -80°C.

4.3.12 Generation of monoclonal antibodies to IGF1R

Monoclonal antibodies against the IGF1R were generated by genetic immunization of mice [163, 164]. As an encouraging positive literature example, TSHR antibodies had been generated by this method successfully [165]. The genetic immunization of two mice was conducted by the cooperation partner Unicus Karlsburg OHG (Karlsburg, Germany) using the pIRESneo-IGF1R-2B5 plasmid described above.

4.3.13 Purification of monoclonal antibodies to IGF1R

Volume of hybridoma cell cultures to produce monoclonal antibodies generally started from around 1.8 L cell culture supernatant. The cell culture supernatant was directly handed to an Äkta Explorer chromatography working station (GE Healthcare, Freiburg) connected to a chromatography column with a column volume (CVol) of 100 ml. Column was filled with 97 ml POROS A50 Protein-A resin (Applied biosystems / Life technologies) in storage buffer (200 mM Na-phosphate-buffer, pH 7.3). The column was equilibrated with 1/3 CVol washing buffer (200 mM NaPP-buffer, pH 7.3), because it was identical to the actual storage buffer. Approximately 1.8 L cell culture supernatant, originating from hybridoma cell culture producing the antibody in a 2.0 L seized superspinner, was applied onto the column. The system was washed with 5.7 CVol washing buffer. The elution step with 2 CVol elution buffer (0.1 M citric acid, pH 2.0) followed, when a distinct ground line separation was assured. The antibody was eluted into preliminary presented neutralization buffer (1 M K_3PO_4, pH 8.0) in a 4-time excess to neutralize pH of the eluted antibody elution. Following elution, the chromatography column was re-equilibrated with 1.5 CVol washing buffer. The solution containing the purified monoclonal antibodies was

dialyzed for 2 days in PBS (150 mM, pH 7.4) in at least 50x (v/v) dialyses volume. Protein content of samples was determined prior and after dialyses by UV-spectroscopy at a wavelength of 280 nm. When precipitates were observed during dialyses, the solution was centrifuged before protein determination. A sterile filtration using 0.2 μm syringe attachment filters (Sartorius, Göttingen) was performed routinely.

4.3.14 Preparation of cell fractions

Wild type HEK293 cells and HEK293-IGF1R-luc cells were grown to confluency in T-75 flasks. Cells were harvested by scraping into PBS, collected by centrifugation at 800 x g and resuspended in 0.5 ml buffer containing 20 mM HEPES-NaOH (pH 7.5), 50 mM NaCl, 10% glycerol and protease inhibitors. The suspensions were homogenized at 4°C by 20 strokes in a glass/ teflon homogenizer and then centrifuged for 15 min at 800 x g, and for 90 min at 70,000 x g minimum. The supernatant (cytoplasmic fraction) was collected, and the pellet (membrane fraction) was resuspended in the same buffer containing 1% triton X-100. Samples from both fractions were measured in a luminometer (Berthold, Bad Wildbad, Germany) for 10 sec, and subjected to electrophoresis in 10% SDS PAGE and transferred to nitrocellulose membranes as well. Membranes were probed overnight at 4°C with anti-luciferase antibody (Promega, Madison, U.S.A.) to detect IGF1R-Luc fusion protein. Bands were visualized using enhanced chemiluminescence Western blotting detection kit (Pierce, Rockford, UK).

4.3.15 Interaction of IGF1R-Luc cells with IGF1

IGF1 was labeled by acridinium NHS ester according to the manufacturer's instructions (Cayman) yielding a preparation of acridinium ester-labeled IGF1 (10^8 RLU/μg IGF1). Confluent cells grown in a 96 well plate were washed with DMEM/F12 medium and incubated for 1 h at 4°C or 37°C with labeled IGF1 (~10^6 RLU/well) diluted in 100 μl of DMEM/F12, 0.1% BSA. Unlabeled IGF1 (0.3 mg/ml) was added together with labeled hormone to test for unspecific binding. Cells were washed with DMEM after incubation, resuspended in PBS containing 2% triton X-100 and lysates were measured in a luminometer (Berthold, Bad Wildbad, Germany) for 10 sec.

4.3.16 Effect of autoantibodies on IGF1R autophosphorylation

Human hepatocellular liver carcinoma cells (HepG2 cells) endogenously expressing human IGF1R were seeded in 96 well plates (10,000 cells/well). Cells were incubated for 24 h in complete DMEM/F12 medium followed by overnight incubation in serum-free DMEM/F12 containing 0.1% BSA. After serum starvation cells were incubated with human Ig (~10 mg/ml) in DMEM/F12 for 15 min to 1h. IGF1 (1 ng/ml) was added or not and cells were incubated for an additional 15 min. Cells were washed with PBS containing phosphatase inhibitors and lysed in buffer (20 mM HEPES-NaOH pH 7.5, 50 mM NaCl,

2% triton-X-100, 10% glycerol, and 1 x phosphatase inhibitor cocktail, Sigma). Cell lysates were analysed by 10% SDS PAGE and blotted onto nitrocellulose membranes. Phosphorylated IGF1R was detected using an anti-IGF1R (Tyr1165/Tyr1166) antibody, which detected directly phosphorylated tyrosine residues in the IGF1R-cytoplasmic domain.

4.3.17 Effect of autoantibodies on cell growth

Human breast adenocarcinoma cells (MCF7 cells) were seeded at 2,500 per well and incubated overnight in complete DMEM/F12 medium. Cells were starved in serum free DMEM/F12 medium containing 0.1% BSA for 5 h followed by addition of 1% serum, 1 ng/ml IGF1 and Ig preparations (~10 mg/ml) isolated from IGF1R-Ab positive or negative serum samples. Cells were incubated for 5 days. The CellTiter-Glo luminescent cell viability kit was used to assess number of viable cells in culture based on quantification of ATP concentrations, according to the manufacturer's instructions. Inhibiting effect of autoantibodies was expressed as Inhibition Index calculated as InI [%] = 100 x [1 − (RLU test Ig) / (RLU negative Ig pool)].

4.4 Human samples

Studies with human samples described in this study have been conducted in according to the principles expressed in the Declaration of Helsinki [166]. The required ethical approvals have been obtained from Essen University (No. 02-1860) and Charité - Universitätsmedizin Berlin (No. EA2/103/10 and no. EA2/132/11), respectively. Written informed consent had been obtained from all participants prior to be included into the analyses. Samples have been analyzed blinded as to the clinical characteristics of the donors.

4.5 Statistical analyses

Experimental analyses were performed in triplicates, wherever possible. Due to sample limitation, especially regarding human serum sample, several experiments were performed in single or double determination. In these cases results were verified at a later date. Number of determinations and of replicated experiments is stated in the figure legend.

Significant differences between two data sets were analyzed with t-test or ANOVA analyses as appropriate. Results are designated as "statistically significant" if their error probability is less than 5%, which means a p-value of 0.05. IGF1R-Ab determination in large numbered human sample collectives was performed in single determination due to very stringent sample limitation. At that point of time, the assay system was characterized very well and reproducibility of results was accepted.

5 Results

5.1 Installation of a novel IGF1R-autoantibody precipitation assay

5.1.1 Schematic presentation of the principle

One of the important input requirements for the antigen specific autoantibody detection assay was to yield a non-radioactive assay. Thus recombinantly-expressed autoantigen, in the present study the IGF1R, was N-terminally fused to a luciferase reporter protein (Figure 5.1). Cell extracts of IGF1R-Luc fusion proteins were prepared. If the extract was combined and incubated in a reaction tube with a sample containing antibodies against the antigen, an antibody-antigen reaction takes place. The antigen-antibody complex was bound and precipitated by a protein-A matrix. Unbound components were removed, and nonspecific binding was reduced by repeated washing and centrifugation steps. The precipitate obtained was detected by a CT luminometer using a luciferase-specific substrate. The relative light units (RLU) obtained were directly proportional to the concentration of aAb in the sample.
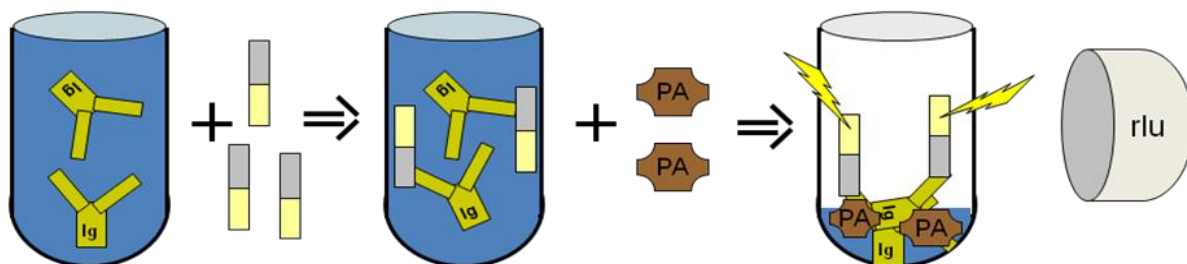
Figure 5.1: *Schematic depiction of the diagnostic aAb assay system using or IGF1R-Luciferase fusion protein as specific autoantigen. Cell extracts of IGF1R-Luc fusion proteins (grey-yellowish rectangle) are prepared and after incubation with a sample containing antibodies (Ig) against IGF1R, an antibody-antigen reaction takes place. The antigen-antibody complex is bound and precipitated by a protein-A matrix (PA). Unbound components are removed and nonspecific binding is reduced by repeated washing and centrifugation. The precipitate obtained is detected by a CT luminometer using a luciferase-specific substrate, yielding relative light units (rlu).*

For reasons of uniformity, it was decided to annotate the assay for detection of IGF1R-aAb "IGF1R-Ab precipitation assay", because the detection of IGF1R-Ab is independent of the antigens origin, which led to immunization initially. It will be discriminated between Ab and aAb in the following text were appropriate.

5.1.2   Expression of recombinant proteins in HEK293 cells

Most of the recombinant proteins used in this study were generated by stable gene integration in a parental HEK293 wild type cell line (see Figure 5.2 and material and methods in 4.3.1). Hereby, a consistent protein expression system with sufficiently high yields could be established and ensures a reproducible assay production.
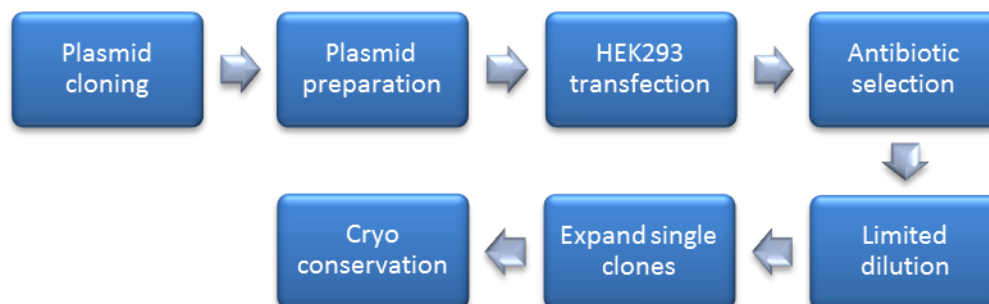

Figure 5.2: *Construction of a stable cell line. This flowchart represents the working steps for construction of a cell line stably expressing a recombinant protein. In short, the gene of interest is cloned into a mammalian expression vector also containing a resistance gene for antibiotic selection. HEK293 cells are transfected with the plasmid and selected by antibiotics. Single clones are generated by limited dilution and expanded independently, which are cryo conserved or checked for protein expression. The whole process needs four to eight month to completion.*

HEK293 cells usually grow adherent on flat surfaces in a monolayer structure. Cells are covered with an adequate volume of appropriate medium for optimal growth. For enabling a more effective large-scale production, stable gene expressing cell clones were adapted from adherent to suspension culture (see Figure 5.3 and material and methods in 4.3.4). To ensure gas exchange and optimal nutrient supply, an adequate mixing of the cell suspension was obligatory. As final adaption step cells were thus transferred into a superspinner culture system (Sartorius) for protein production (Figure 5.4). For a standard medium-scale cultivation process of a cell line stably expressing a recombinant receptor, and preparation of cell extract thereof, six T-Flasks with an area of 150 cm^2 each were used for adherent culture conditions. For a large-scale preparation in a serum-free suspension culture process, a superspinner culture system with 1.0 L working volume was used.
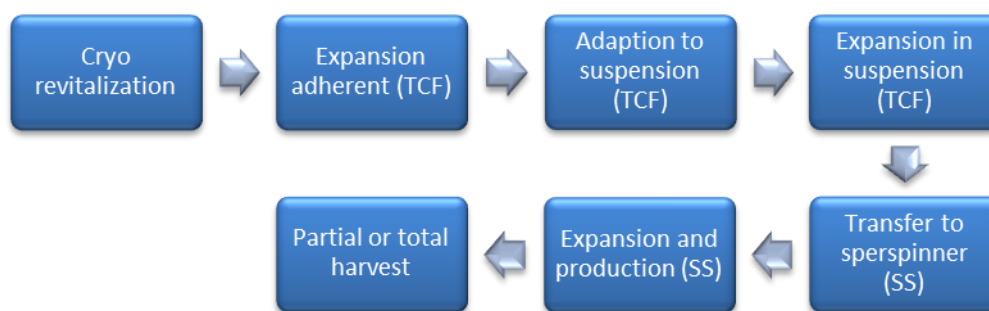
Figure 5.3: *Production process of recombinant IGF1R.* *This flowchart presents the production process of a stable cell line expressing recombinant IGF1R. In short, cells stably expressing the IGF1R are revitalized, cultivated and expanded in a tissue culture flask (TCF), growing in adherent manner (with 10% FCS media supplementation). Cells are adapted to serum-free media and growth in suspension followed by expansion in several TCF's. Suspension cells are transferred to a superspinner system (SS) and expanded to final spinner volume for production. Cells are harvested at high cell density, if nutrient limitation or decreased vitality is obtained. A partial harvest of the spinner volume may be appropriate if production should be maintained.*

Following the entire harvest of six T-Flasks, a pellet net weight of 1.2 g was yielded. When harvesting 1 L of suspension culture from the superspinner, 3.0 g pellet net weight was obtained (Table 5.1).

A

B
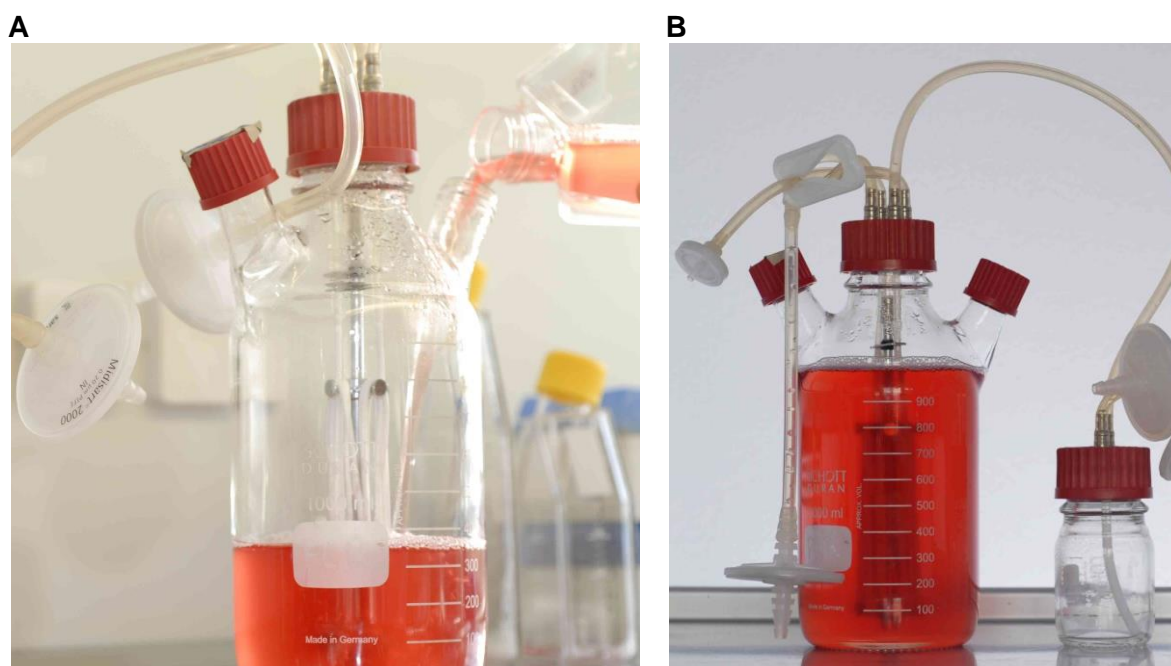
Figure 5.4: *Superspinner system for suspension culture.* *The system was available in sizes of 1.0 or 2.0 liter. After adaption of adherent cells to serum-free medium and suspension culture, cells were transferred into super spinner system. The tubular membrane for bubble free gas exchange was wounded around the vertical, rotatable stirrer and connected to the gas exchange system (air). Suspension was stirred when spinner was placed on a magnetic mixer inside the 37°C incubator.*

Table 5.1: *Comparison of adherent and suspension culture condition at stable gene expression of IGF1R-luc in HEK293 cells.*

Culture condition	System	Volume / Area	Quantity	Yield (entire harvest)
Adherent	T-Flask	150 cm^2	6	1.2 g
Suspension	Superspinner	1 L	1	3.0 g

The relative luciferase activity (RLU) of extracts from cells cultivated either adherent or in suspension were comparable, with a lower yield when cultivated under suspension conditions (Figure 5.5).

Figure 5.5: *Stable gene expression of IGF1R-luc in HEK293 cells. Comparison of cell extracts from adherent cultures and suspension cultures in a superspinner system. Relative luciferase activity was determined from 5 µl of a 1 to 10 diluted IGF1R-Luc cell extract using a luminometer (n=3, no significant difference was determined, p = 0.177; RLU, relative light units).*

For characterization of IGF1R-autoantibody interaction and continuative experiments, an IGF1R-fusion was engineered harborin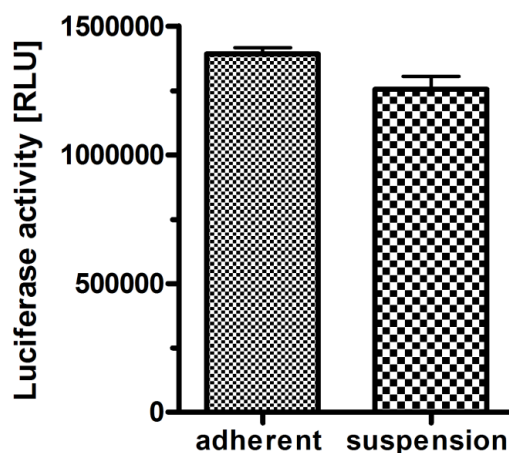g a peptide tag (PGA) at the C-terminus and was overexpressed in HEK293 cells. The procedure for expressing the construct was similar to the IGF1R-Luc fusion. To control its correct function and expression, 10 µl of a 1 to 3 diluted IGF1R-PGA cell extract were incubated in 200 µl assay buffer in anti-PGA peptide antibody coated tubes (ICI, Berlin) and binding capacity of acridinium labeled IGF1 as a tracer molecule to each coated tube was determined (Figure 5.6, column 1). The use of unlabeled IGF1 in wide excess (10 µg/ml) in the competition sample (column 2) resulted in a reduction of the signal by 89%, based on competition with acridinium labeled IGF1 with the hormone binding site of the receptor. When HEK293 wild type extract was used (column 3), only an artificial binding of the labeled hormone was possible, while no binding of labeled IGF1 occurred when using buffer instead of any cell extract (column 4). Stability of the tracer and longevity of the constructed assay was verified by letting sit tubes, containing samples identically to those presented in column 1, after last washing step for

60 minutes under not controlled conditions on the bench top (column 5). A slightly higher value for labeled hormone binding was observed in these samples.
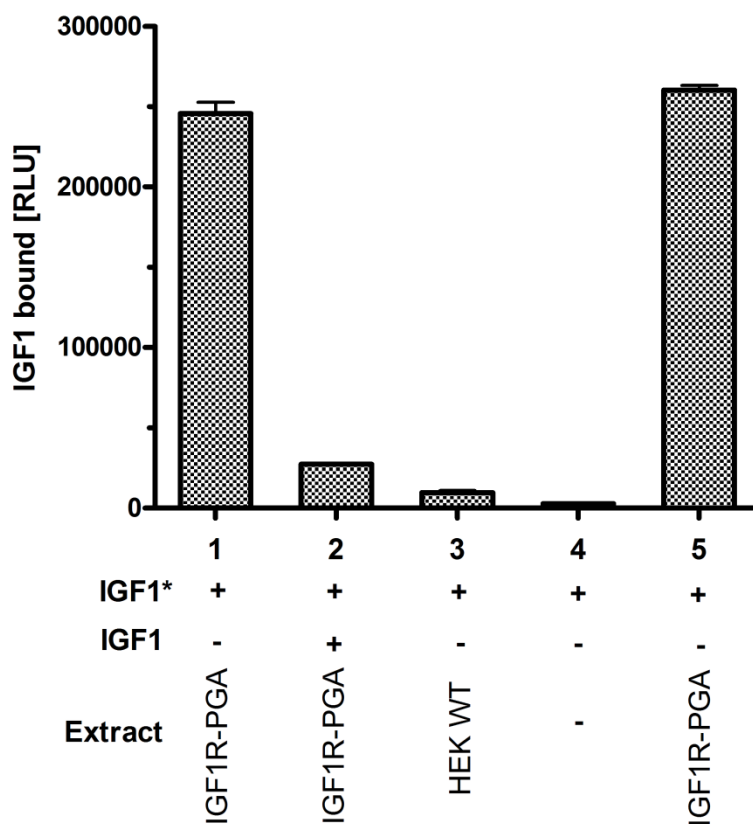
Figure 5.6: *Control of overexpression of IGF1R in HEK293 with a C-terminal peptide tag. 10 µl of a 1 to 3 diluted extract from IGF1R-PGA transfected cells (column 1,2 and 5) or wild type cells (column 3) were adjoined to anti-PGA peptide antibody coated tubes in 200 µl assay buffer and binding capacity of acridinium labeled IGF1 tracer (IGF1*) was determined. 10 µg/ml unlabeled IGF1 (IGF1) was used as competition control in one sample in single determination (column 2). In another sample, no extract was added, to exclude matrix binding of the tracer (column 4). Tracer stability and longevity of the constructed assay was proved by letting sit tubes after last washing step for 60 minutes on bench top under uncontrolled conditions (column 5). All conditions have been carried out in quadruplicates except stated otherwise.*

Stable transfected cells expressing the IGF1R-PGA fusion have been recloned to ensure the stability of the gene insertion and guarantee consistent high-level protein expression with the chosen clone. To this end, cells were stepped again into the complete cloning process from clone separation to single cells up to cryo stocks and extract preparation from the T-flask culture size. Variable amounts of cell extract from two independent reclones were analyzed as described previously to obtain a dimension for hormone binding capacity including functionality and amount of receptors incorporated in the cell extracts (Figure 5.7). Using 2.5 µl extract of each, those from reclones produce a slightly higher signal compared to the original clone. This changed the requirement to only 5 µl

extract per assay. The signal originating from the original clone sample was highly comparable with the one from both tested reclones when using 10 µl extract addition (Figure 5.7, A and B). Signal ratio from IGF1R-PGA containing extract to crude extract from untransfected HEK293 cells was determined to 23-fold (Figure 5.7, B).

A

B
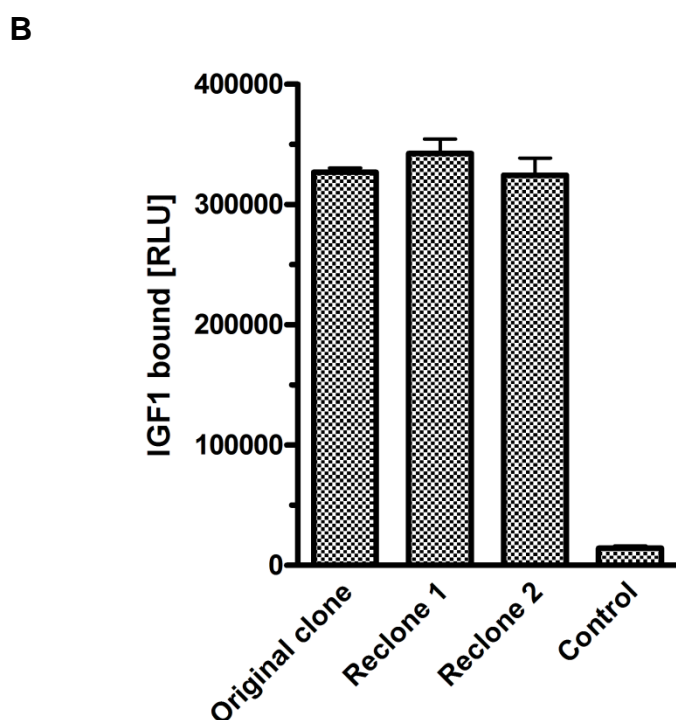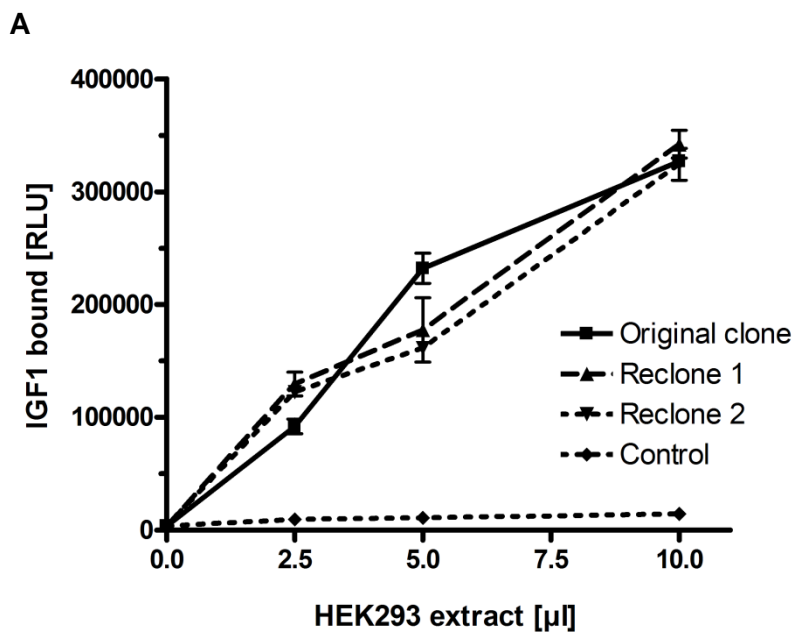
Figure 5.7: *Recloning IGF1R-PGA expressing HEK293 cells.*

(A) IGF1R-PGA over-expressing cells were recloned and their quality compared to the previous clone. Cell extracts of the original clone, two reclones and untransfected HEK293 cells (control) were immobilized onto anti-PGA antibody coated tubes in rising amounts in an equal volume assay buffer. Acridinium labeled IGF1 was added to observe hormone binding capacity including functionality and amount of receptors incorporated in indicted extracts. Error bars represent mean +/- SD from replicates.

(B) Presentation of the results using 10 µl cell extracts. Error bars represent mean +/- SD from replicates.

5.1.3 Biological suitability of expressed receptor

Untransfected HEK and HEK293-IGF1R-Luc cells showed binding of acridinium ester-labeled IGF1 which could be competed for by unlabeled IGF1 hormone (Figure 5.8). Binding of labeled IGF1 to HEK293-IGF1R-Luc cells was clearly higher when compared to untransfected HEK293 cells. Cells were incubated in identical experimental setups at 37°C and 4°C. Temperature reduction was chosen to mimic a minimum cell metabolism and membrane and receptor action at the 4°C sample, because of concerns that free acridinium or a fragment of the labeled IGF1 might get internalized by the cells and display a positive signal for bound IGF1. After lowering the temperature to 4°C, the binding behavior was nearly identical to the one observed before at 37°C. Thus the labeled hormone was likely retained on the outer surface of the cell membrane and surface binding was accomplished.
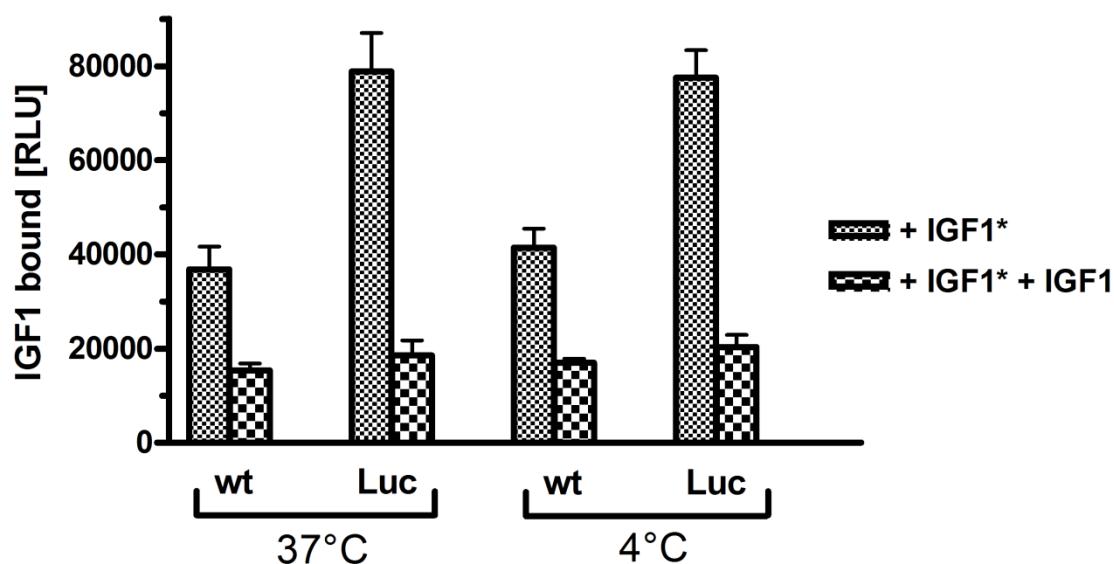
Figure 5.8: *Interaction of IGF1 with wild-type (wt) and IGF1R-luc (Luc) expressing HEK293 cells. Cells were incubated at 37°C or 4°C with acridinium-labeled IGF1 (IGF1*) in the presence or absence of an excess of unlabeled IGF1. Recombinant IGF1R-Luc fusion protein was successfully inserted into the plasma membrane and capable of IGF1 binding. Each value represents the mean +/- SD of quadruplicate measurements. This experiment was replicated once with the same results.*

These results indicate a successful overexpression, correct processing and functional insertion of the IGF1R-Luc fusion protein into the plasma membrane. This notion was supported when the majority of recombinant IGF1R fusion protein was found in the membrane fraction of stably transfected HEK293-IGF1R-Luc cells (Figure 5.9). Subcellular fractions were prepared from either HEK293 cells stably expressing IGF1R-Luc or HEK293 wild-type cells. The localization of the recombinant fusion protein was determined in the cell fractions by measuring total luciferase activity in membrane and

cytosolic fractions of HEK293-IGF1R-Luc cells (Figure 5.9, A). The determination of luciferase activity showed that integration of IGF1R-Luc was the cause of 71% of total luciferase activity, while only 29% of total luciferase activity was detected in the cytosolic fraction (Table 5.2). Western blot analysis has been performed of cell fractions from wild type HEK293 cells (Figure 5.9, B, lanes 1-3) and HEK293-IGF1R-Luc cells (lanes 4-6). Equal amounts of crude extracts (lanes 1, 4), membrane fraction (lanes 2, 5) and cytosolic fraction (lanes 3, 6) were subjected to electrophoresis, blotted and probed by anti-luciferase antibody (Promega, Mannheim). The blot showed that the majority of recombinant IGF1R-Luc fusion protein was detected at 100/130 kDa and was associated with the membrane fraction, compared to the lane containing the crude extract. Only faint signals were identified from cytosolic fraction. No signal was detected in blotted fractions from HEK293 wild type cells. Thus, the majority of recombinant IGF1R-Luc fusion protein was associated with the membrane fraction and demonstrated a functionally integration and expression of IGF1R-Luc fusion protein, supporting the preliminary results presented above (Figure 5.5 to Figure 5.8).

Table 5.2: *Results and calculation steps of subcellular distribution of IGF1R-Luc expression in stable HEK293 cells. After preparing subcellular fractions, from either HEK293 cells stably expressing IGF1R-luc or HEK293 wild type cells, the localization of the recombinant fusion protein was determined in the cell fractions by measuring total luciferase activity. Total RLU were calculated by adding multiplication factors depending on dilution and volume ratios. The experiment has been reproduced with nearly identical results.*

Fraction	membrane	cytosolic
MW of quadruplicates raw data [RLU]	2522020	866717
SD [RLU]	217554	70650
SD [%]	8,6	8,2
Total volume [µl]	200	2400
Measured volume [µl]	2	2
Factor for total RLU	100	1200
Dilution for measurement	10	1
Factor for total RLU with dilution	1000	1200
Total RLU	2522019500	1040060700
Fraction RLU [%]	70,8	29,2

A

B
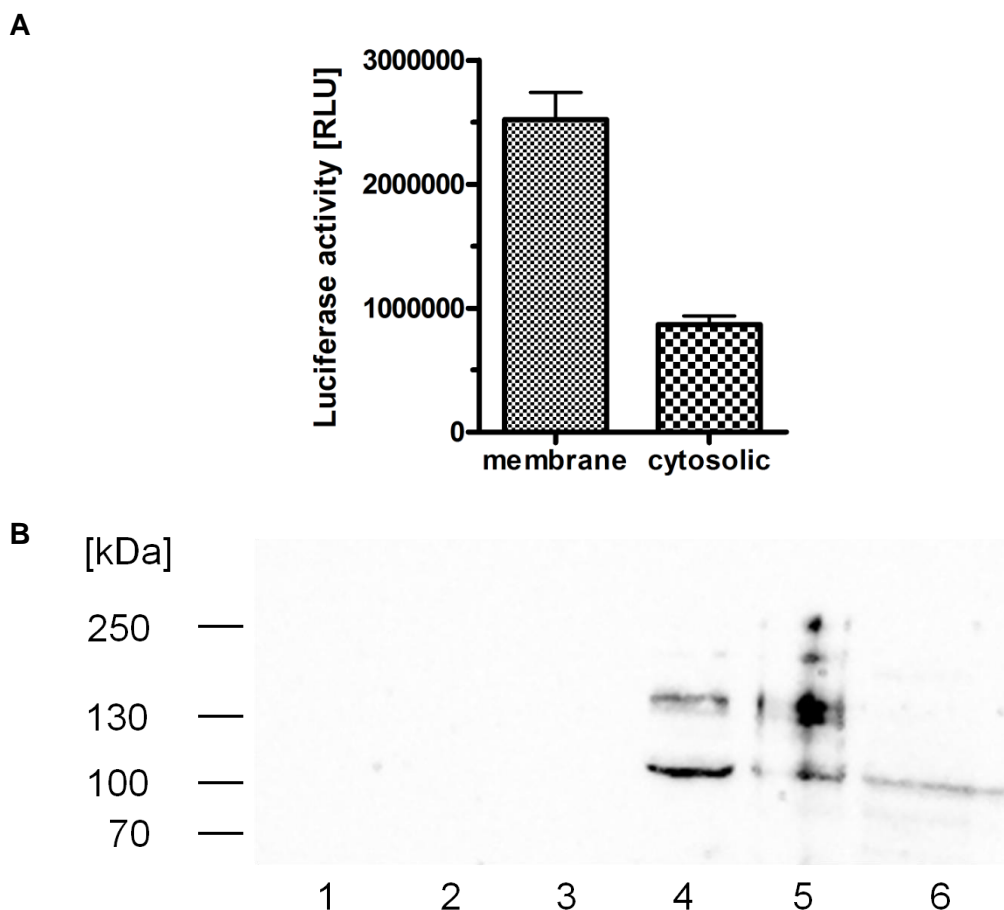
Figure 5.9: *Subcellular distribution of IGF1R-Luc expression in stable HEK293 cells. After preparing subcellular fractions, from either HEK293 cells stably expressing IGF1R-luc or HEK293 wild type cells, the localization of the recombinant fusion protein was determined in the cell fractions. (A) Total luciferase activity was determined in membrane and cytosolic fractions of HEK293-IGF1R-Luc cells following cell fractionation. Each value represents the mean +/- SD of quadruplicates. (B) Western blot analysis of cell fractions from wild type HEK293 cells (1-3) and HEK293-IGF1R-Luc cells (4-6). Equal amounts of crude extract (lanes 1, 4), membrane fraction (lanes 2, 5) and cytosolic fraction (lanes 3, 6) were subjected to electrophoresis, blotted and probed by anti luciferase antibody. The majority of the recombinant IGF1R-Luc fusion protein detected at 100/130 kDa was associated with the membrane fraction.*

5.1.4 Buildup of the IGF1R-Ab assay

For basic characterization of the new assays, various parameters were tested. Dilution of IGF1R-Ab serum samples, recovery of positive signals and stability of the assay system was investigated. Linearity of the signals, potential interference by matrix components, and stability of the autoantibodies in serum preparations were determined as well.

5.1.4.1 Interference of IGF1 with the IGF1R-Ab assay

Free IGF1 hormone is necessarily present in human serum. Its concentration varies in a normal population dependent on sex and age, and may reach values of up to 200 µg/l in patients [167, 168]. We decided to examine concentrations which may range up to 10 mg/l supplemented recombinant IGF1. For reasons of simplicity it was decided to label the annotation of the Y-axis with "IGF1R-Ab" from now on; well knowing that this term does not discriminate between aAb and Ab, but the indication Ab does obviously include aAb.
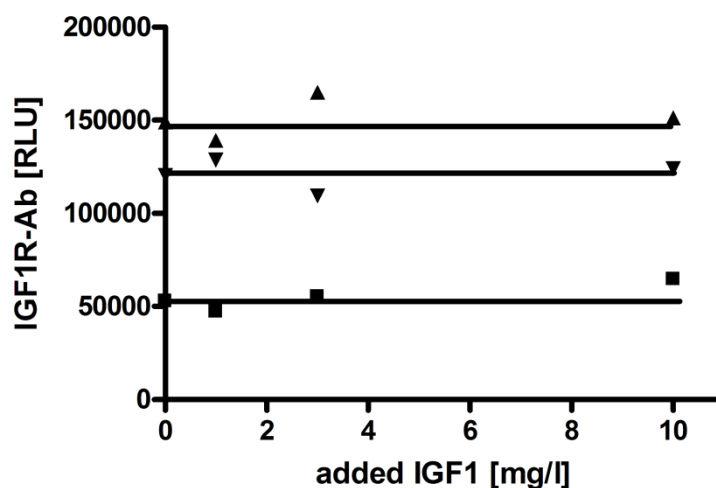
Figure 5.10: *Effect of IGF1 on the IGF1R-Ab assay. Increasing concentrations of IGF1 were added to three different IGF1R-Ab positive serum samples prior to immunoprecipitation and luciferase measurements. Presence of IGF1 in concentrations found in human serum or exceedingly high levels do not interfere with the IGF1R-Ab assay. Each value represents the mean of duplicate measurements. Negative control sera yielded around 5000 RLU under these conditions.*

5.1.4.2 Matrix effects

Matrix effects were tested by combining one positive and one negative serum in a 1:1 ratio, and analyzing the IGF1R-Ab concentrations in these mixtures. The measured values correspond to the theoretical arithmetic mean of both samples, indicating that no matrix effects were interfering with the IGF1R-Ab assay (Figure 5.11).
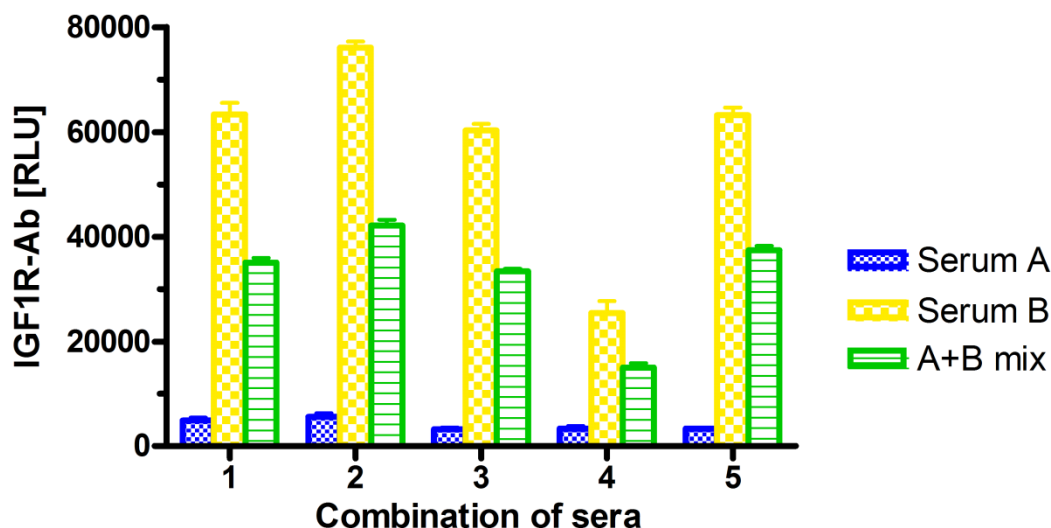
Figure 5.11: *Matrix effects. Control (blue, serum A) and IGF1R-Ab positive (yellow, serum B) serum samples were combined (green, A+B mix) by equal volume mixing and analyzed for IGF1R-Ab concentrations. The signals obtained in the IGF1R-Ab assay correspond to the theoretical arithmetic mean of the original samples indicating absence of matrix effects during the measurements.*

5.1.4.3 Serial dilution

Five different sera positive for IGF1R-Ab were selected and serially diluted. The measurements yielded concentration-dependent readings indicative of a good proportional increase of the IGF1R-Ab assay signal with IGF1R-Ab concentration (Figure 5.12).
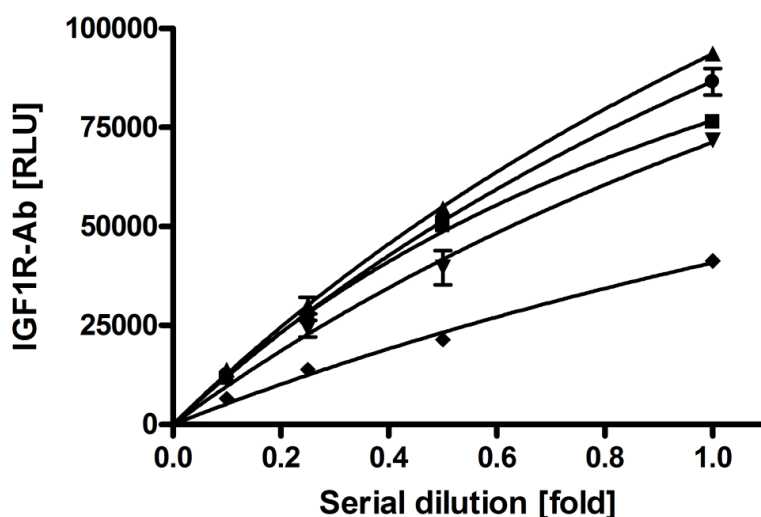
Figure 5.12: *Serial dilution of positive sera. The monoclonal antibody to the IGF1R-α-subunit (Millipore) was diluted using sample buffer and measured by the immunoprecipitation assay as described. Average RLU values from triplicate measurements are given in a logarithmic scale and the cutoff criterion for positivity of a present antibody is shown as dotted line.*

This result was verified with a commercial monoclonal antibody against the IGF1R α-subunit (Millipore, Billerica, USA). Stepwise dilution of the IgG preparation (30 µg IgG/ml) yielded a concentration-dependent signal decline. The cutoff criterion for positivity was reached at 15 ng IgG/ml of the monoclonal antibody, taking twice IGF1R-Ab value of the zero-sample as a basis, which contained no antibody (Figure 5.13).
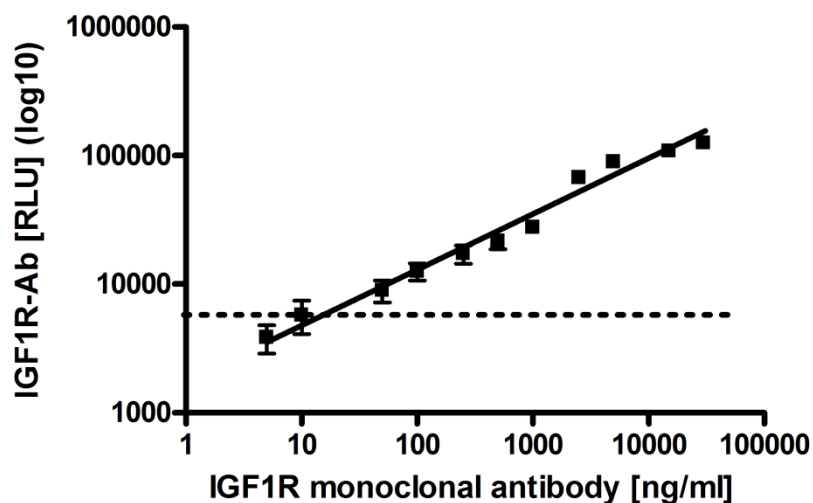
Figure 5.13: *Serial dilution and determination of detection limit with a commercial monoclonal antibody. The monoclonal antibody to the IGF1R-α-subunit (Millipore) was diluted using sample buffer and measured by the immunoprecipitation assay as described. Average RLU values from triplicate measurements were given at a logarithmic scale and the cutoff criterion for positivity of a present antibody was shown as dotted line.*

5.1.4.4 Stability of the autoantigen under assay conditions

Stability of the IGF1R-Ab in serum was determined by long-term storage experiments. As expected from the known nature of IgG molecules, signal intensities in the IGF1R-Ab assay were stable after samples had been incubated at 37°C or 4°C over time periods of up to 10 days using a pool of 5 sera as test sample (Figure 5.14).
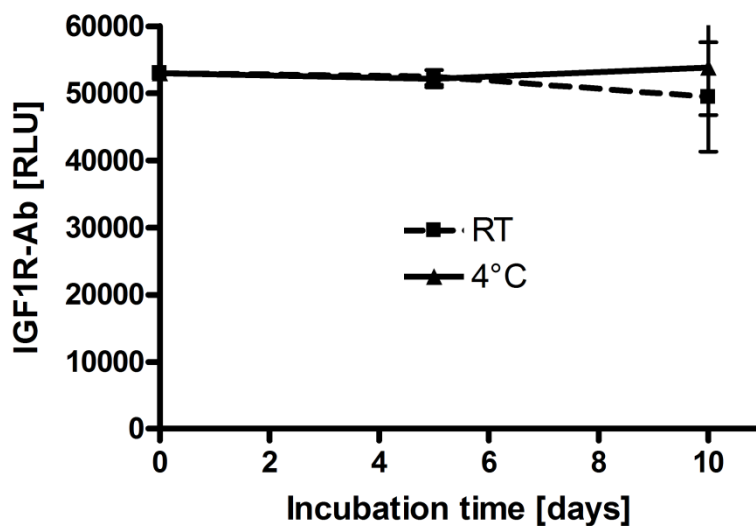
Figure 5.14: *Stability of the autoantigen under assay conditions. A pool sample from five positive sera was incubated at room temperature (RT) and 4°C for given periods of time and analyzed in the IGF1R-Ab assay. The signals obtained indicate stability of the IGF1R-Ab in serum over extended periods of time at both RT and 4°C. This experiment was replicated once with the same results.*

5.1.4.5 Comparison of serum to cleaned up IgG samples

Five different control and five IGF1R-Ab-positive serum samples were selected and their Ig prepared. The precipitation assay was conducted in order to verify that the IGF1R-Ab assay does indeed determine autoantibodies against the IGF1R. Only the purified Ig samples from positive IGF1R-Ab sera but not from control samples yielded luciferase signals after immunoprecipitation. The relative signal strengths from positive and negative samples and within the group of IGF1R-Ab-positive samples were similar in both data sets independent of prior Ig isolation (Table 5.3).

Table 5.3: *Comparison of crude serum and isolated Ig preparations in the IGF1R-Ab assay. The immunoprecipitation activities are expressed as RLU bound. Each value represents the mean of duplicate measurements. Analyzed samples were marked in ascending order.*

	IGF1R-Ab in Serum [RLU]	Relative IGF1R-Ab in serum, % of max	IGF1R-Ab in isolated Ig [RLU]	Relative IGF1R-Ab in Ig, % of max
1	417	0	238	0
2	619	0	181	0
3	781	1	392	1
4	669	0	414	1
5	348	0	293	0
6	121585	83	70472	92
7	145972	100	76178	100
8	130683	90	62441	82
9	55840	38	23002	30
10	131560	90	49699	65

5.1.5 Characterization of IGF1R-Ab assay

Coefficients of variation (CV) describe the ratio of the standard deviation to the mean, which includes the extent of variability in relation to the mean of the population. Thus IGF1R-aAb were determined in the same serum samples by repeated measurements of 5 replicates of the same sample in 4 independently performed assay sets in the IGF1R-Ab luciferase precipitation assay. To visualize the applied methodology more clearly, the individual results are illustrated in consecutive tables including the data of the experiments (Table 5.4).

Table 5.4: *Data obtained for determination of inter and intra assay CV´s. Data of 4 independently executed IGF1R-Ab luciferase precipitation assays for 4 serum samples in quintuplicates. Replicates mean and SD of replicates were determined for every serum sample in each set. The %-CV for every sample was calculated by dividing the standard deviation of the 5 replicates by the replicates mean, multiplied by 100. Table is continued on the following page.*

IGF1R-Ab-Luc assay	RLU			
Assay set 1	Serum 1	Serum 2	Serum 3	Serum 4
Result 1	3530	3896	4291	13089
Result 2	4276	3134	3685	15181
Result 3	4280	3750	4647	13464
Result 4	4160	4176	4771	14719
Result 5	3175	4742	5284	14796
Replicates mean set 1	3884	3940	4536	14250
SD of replicates set 1	504	589	594	915
%-CV of 5 replicates set 1	13.0	14.9	13.1	6.4
Assay set 2	Serum 1	Serum 2	Serum 3	Serum 4
Result 1	3497	2931	3270	10617
Result 2	3300	3559	3540	11240
Result 3	5362	3126	3950	12791
Result 4	3818	3273	3830	12484
Result 5	3663	3657	3986	11467
Replicates mean set 2	3928	3309	3715	11720
SD of replicates set 2	824	301	304	900
%-CV of 5 replicates set 2	21.0	9.1	8.2	7.7
Assay set 3	Serum 1	Serum 2	Serum 3	Serum 4
Result 1	2246	2111	2755	9758
Result 2	2417	1750	2759	11028
Result 3	2053	1858	2881	10035
Result 4	2293	1767	2475	9916
Result 5	2087	1852	2832	10076
Replicates mean set 3	2219	1868	2740	10163
SD of replicates set 3	150	145	157	499
%-CV of 5 replicates set 3	6.8	7.7	5.7	4.9
Assay set 4	Serum 1	Serum 2	Serum 3	Serum 4
Result 1	2049	1419	2158	8033
Result 2	1982	1592	2461	8398
Result 3	2305	1694	2290	8974
Result 4	2505	1805	2464	9258
Result 5	2421	2102	2723	9336
Replicates mean set 4	2252	1722	2419	8800
SD of replicates set 4	229	255	213	565
%-CV of 5 replicates set 4	10.2	14.8	8.8	6.4

Proceeding and auxiliary calculations for determination of the inter assay CV is presented in Table 5.5. Determination of the intra assay CV is presented subsequently in Table 5.6. The inter assay CV for the IGF1R-Luc precipitation assay was determined to be 13.6%, the intra assay CV was determined to be 9.9%.

Table 5.5: *Inter assay CV. The replicates mean for each sample was used to evaluate the overall mean, standard deviation, and overall %-CV for each sample in all assays. Results were declared relative to standard serum 1 to ensure comparability of every assay set. The average of sera 2 to 4 %-CV is reported as the inter assay CV.*

Inter assay CV	Serum 1	Serum 2	Serum 3	Serum 4
Overall mean of 4 replicate means	1.00	0.87	1.11	3.78
SD of 4 replicate means	0.00	0.11	0.13	0.66
Overall %-CV of 4 replicate means	0.0	12.2	11.3	17.4
		Inter assay CV [%]		13.6

Table 5.6: *Intra assay CV. The average of the individual set's of %-CV values is reported as the intra-assay CV.*

Intra assay CV	Serum 1	Serum 2	Serum 3	Serum 4	Average %-CV set
Set 1 %-CV of 5 replicates	13.0	14.9	13.1	6.4	11.9
Set 2 %-CV of 5 replicates	21.0	9.1	8.2	7.7	11.5
Set 3 %-CV of 5 replicates	6.8	7.7	5.7	4.9	6.3
Set 4 %-CV of 5 replicates	10.2	14.8	8.8	6.4	10.0
			Intra assay CV [%]		9.9

5.2 Installation of a IGF1R-Ab bridge assay

For a simplification of the previously established IGF1R recombinant autoantigen specific precipitation assay, the idea for the installation of an ELISA-like method for detecting highly specific autoantibodies to the IGF1R raised up. The antigen IGF1R was presented as recombinant expressed receptor molecule immobilized to an 2B5-antibody-coated tube using the 2B5-peptide tag fused C-terminal to IGF1R. After subjecting serum containing antibodies to the IGF1R and repeating washing steps, an IGF1R-Luc fusion was added. The second variable chain region of the antibody bound IGF1R-Luc simultaneously and luciferase activity was determined following washing. The bridge assay was designed as an experimental assay format, in which the antibody links ("bridges") two autoantigen molecules and is therefore highly specific.

5.2.1 Buildup of the IGF1R bridge assay

In the first attempt performing the IGF1R-IGF1R bridge assay, the recombinant IGF1R extract with C-terminal peptide tag was used in a dilution of 1 to 20, which means 10 µl extract in 200 µl working volume in the assay tubes. Extract containing the IGF1R-Luc fusion was used in a 1 to 10 dilution. These assumptions were based on the data of previous experiments (see 5.1.2).

The first test sample in the newly designed assay format was a patient serum, previously determined as highly positive in IGF1R-Ab in the precipitation assay. This serum was used in serial dilution with factor 4 (Figure 5.15). The "undiluted" sample was applied directly into the assay system, but represented a 1 to 2 overall diluted sample, because half of the working volume per tube was necessary for assay buffer. When using undiluted strongly positive IGF1R-Ab serum in the IGF1R-IGF1R bridge assay, an IGF1R-Ab signal of more than 60,000 RLU was observed. With a fourfold dilution of the serum the signal decreased to 60% of the previous one, with an additional four time dilution, signal decreased by approximately one half. Compared to the signal from undiluted serum, the signal from the 1 to 16 dilution decreased by two thirds and was still 3.7-fold above background signal. During a serum dilution of 1 to 64, the RLU value drew near the background, while the background was definitely reached at a 1 to 256 dilution.

A

Serum dilution	IGF1R-Ab [RLU]
undiluted	64651
1/4	38829
1/16	20269
1/64	8135
1/256	5389
background	5369

B
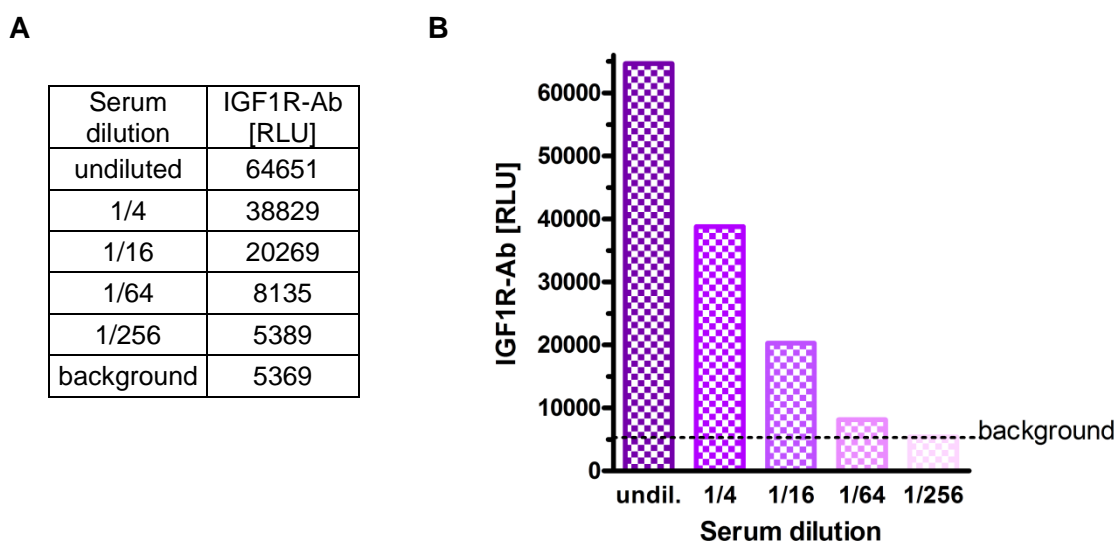
Figure 5.15: *Positive IGF1R-aAb serum in the IGF1R-IGF1R bridge assay.* *The IGF1R-Ab positive patient serum sample was serially diluted by factors of 4-times and subjected to the IGF1R-IGF1R bridge assay. Undiluted serum sample was applied directly into the assay system. Due to the 1/1 (v/v) necessity for the presence of assay buffer, an overall assay dilution of 1 to 2 was reached in the sample denoted as "undiluted". (A) Table including the raw data of the serial serum dilution with IGF1R-Ab level and the background sample. (B) Sample values from the serial*

dilution of the positive serum are presented in columns, the background value is represented as a dotted line. The result was replicated once with the same results.

As a second test sample, the two IGF1R molecules in the IGF1R-IGF1R bridge assay were assayed by a commercially available antibody targeting the IGF1R α-subunit (Millipore, Billerica, USA). The antibody was used in a serial dilution with a factor of 4 from 50 µg/ml, corresponding to absolute antibody concentrations of 50 µg/ml down to 0.05 ng/ml (Figure 5.16). Starting from the lowest concentration, a rapid dependent increase in signal intensity to around 470,000 RLU was observed up to a concentration of 781 ng/ml of the commercial antibody (Figure 5.16, B). From 781 ng/ml to a maximum concentration of 50 µg/ml, a non-linear slab of the IGF1R-Ab signal from below 500,000 to more than 800,000 RLU was observed. Using only 3 ng/ml antibody, a signal more than 2-fold higher than background values was reached, which can be set as the limit of detection (LOD). When generating a logarithmic depiction of the signals from the applied antibody, a characteristic type of antibody-binding curve is generated (Figure 5.16, C).

B

A

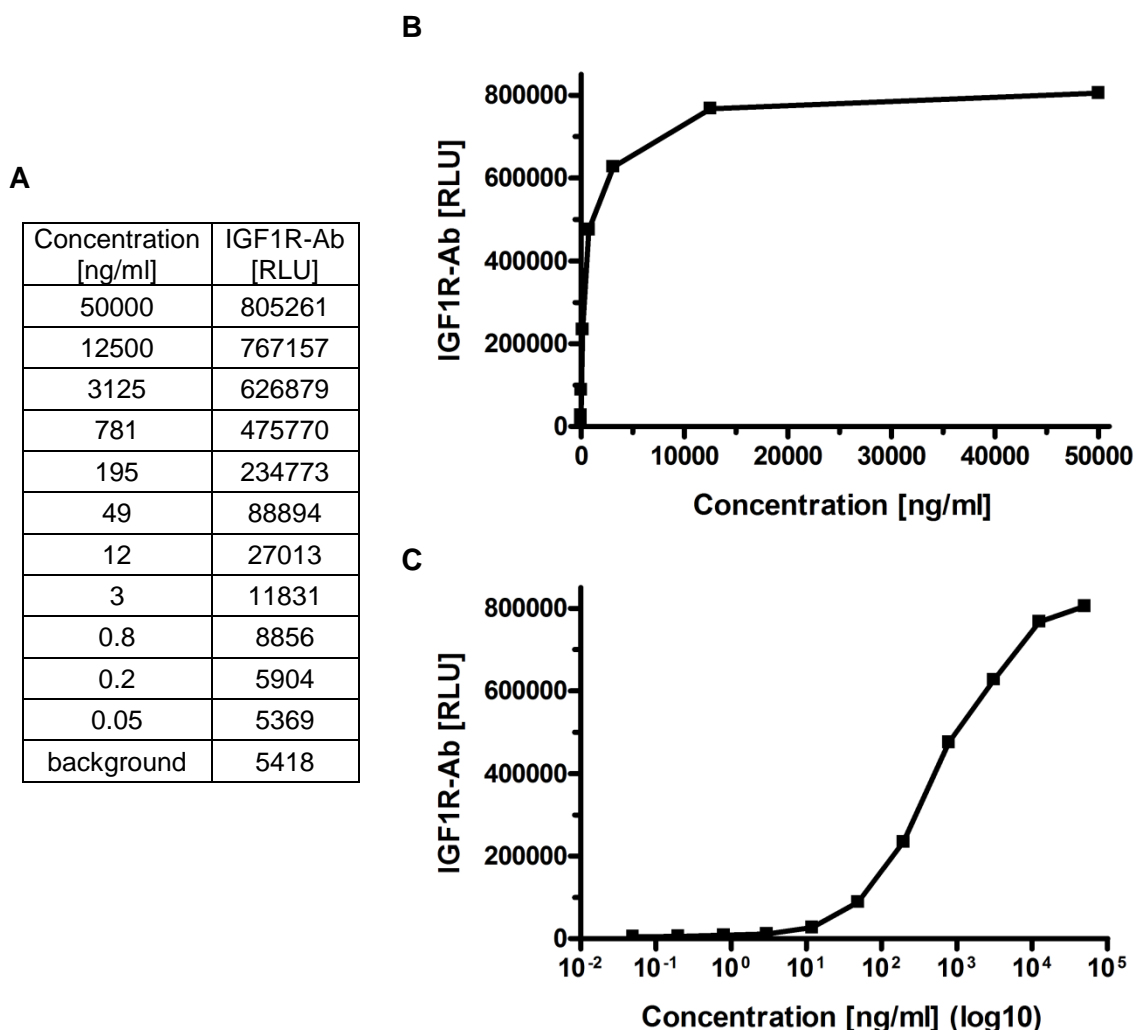| Concentration [ng/ml]	IGF1R-Ab [RLU]
50000	805261
12500	767157
3125	626879
781	475770
195	234773
49	88894
12	27013
3	11831
0.8	8856
0.2	5904
0.05	5369
background	5418

C

Figure 5.16: *Commercial anti-IGF1R α-subunit antibody in the IGF1R-IGF1R bridge assay*. (A) Table including raw data of IGF1R-Ab levels in various concentrations of a serial dilution and a

background sample. (B) IGF1R-Ab detection created by a commercial antibody in a serial dilution starting at 50 µg/ml with factor 4, presented with X-axis in linear scale and (C) presented with X-axis in logarithmic scale. The result was replicated once with the same result.

5.2.2   Adaptation of the assay format for routine use

An assay system on the step from common basic research to routine use and high sample throughput has to fit more stringent criteria on quality on the one hand, but in the current stage more important, needs to be superior in terms of practicability and ease of application on the other hand. A set of pre-experiments was thus performed in order to test the possibility of further development and routine production.

Lyophilization of IGF1R coated tubes

The IGF1R-IGF1R bridge assay comprises 4 steps, starting with two coating steps to the reaction tube, by firstly the anti-peptide tag antibody and secondly the peptide tagged IGF1R as bait. Because of the complexity of reproducibly binding these components to the tubes, a simplification of these steps is highly desirable. In several experiments, anti-2B5 peptide antibodies or anti-PGA peptide antibodies, respectively, were used as capture antibody for the tagged IGF1R. These antibodies were lyophilized to high capacity (star shaped bottom) tubes, seizing a volume of 5 ml (ICI, Berlin). The second coating step in the assay includes the binding of tagged IGF1R as bait (the first antigen to bind the autoantibody). Successful lyophilization of bound IGF1R would make the assay easier by reducing the number of working steps and decreasing the incubation times at once. IGF1R-PGA cell extracts were bound to anti-PGA coated tubes at 4°C over night and lyophilized after a washing and blocking step. Biological activity of the immobilized receptor was tested by determination of relative IGF1 binding capacity using acridinium labeled hormone (Figure 5.17). IGF1 binding capacity of tubes, at which the IGF1R antigen was lyophilized to, was 70% of the individually coated non-lyophilized samples. First differences appeared when 5 µl of cell extract containing the IGF1R was used and the differences increased slightly to the use of 20 µl extract, at which point the IGF1 binding capacity reached nearly a plateau in both sample sets, individually coated tubes and lyophilized antigen containing tubes. When the same amount of HEK293 wild type extract was used as control, the signals obtained for the lyophilized samples were slightly higher as compared to individually coated tubes.
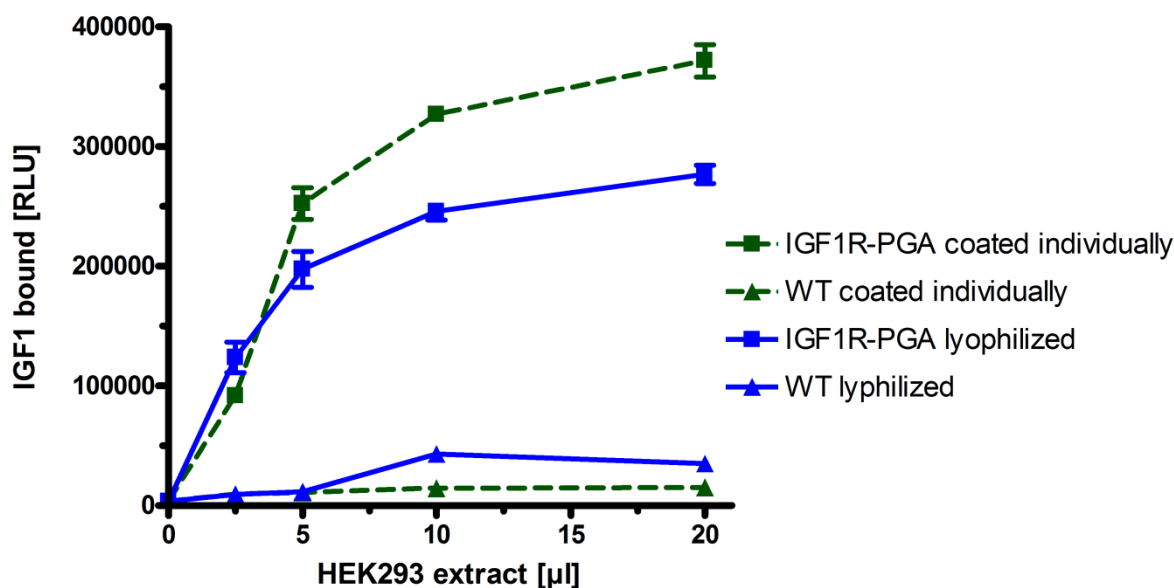
Figure 5.17: *Lyophilization of IGF1R to anti-peptide tag antibody coated tubes. Different amounts of IGF1R extract were bound by the fused peptide tag to anti-peptide tag antibody coated tubes at 4°C over night and then lyophilized. Indicated amounts of protein extract were added in a total volume of 200 µl per tube. HEK293 wild type extracts (WT) under the same conditions and samples in the experiment with individually coated tubes served as control. IGF1 binding capacity of the immobilized receptor was determined using acridinium labeled hormone. Error bars represent +/- SD from three replicates.*

Comparison of anti-peptide tag antibody coated tubes

As basic carrier material for the IGF1R-antigen presentation in the assay star-shaped bottom plastic tubes with a total volume of 5 ml were used, providing a working volume of 200 µl. Monoclonal antibodies to the peptide tag of the IGF1R-peptide tag fusion protein (IGF1R-PGA) served as linker between the tubes and the antigen. Two lots of antibody-coated tubes were provided (ICI, Berlin), lot CTSP008.001 and lot CTSP009.001 (in short: lot 008 and 009). Lots differed by the antibody batches used for production of the antibody-coated tubes. Using various amounts of IGF1R-PGA fusion protein containing cell extract, the binding curve for coated tubes from lot 009 obtained three times higher IGF1 binding capacity compared to lot 008 tubes (Figure 5.18). HEK293 wild type extract served as control, while obtained signals represent a bottom line throughout rising extract amounts.

Figure 5.18: *Comparison of different lots of anti-peptide tag antibody coated tubes. Binding capacity of the IGF1R antigen to different lots of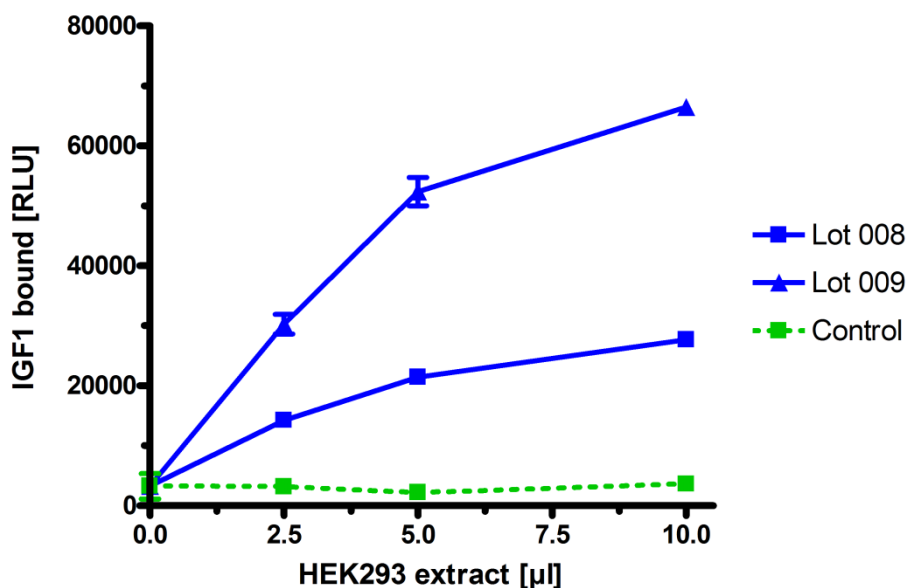 coated tubes was determined. Indicated extract amounts were added in a total volume of 200 µl per tube. HEK293 wild type extracts (WT) under same conditions served as control. Binding capacity of applied receptor amounts was scored using acridinium labeled IGF1 hormone binding to immobilized receptors. Error bars represent +/- SD from replicates.*

Baculovirus-based IGF1R-ED antigen production as promising model

A promising model to gain a large amount of antigen with less effort than using HEK cells, is the baculovirus expression system in insect cell culture. It was reported to be a quick performing recombinant protein expressing system [169, 170], which has proven successful for the production of many recombinant proteins [171, 172]. The baculovirus expression system provided ready to use protein in insect cell culture supernatant. Unfortunately, the expression, secretion and correct folding of a hormone-binding extracellular domain of IGF1R did not work in this case. Hormone binding capacity could not be detected (data not shown). This might be due to inadequate post translational modifications in the insect cell expression system, or because of missing functionality of the extracellular domain when expressed without transmembrane domains.

Miniaturization of assay format

First experiments to miniaturize the assay have been performed. The necessity arose out of missing upscale capabilities of experiment numbers in the coated tube assay format. This was based on relatively high labor input, because every tube has been handled individually in each assay step. An additional purpose was crucial reduction of sample amount, especially when human serum was analyzed. Thus preliminary experiments were

performed on a 96-well microtiter plate using the IGF1R-IGF1R bridge assay including a working volume of 100 µl per well and a commercially available antibody against α-subunit of IGF1R (Millipore). To this end, a 96-well white luminescence compatible plate (Greiner, Frickenhausen) was coated with 0.2 µg anti-2B5 peptide monoclonal antibody per well as described. IGF1R-2B5 containing extract was immobilized to the coated tube, followed by incubation with antibody solution in desired concentration and interaction as antibody-antigen complex. The assay was completed by detection of the relative luciferase fluorescence from the autoantibody-bound IGF1R-Luc antigen as detector. The anti-IGF1R antibody was applied in serial dilution with factor 2, beginning at 10,000 ng/µl decreasing to 5 ng/µl. A monoclonal antibody against FABP (InVivo-Lot: AK2025/01), consequently not binding IGF1R, was included as control in a comparable concentration range. Using the commercially available antibody against α-subunit of IGF1R, a rapid signal increase was observed already in minor concentration range, climbing to a plateau at around 1250 ng/µl (Figure 5.19, A). When concentration values were plotted in logarithmic scale, a characteristic sigmoid antibody-binding curve resulted (Figure 5.19, B).
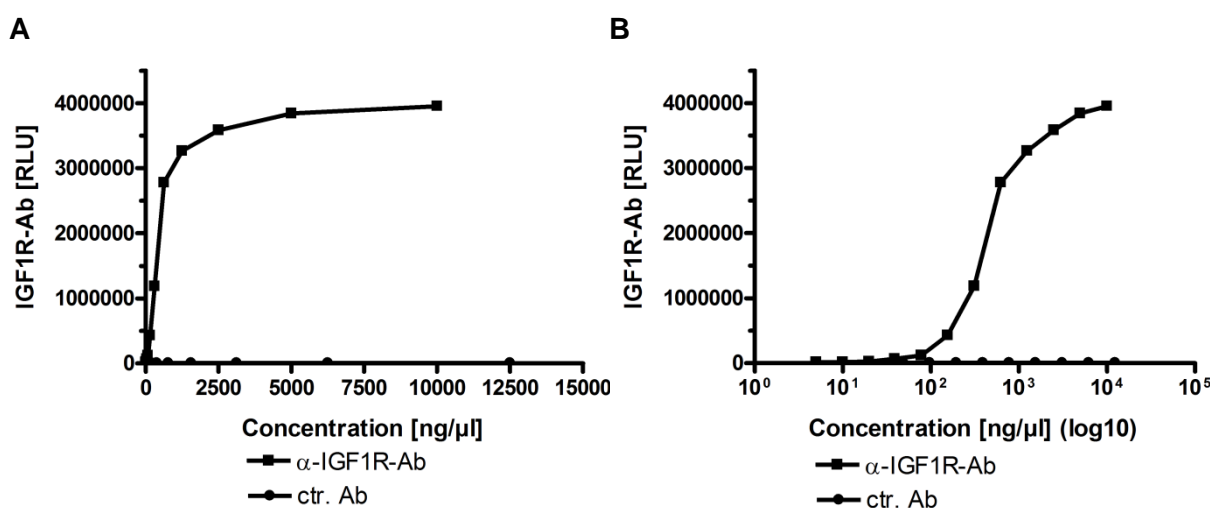
Figure 5.19: *Miniaturization of IGF1R-IGF1R bridge assay on 96-well microtiter plate. IGF1R-Ab detection was accomplished by a commercial antibody anti-IGF1R α-subunit in the IGF1R-IGF1R bridge assay. The antibody was applied in serial dilution with factor 2 (filled squares); an unrelated monoclonal antibody not binding IGF1R (InVivo-Lot: AK2025/01) was included as control (filled circles). Results are presented in graphs (A) with Y-axis in linear scale and (B) with Y-axis in logarithmic scale. Data points represent mean of double determination, the experiment was replicated once with the same results.*

5.3 Generation of monoclonal antibodies to the IGF1R

Monoclonal antibodies to the IGF1R were generated and produced in a fruitful cooperation project. The project was split between the cooperating experts according to their particular field of expertise. The flowchart illustrates the complexity of the work and the individual steps taken to raise, isolate and generate the antibodies needed (Figure 5.20). The Project started with creation of an IGF1R-expression plasmid at the Institute for Experimental Endocrinology (Charité, Berlin; subsequently abbreviated as "IEE"). Genetic immunization of mice was performed by Unicus Karlsburg OHG (Karlsburg, Mecklenburg; subsequently "Unicus") using the pIRESneo-IGF1R-2B5 expression plasmid from IEE. Following immunization, Unicus created hybridoma fusions and separated clones. Their cell culture supernatant was analyzed at IEE with an anti-mouse-Ab assay, detecting specifically binding to IGF1R in 96-well format. Antibodies from hybridoma cell culture supernatant bound to immobilized anti-mouse antibodies and antigen specific antibodies were detected by binding additionally to IGF1R antigen fused to luciferase (IGF1R-Luc). Clones generated highest Luc-signals were chosen and further subcloning took place at Unicus. This procedure was repeated two times, leading to a reduction of the initially identified 376 clones to 48 subclones, and finally to 31 new reclones. From those clones, the five best were selected as final production clones and hybridoma cell culture was upscaled at InVivo BioTech Services GmbH (Hennigsdorf; subsequently "InVivo Biotech"). Purification and quality control experiments were performed at InVivo Biotech as well.

Unicus　　**IEE Charité**　　**InVivo Biotech**
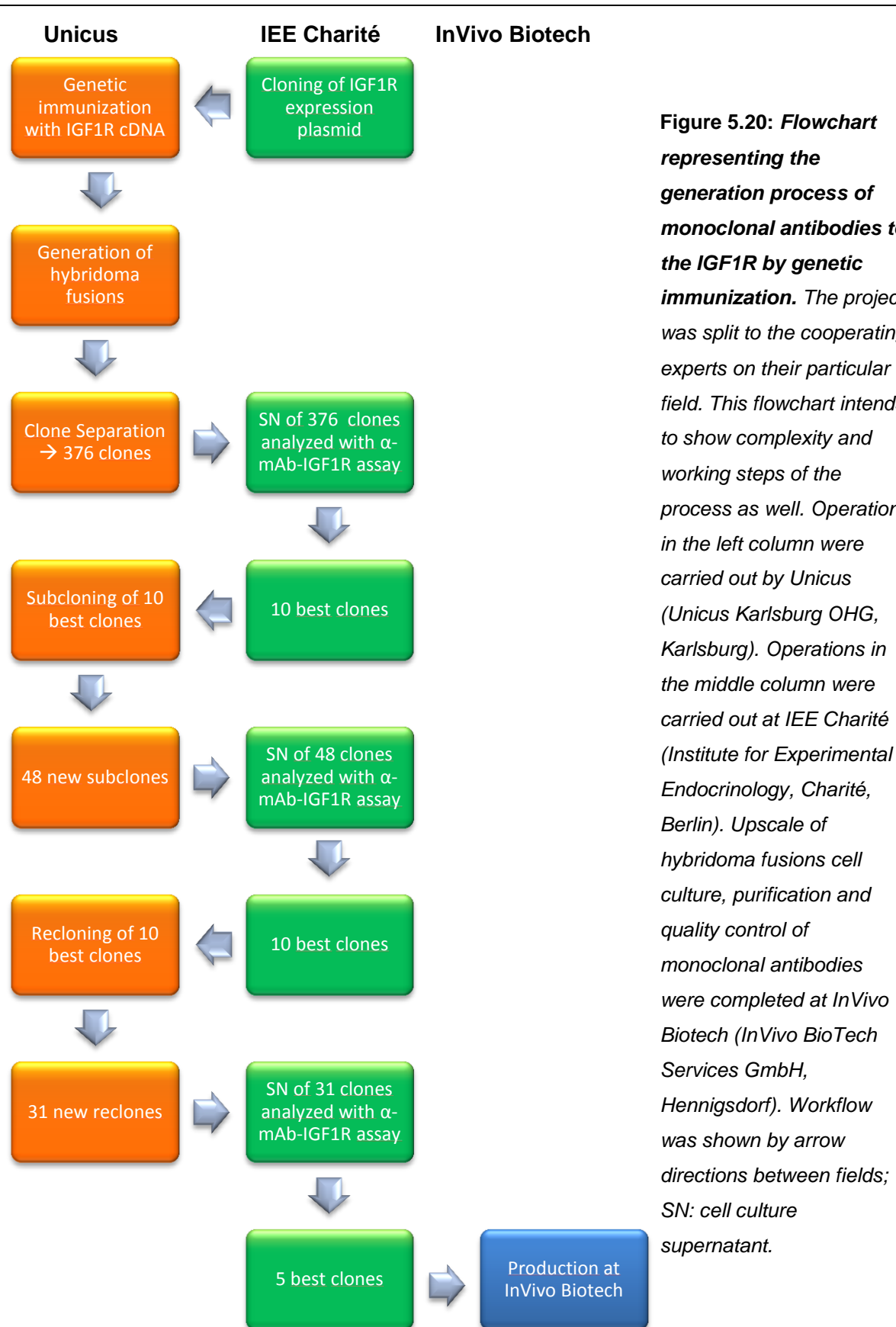
Figure 5.20: *Flowchart representing the generation process of monoclonal antibodies to the IGF1R by genetic immunization.* The project was split to the cooperating experts on their particular field. This flowchart intends to show complexity and working steps of the process as well. Operations in the left column were carried out by Unicus (Unicus Karlsburg OHG, Karlsburg). Operations in the middle column were carried out at IEE Charité (Institute for Experimental Endocrinology, Charité, Berlin). Upscale of hybridoma fusions cell culture, purification and quality control of monoclonal antibodies were completed at InVivo Biotech (InVivo BioTech Services GmbH, Hennigsdorf). Workflow was shown by arrow directions between fields; SN: cell culture supernatant.

5.3.1 Screening of hybridoma clones

Following the first cultivation of hybridoma B cell / myeloma fusions, the first screening round of 376 samples of hybridoma clone cell culture supernatants was performed in a micro titer plate format by measuring the binding potential of the antibodies from the supernatants to immobilized to the IGF1R antigen fused to luciferase (IGF1R-Luc). To this end, the mouse antibodies were first immobilized to the 96 well surface by an anti-mouse IgG. Results of single determination were displayed relative to the mean value of two medium controls as "relative titer" in each individual assay plate. The best performing 10 clones were selected and are presented in Table 5.7. These clones were subcloned and hybridoma cell culture supernatant of 48 subclones was analyzed as described previously. Again the 10 best performing clones were selected and are presented in Table 5.8.

Table 5.7: *Best performing 10 clones out of 376 binding specifically to the IGF1R. Results are displayed relative to the mean of medium control samples for each assay plate individually. "Clone name" indicates the plate and position of examined clone on the cell culture plate.*

Table 5.8: *Best performing 10 subclones out of 48 binding specifically to the IGF1R. Results are displayed relative to the mean of medium control samples and denote the mean of double determination. "Clone name" indicates ancestry of examined clone and position on the cell culture cloning plate.*

Clone name	Relative titer
p1, B12	1,93
p2, B08	2,92
p2, E10	2,45
p2, F12	2,15
p3, G02	1,94
p3, H02	2,25
p4, C01	2,75
p4, E02	2,61
p4, F01	3,13
p4, F03	2,90

Clone name	Relative titer
4F1 E1	3,54
4F1 F3	3,39
2B8 F9	4,30
2B8 H12	3,11
4C1 F7	3,11
4C1 G8	2,83
4C1 H7	2,81
2E10 E8	4,14
1B12 H4	2,28
1B12 H6	2,05

These subclones were re-cloned again and hybridoma cell culture supernatant of 31 re-clones was analyzed as described previously. The 5 best performing re-reclones were selected; their "relative titer" is presented in Table 5.9. Those five clones have been selected for culture upscale and antibody purification.

Table 5.9: Best performing 5 re-reclones out of 31 binding specifically to the IGF1R. *Results are displayed relative to the mean of medium control sample and provide the mean of double determinations. "Clone name" indicates ancestry of examined clone and position on the cell culture cloning plate.*

Clone name	Relative titer
4F1 E1 E2	21,04
4F1 E1 E5	20,86
4C1 F7 F5	8,98
4C1 F7 G2	16,39
1B12 H4 G6	13,99

5.3.2 Antibody production and purification from hybridoma clones

Selected cryo conservations of hybridoma clones previously chosen (Table 5.9) were obtained from Unicus, then revitalized and cultivated at InVivo Biotech as described in material and methods (section 4.3.13). Culture volume was expanded for each clone continuously to superspinner batch culture format. Hybridoma cell culture supernatants were then harvested and supplied to a protein-A purification process (Figure 5.21).

AK2046/01 (clone 551/E5) was chosen as example to illustrate the purification process of all selected clones. Purification was performed via an Äkta Explorer HPLC chromatography system connected to a chromatography column with a column volume (CVol) of 100 ml. Column was filled with 97 ml POROS A50 Protein-A resin in storage buffer. The column was equilibrated with 1/3 CVol washing buffer. Then, a total volume of 1750 ml cell culture supernatant, originating from hybridoma cell culture producing the antibody in a 2 L seized superspinner, was loaded onto the column. Addition of the antibody-containing sample resulted in a sudden increase of A_{280}-values (Figure 5.22). The antibodies bound to the protein-A matrix in the column and components of cell culture medium rushed through the column. The system was washed with 5.7 CVol washing buffer, while A_{280} values decreased again. The elution step with 2 CVol elution buffer followed, when a distinct ground line separation was ensured. The antibody was eluted after adding 0.55 CVol elution buffer, resulting in a strong increase in A_{280} absorption. The formed peak ended after 1.35 CVol elution buffer had been added. Thus a total volume of 0.80 CVol contained the majority of the antibody, which equals approximately 76 ml. The antibody was eluted into 30 ml of neutralization buffer. Following elution, the chromatography column was re-equilibrated with 1.5 CVol washing buffer. The total yield of eluted antibody was 227 mg with a concentration of 2.14 mg/ml. The solution was dialyzed for 2 days in PBS (150 mM, pH 7.4). Following dialysis and filtration via a 0.22 µm membrane, the antibody yield was 222 mg with a concentration of 1.65 mg/ml (compare to Table 5.10).
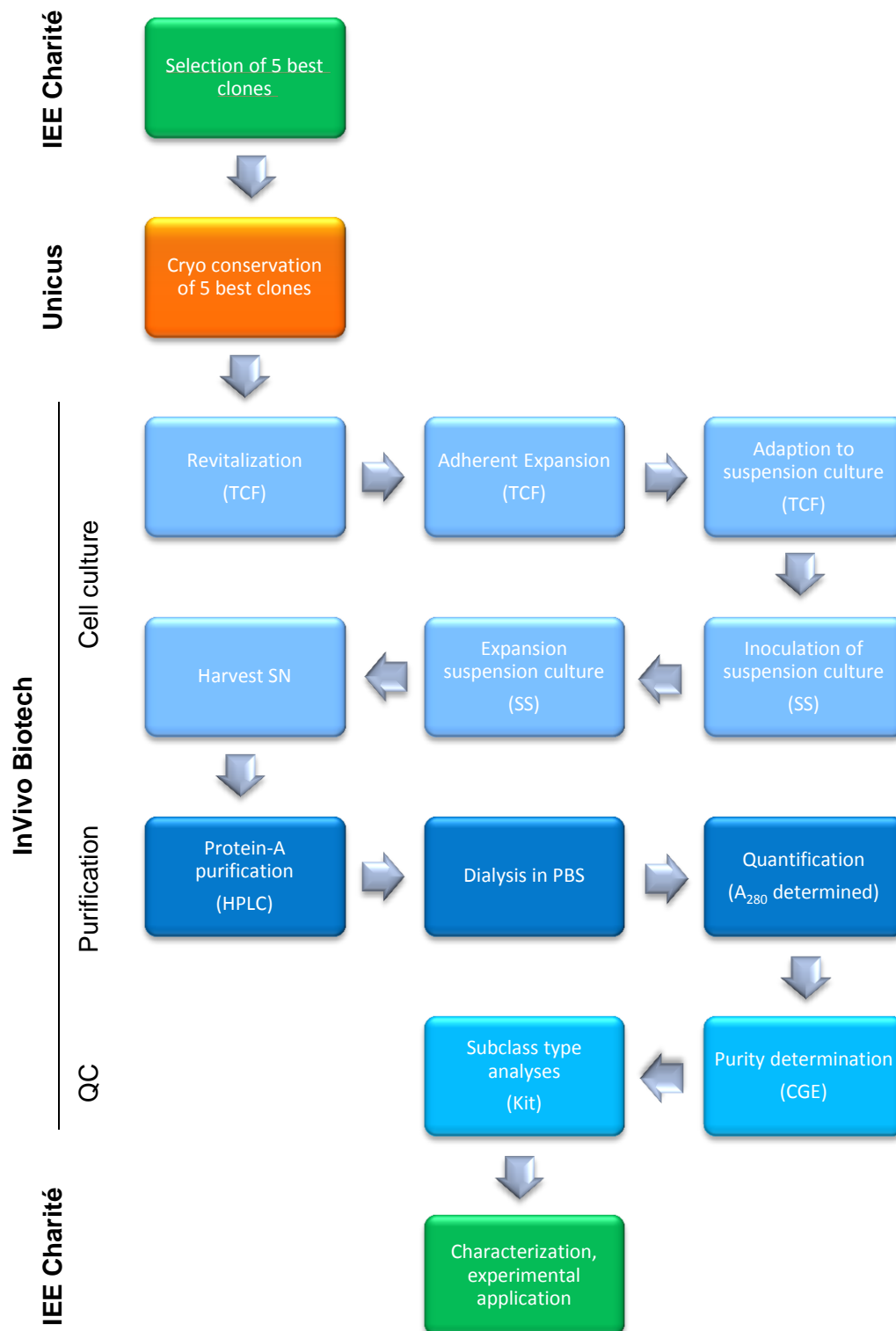
Figure 5.21: *Flowchart representing the production and purification process of monoclonal antibodies to the IGF1R, including the quality control. Workplaces where operations were carried out are entitled at the left and indicated in fitting colors (IEE Charité: Institute for Experimental Endocrinology, Charité, Berlin; Unicus: Unicus Karlsburg OHG, Karlsburg; InVivo Biotech: InVivo BioTech Services GmbH, Hennigsdorf). After selection of the five best performing hybridoma clones producing antibodies against the IGF1R, cryo conservations of these were*

provided and revitalized in tissue culture flasks. The adherent cell culture of the hybridoma fusions was expanded and adapted to suspension culture. Thereupon, a super spinner culture system was inoculated from suspension culture adapted cells originating from the tissue culture flasks. Spinner culture was expanded to desired volume and cell culture supernatant was harvested. Purification of the antibodies was performed by a protein-A purification process using an Äkta Explorer HPLC chromatography system. After elution, the antibody solution was dialyzed into PBS and quantified by UV-spectroscopy. Quality control was carried out by running a CGE and analyzing the antibody subclasses. Purified antibodies were then biochemically evaluated and characterized by experimental approaches. The working system was specified in brackets beneath every working step; TCF: tissue culture flask, SS: superspinner, HPLC: high pressure liquid chromatography, CGE: capillary gel electrophoresis. Workflow is shown by arrow directions between fields; QC: quality control; SN: cell culture supernatant.
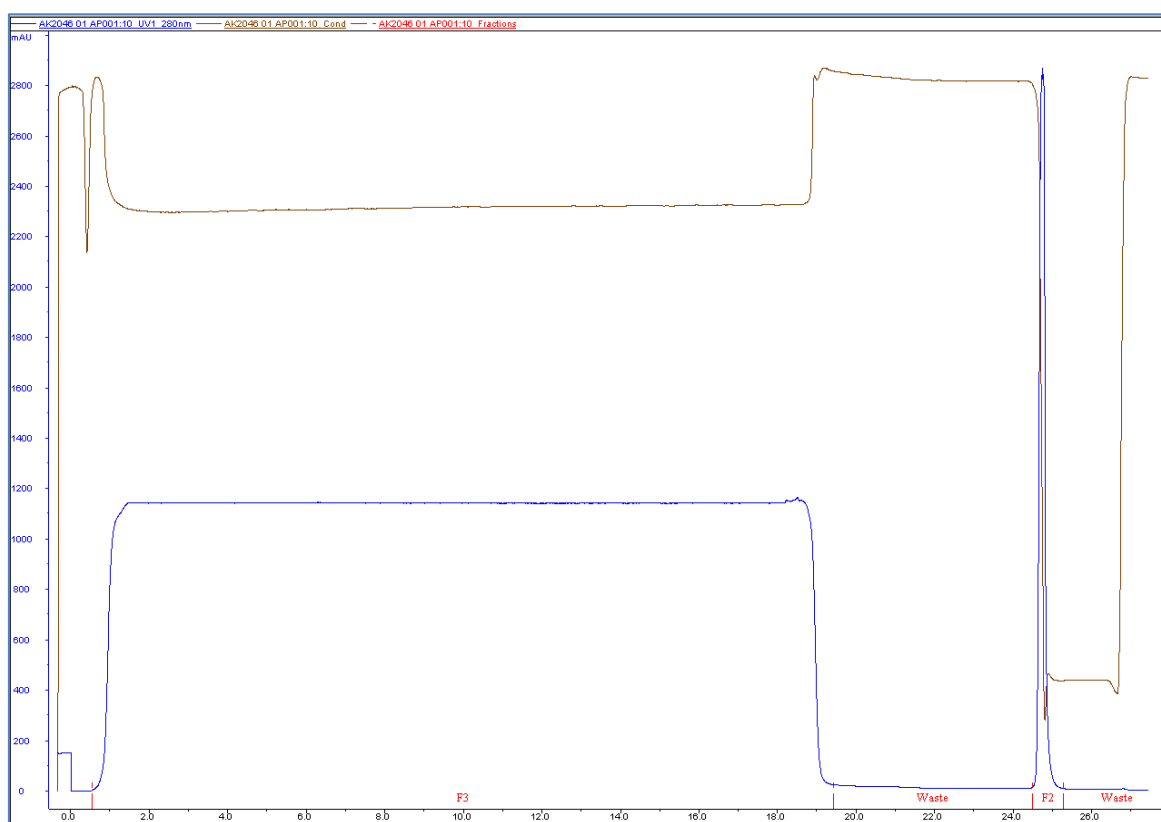
Figure 5.22: C*hromatogram of antibody purification process for AK2046/01 (clone 551/E5).*
X-axis represents column volumes (CVol), Y-axis represents A_{280}-values measured directly in the chromatography system, when the flow passed the chromatography column. Blue lines indicate A_{280}, brown line the conductivity. Fractions collected were labeled in red. The chromatography column contained 97 ml POROS A50 Protein-A resin, which was equilibrated with 1/3 volume of washing buffer, followed by the load of hybridoma cell culture supernatant onto the column for approx. 18 CVol. The system was washed with 5.7 CVol of washing buffer followed by antibody elution with 2 CVol of elution buffer and re-equilibration of the column with 1.5 CVol washing buffer.

Table 5.10: *Yield of anti-IGF1R antibodies after purification. Five selected antibody producing clones were revitalized and cultivated at InVivo Biotech in a 2 L superspinner culture system or two 1 L super spinner culture systems per clone. Protein concentration was determined by A_{280nm} measurement using an extinction factor of 1.35 (1 A_{280nm} = 1.35 mg/ml).*

Clone	Batch	Culture system	Total yield [mg]	Concentration [mg/ml]
551/E2	AK2045/01	2 L SS	220	1.15
551/E5	AK2046/01	2 L SS	222	1.65
551/F5	AK2047/01	1 L SS	78	1.00
	AK2047/01B	1 L SS	74	0.84
551/G2	AK2048/01	1 L SS	66	1.00
	AK2048/01B	1 L SS	63	0.50
551/G6	AK2049/01	1 L SS	1.5	0.17
	AK2049/01B	1 L SS	12	0.60

Antibodies originated from hybridoma clones 551/E2 and 551/E5 were purified in one batch. When two 1 liter seized superspinner systems have been prepared for generation of 2 liter hybridoma cell culture supernatant (clones 551/F5, 551/G2 and 551/E6), the antibodies were purified independently and the batch number of one spinner was complemented by a "B". The yield of purified antibodies reached from 63 mg to 111 mg per liter of hybridoma cell culture from every clone (Table 5.10). Yields of purified antibodies from clone 551/G6 represent an exception with 1.5 mg and 12 mg per liter cell culture, respectively. The protein concentration following dialysis and filtration of antibodies reaches from 0.50 to 1.65 mg/ml, again with the exception of one batch originating from clone 551/G6 with a protein concentration of 0.17 mg/ml.

5.3.3 Quality control of purified antibodies

Samples of purified antibodies (Table 5.10) and a protein ladder were subjected to capillary gel electrophoresis under reducing conditions. The resulting density plot was arranged as a gel picture (Figure 5.23) and normalized to internal standards included in every sample (240, 7 and 4.5 kDa).
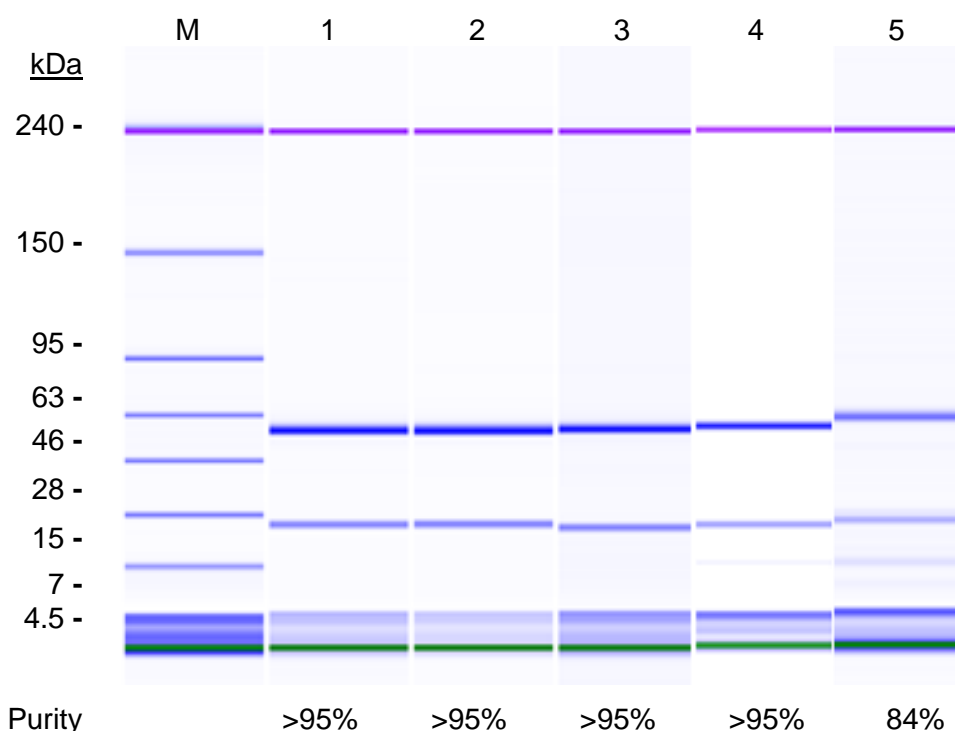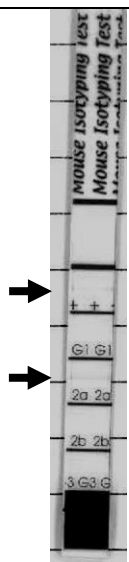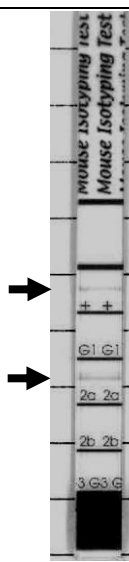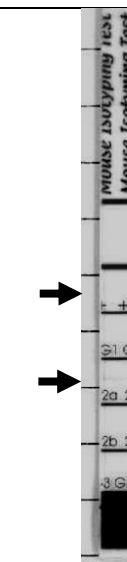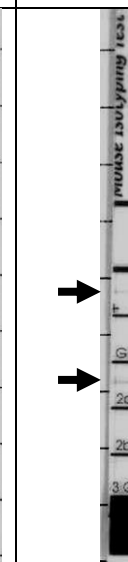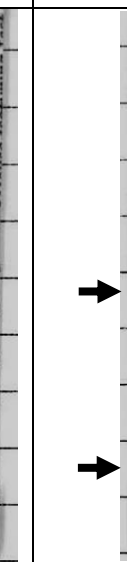
Figure 5.23: *Capillary gel electrophoresis of purified antibodies. 4 µl of protein ladder (Lane M) or antibody samples (Lane 1: AK2045/01; lane 2: AK2046/01; lane 3: AK2047/01; lane 4: AK2048/01; lane 5: AK2049/01B) were subjected to capillary gel electrophoresis under reducing conditions, normalized to internal standard fragments with sizes of 240, 7 and 4.5 kDa included in each sample. Purity was calculated by Agilent bioanalyzer software.*

In lanes 1-3, representing antibodies AK2045/01, AK2046/01 and AK2047/01, a distinct separation of focused bands of heavy chains between 50 and 60 kDa and light chains around 25 kDa was clearly visible, which correlated with the expected molecular weights of around 50 kDa for an antibodies heavy chain and around 25 kDa for an antibody light chain. No further bands appeared between internal marker bands for 240 and 7 kDa fragments, which indicated no impurities. Purity was calculated by Agilent bioanalyzer software to >95% for all three samples, which represented the maximum of purity obtainable in this analysis system. Bands between internal marker bands of 7 and 4.5 kDa had systemic character and had been observed previously. Lanes with antibody samples of AK2048/01 (lane 4) and AK2049/01B (lane 5) showed the same expected pattern as described for the first three analyzed antibodies, while an additional slightly distinct protein band appearing at around 15.3 kDa with a presence status of 4.0%. Nevertheless, the purity grade was calculated to >95%. The band representing the heavy chain of AK2049/01B was located nearby the 63 kDa protein marker fragment. An additional distinct protein band appeared at around 15.3 kDa with a presence status of 11.5%. Purity for AK2049/01B was stated at 84%.

5.3.4 Subclass type analyses

Antibody subclasses of these 5 clones were determined using the mouse monoclonal antibody isotyping kit (MMT1, AbD serotec, Puchheim, Germany) with an antibody concentration of 1 μg/ml. Photographs of the front side of the isotyping strip are shown in Table 5.11 for every batch analyzed. Black arrows indicate a distinct band on the carrier material. The upper black arrow displays the internal test's positive control, which showed up in all five samples. On those stripes analyzing the antibody batches AK2045/01, AK2046/01, AK2047/01 and AK2048/01, a second band became visible at the position for heavy chain subclass IgG2a. For batch AK2049/01B a band appeared at IgG3 position. Detection fields for the other potential subclasses IgA, IgD, IgE and IgM on the back side of the strip showed no band (not shown). The light chain subclass was determined to kappa for all five batches of produced antibodies, while the field for lambda subclass of the light chain showed no band (not shown).

Table 5.11: *Subclass type analyses from selected monoclonal anti-IGF1R antibodies. Antibody subclasses were determined using the mouse monoclonal antibody isotyping kit MMT1 with an antibody concentration of 1 μg/ml. Batch numbers of the antibodies are displayed at the front row with appropriate photographs of the isotyping strip underneath. Black arrows indicate a distinct band on the carrier material. Results for heavy and light chain are summarized in rows 3 and 4, while photographs of the backside of the strip with determination of potential other heavy chain isotypes and light chain subclass are not presented here.*

Batch no.	AK2045/01	AK2046/01	AK2047/01	AK2048/01	AK2049/01B
Isotyping strip					
Heavy chain	IgG2a	IgG2a	IgG2a	IgG2a	IgG3
Light chain	kappa	kappa	kappa	kappa	kappa

5.3.5 Binding of purified monoclonal antibodies to their antigen IGF1R

To test if the positive hybridoma clones, which have previously been chosen for upscale production and purification, do contain antigen-specific antibodies to the IGF1R, they were tested with the previously described assay format on a 96-well plate (see section 5.3.1). In short, monoclonal antibodies bound to anti-mouse antibodies, which were immobilized at the plate surface. Antigen-specific binding was detected by adding IGF1R antigen fused to luciferase (IGF1R-Luc). For first analysis, dilutions in PBS of 1 to 10, 1 to 100 and 1 to 1000 of the supplied material were tested (Figure 5.24).
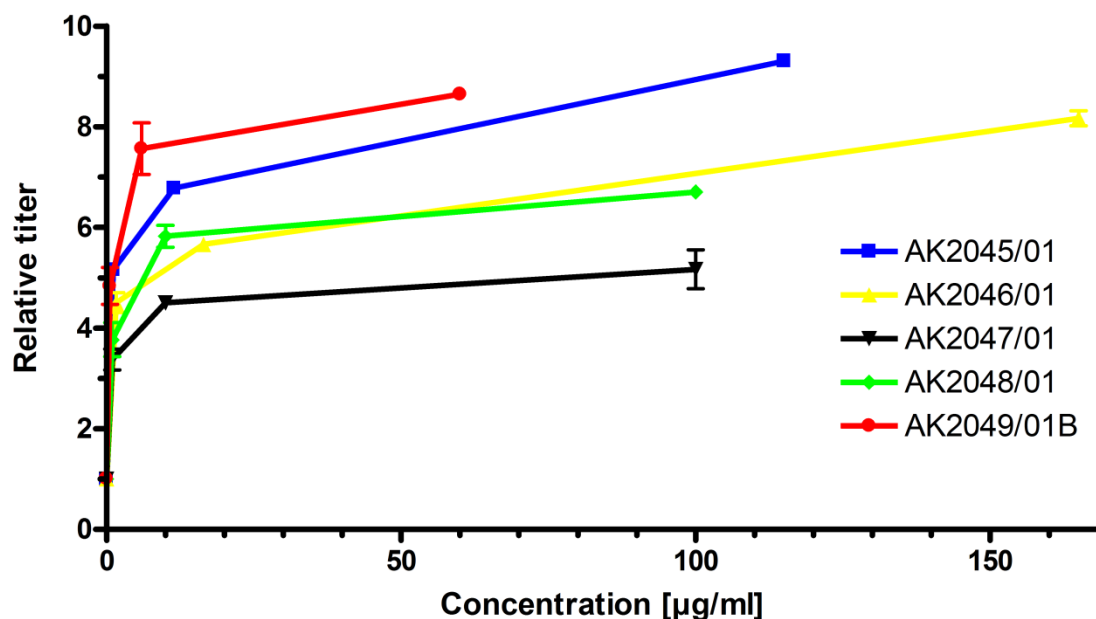
Figure 5.24: *Specific binding of monoclonal antibodies against IGF1R. Different concentrations of purified antibody solution were bound to anti-mouse antibodies on a 96-well plate Antigen specificity was tested by binding IGF1R-Luc fusion protein, and resulting luciferase activity was detected. Results are presented as "relative titer" in relation to the PBS control sample set to 1.0. The experiment was performed in duplicate; bars represent the range of double determinations.*

Each of the five chosen monoclonal antibodies against the IGF1R showed relative titers between 5 and 9.5 at their maximal concentration. Saturation of the signal started in all antibodies between dilution step two and three.

5.4 Biological and molecular actions of IGF1R-Ab

Receptor-specific autoantibodies may positively or negatively affect ligand binding or directly stimulate or inhibit the receptor-dependent signaling as best exemplified by autoimmunity against the TSH receptor [173]. The interactions of the IGF1R-aAb with the IGF1R were thus analyzed in further detail. Investigation of the functional activity of

IGF1R-aAb, their effect on the IGF1R itself but also on the viability and proliferation of mammalian cells in general were included in this section as well.

5.4.1 Precipitation of IGF1R by IGF1R-Ab containing sera

Five positive and five negative serum samples for IGF1R-Ab, which obtained a low or high signal in the IGF1R-Ab luciferase precipitation assay, were tested for immunoprecipitation of a peptide-tag bearing receptor fusion protein (IGF1R-PGA) from cell extracts (Figure 5.25). Protein-A precipitated proteins were subjected to SDS electrophoresis, blotted and detected by an antibody specifically recognizing the PGA14 affinity tag located on the IGF1R-fusion protein. Western blot analysis of immunoprecipitated IGF1R samples using the five control serum samples (lane 1-5) or IGF1R-Ab positive serum samples (lane 6-10) showed considerably higher signals for IGF1R in the lanes of positive serum samples than in the control lanes. Thus, the IGF1R-Ab positive samples efficiently recognized and immunoprecipitated the IGF1R-PGA autoantigen, but the control sera did not.
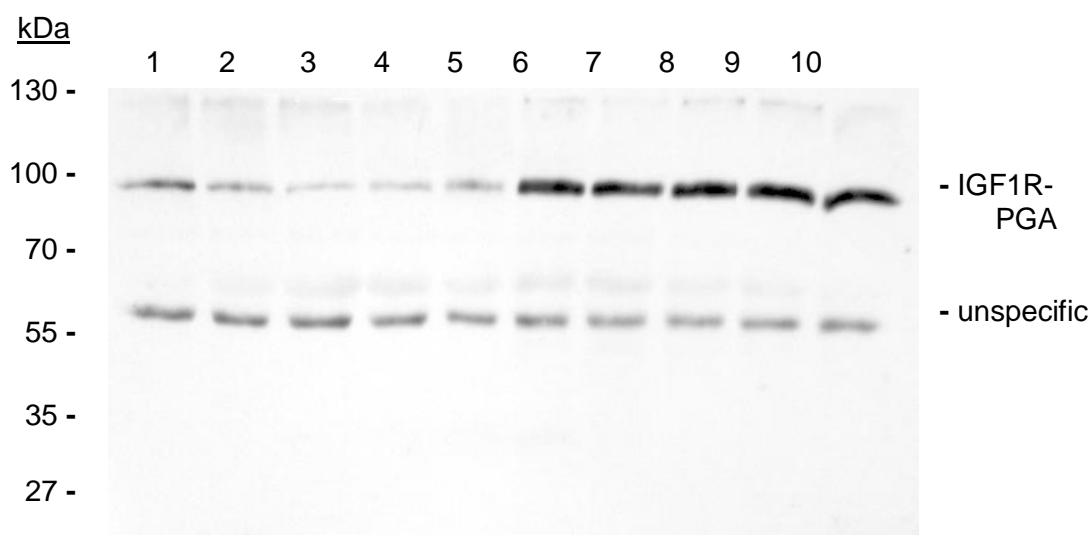
Figure 5.25: *Precipitation of recombinant IGF1R from cell extracts by IGF1R-Ab containing sera. Western blot analysis of IGF1R from cell extract after immunoprecipitation by protein A using five serum samples with low (1-5) or high (6-10) signals in the IGF1R-Ab luciferase precipitation assay. Precipitated proteins were subjected to SDS electrophoresis, blotted and probed by an antibody recognizing the PGA14 affinity tag located on the IGF1R-fuion protein (IGF1R-PGA).*

5.4.2 IGF1R-Ab inhibit signal transduction of IGF1R

HepG2 cells were incubated after serum starvation in the presence of control and IGF1R-Ab positive Ig preparations, respectively. IGF1R activation state was monitored by phosphotyrosine-specific antibodies.

Under basal conditions, which represent an assay for activating IGF1R-Ab, Ig from IGF1R-Ab positive serum samples were not stimulating IGF1R activity, and no consistent effects of the Ig on IGF1R autophosphorylation were observed (Figure 5.26, A). In

contrast, in the assay for detection of inhibiting activity of IGF1R-Ab, IGF1-induced autophosphorylation of IGF1R was observed in IGF1R-Ab negative sera (Figure 5.26, B, lanes 1-5). Ligand-induced activation of IGF1R by IGF1 was shown by a specific increase in the lower phosphorylated IGF1R band, which was efficiently abrogated by all IGF1R-Ab positive Ig preparations tested (Figure 5.26, B, lanes 6-10). Phosphorylated beta-subunit of IGF1R was detected using anti-IGF1R (phospho-Tyr1165/-Tyr1166) antibody. Equal loading and membrane transfer in both analyses was verified by actin staining.
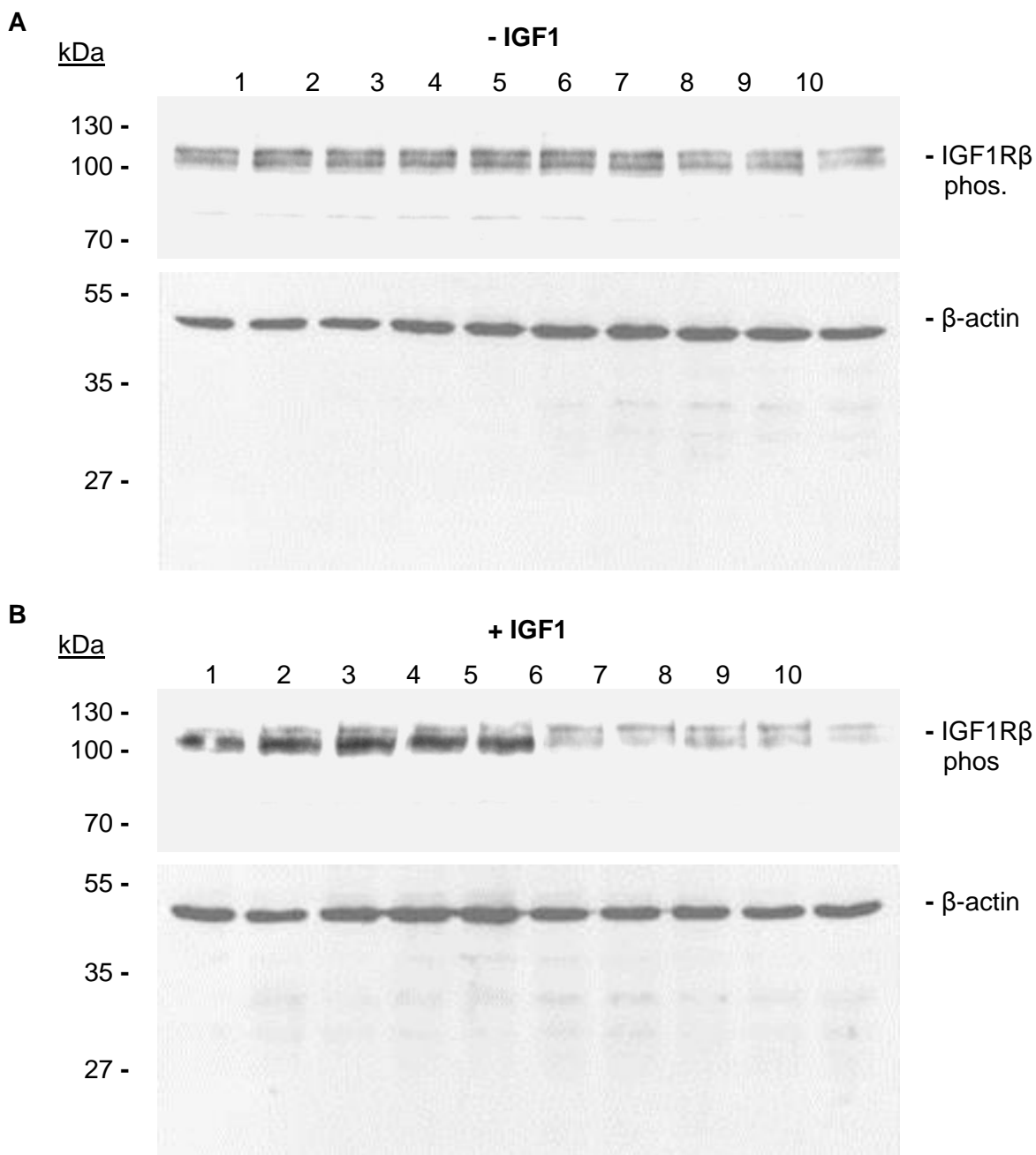
Figure 5.26: *Biological effects of isolated Ig from IGF1R-Ab positive or negative serum samples on autophosphorylation of the IGF1R. Ig isolated from five control (1-5) and five IGF1R-Ab positive serum samples (6-10) were incubated with HepG2 cells either in absence (A) or*

in presence (B) of exogenous IGF1 (1 ng/ml). Phosphorylated IGF1R in cell lysates was detected by Western blot analysis using anti-IGF1R (phospho-Tyr1165/-Tyr1166) antibody. Equal loading and membrane transfer in both analyses was verified by actin staining. This experiment was replicated once with the same results.

IGF1R autoantibodies did not stimulate IGF1R phosphorylation, but reduce the IGF1 dependent receptor phosphorylation and can thus be considered as IGF1 antagonists.

5.4.3   IGF1R-Ab inhibit IGF1-dependent proliferation

In agreement with these previously noticed inhibitory effects of the IGF1R-Ab on IGF1R activation, ATP concentrations of IGF1-stimulated MCF-7 cells were monitored (Figure 5.27).
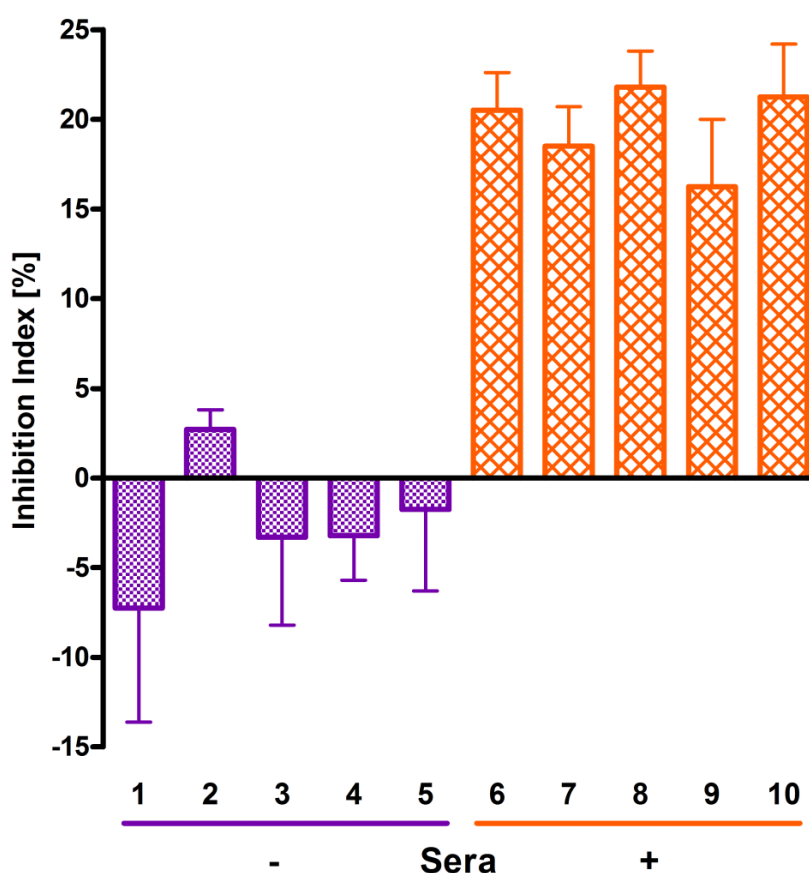
Figure 5.27: *Effect of IGF1R-Ab on cell growth (viability / proliferation). Ig isolated from five serum samples with low (1-5) or high (6-10) signals in the IGF1R-Ab assay were incubated with MCF7 cells in the presence of 1 ng/ml of IGF1 for 5 days. Number of viable cells was determined based on quantification of ATP. The inhibition index illustrates the potential of the Ig to reduce number of viable cells. Each value represents the mean +/- SD of quadruplicate measurements.*

ATP concentrations of IGF1-stimulated MCF-7 cells were reduced upon co-incubation with all analyzed Ig from positive sera by up to 25% from IGF1R-Ab negative sera reflecting modulatory effects of the aAb on IGF1-dependent cell proliferation, apoptosis or

both. ATP concentrations of IGF1-stimulated MCF-7 cells stayed on a comparable level or increased slightly after incubation with Ig from IGF1R-Ab negative sera.

5.4.4   IGF1R-Ab antagonize IGF1 binding to the IGF1R

An IGF1 competition assay was performed *in vitro* in tube format using IGF1R-2B5 fusion protein as hormone acceptor. As basal experimental setup, a similar one as described for the determination of binding capacity of recombinantly expressed receptor protein was chosen (e.g. section 4.1.5). Therein, the biological accuracy and suitability of hormone binding was proved. After adding control or serum samples to the immobilized IGF1R, acridinium labeled IGF1 was supplemented to identify an inhibitory effect of pre-added aAb on hormone binding. Samples without serum served as reference point for the inhibition index, when set to 0% of inhibition while showing 100% of possible binding capacity at the receptor. Inhibition index was referred to the B100 sample, as previously described, after data being normalized to RLU obtained from wild type cells (data not shown). Competition samples using 50 or 5 µg/ml unlabeled IGF1-hormone served as assay competition and functionality controls of the recombinant receptors. Both amounts of unlabeled IGF1 were able to compete successfully the labeled IGF1 from its receptor binding site, represented by inhibition indices of nearly 97% for 50 µg/ml or 92% for 5 µg/ml unlabeled IGF1 (Figure 5.28, A). Negative samples as well as a mixture of negative serum samples obtained inhibition indices between 5 and 25%. The positive serum samples as well as a mixture of positive serum samples yielded inhibition indices up to 36%. The box plot of IGF1R-Ab negative and positive samples showed very similar mean values of 19.2% inhibition index for negative and 20.1% for positive samples (Figure 5.28, B). While the interquartile range was nearly identical, IGF1R-Ab positive sample were much more scattered, ranging from 2 to 36% inhibitory index.

A

B
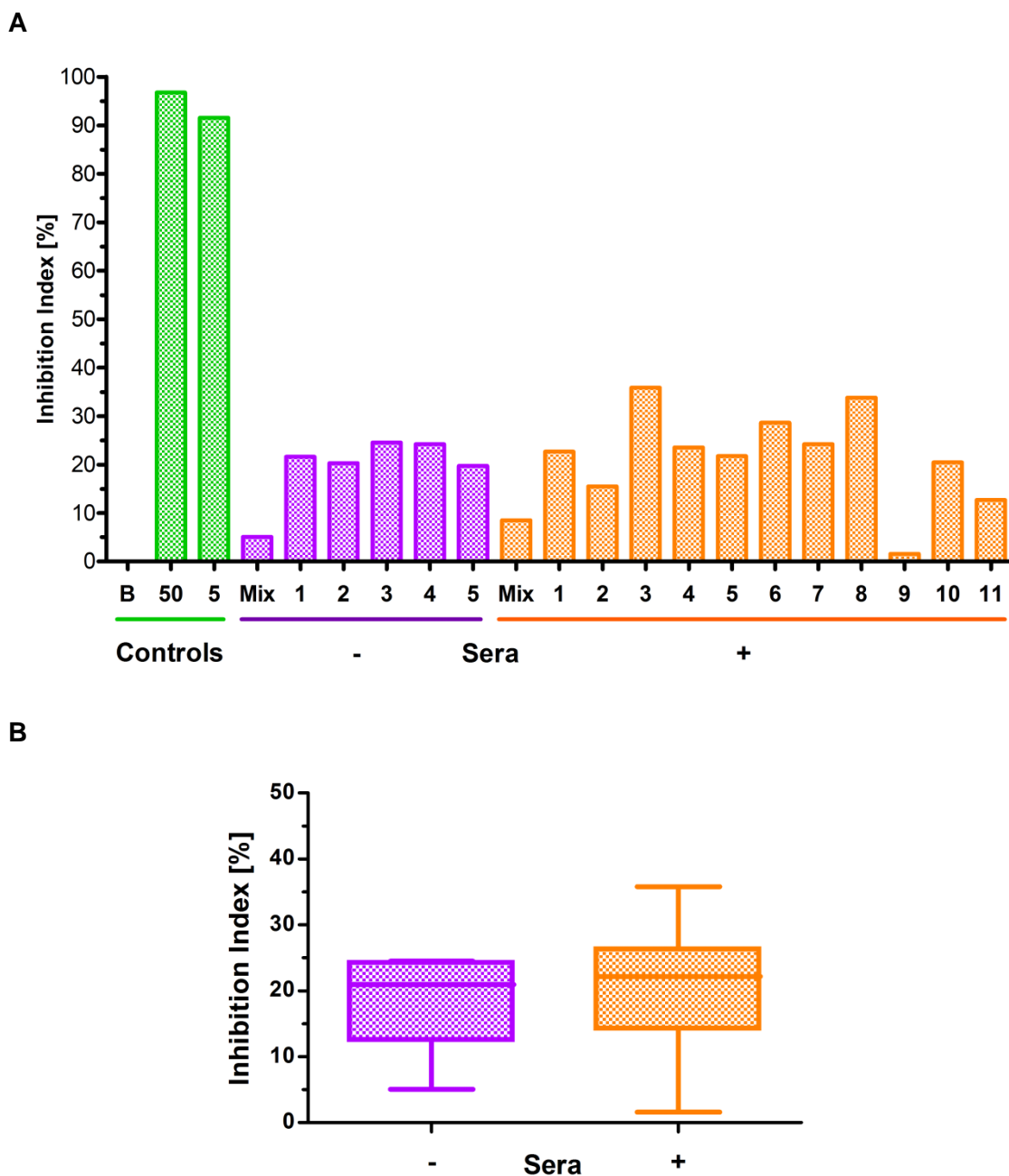
Figure 5.28: ***Effect of IGF1R-Ab on IGF1 hormone binding.*** *(A): Competitive effects from IGF1R-Ab negative and positive sera in the IGF1-hormone competition assay on the IGF1R (negative samples n = 6, including 1 mix of negative sera; positive samples n = 12, including 1 mix of positive sera. Binding-100%-sample (B) without serum served as reference point for the inhibition index, competition samples using 50 (50) or 5 µg/ml (5) unlabeled IGF1-hormone served as assay binding controls. Controls were performed in multiplies, displayed as mean; serum samples were performed in single determination due to serum limitations. Comparable results were obtained in an additional independently performed experiment. (B): Boxplot showing distribution of the inhibition index from IGF1R-Ab negative and positive sera in the IGF1 competition assay on the IGF1R. Presented sera correspond to the same ones shown in (A). The inhibition index illustrates the potential of the IGF1R-Ab to block IGF1 binding to the IGF1R.*

5.4.5 IGF1R analysis for the antigenic domain

Next, the binding capacity of IGF1R autoantibodies to different parts of the extracellular domain of IGF1R was investigated. The extracellular and trans-membrane domain of IGF1R was virtually cut in 4 pieces of around 200 to 250 amino acids in size each (Table 5.12). Epitope 1 enclosed the N-terminus of the mature receptor (aa 31-273), while epitope 2 contained the adjacent part of the α-subunit (aa 264-506). Epitope 3 covered the C-terminal piece of the α-subunit (aa 497-737), whereas epitope 4 (aa 738-938) enclosed the short extracellular part of the β-subunit. Schematic depiction of the epitopes engineered and originating from IGF1R are presented below (Figure 5.29). Fusion proteins between cDNA for these 4 epitopes and cDNA for luciferase were constructed and recombinantly expressed in HEK293 cells. The plasmid construction was described in 4.2.2.

Table 5.12: *Description of constructed epitopes of IGF1R. The amino acid sequence from the mature human IGF1 receptor is given for every epitope, their position in correlation to the whole receptor and the length of the epitope sequence fused to luciferase.*

Epitope	Amino acid (aa)	Position	Length (aa)
1	31-273	N-terminus of IGF1R	243
2	264-506	middle part of α-subunit	243
3	497-737	C-terminal part of α-subunit	241
4	738-938	N-terminal part of β-subunit	201
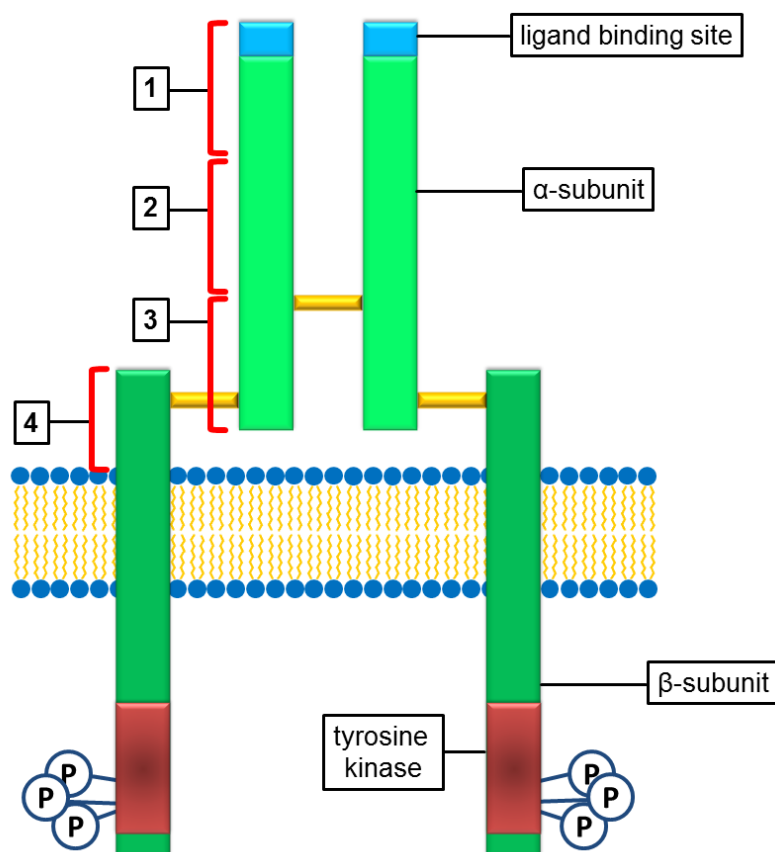
Figure 5.29: *Schematic depiction of the IGF1R domains selected for epitope analyses. Fusion proteins were constructed between the indicated epitopes of the receptor and luciferase. Positions of epitopes were indicated by red braces, did partially overlap, or border each other directly. Epitope 1 enclosed the N-terminus of the mature receptor (aa 31-273), while epitope 2 contained the adjacent part of the α-subunit (aa 264-506). Epitope 3 covered the C-terminal piece of the α-subunit (aa 497-737). Epitope 4 (aa 738-938) enclosed the short extracellular domain of the β-subunit. The elements are presented schematically and not necessarily at scale. Adapted from Figure 2.2.*

Extracts prepared from the cells expressing the IGF1R-epitope luciferase-fusion proteins were used for detection and characterization of IGF1R autoantibodies in human sera by immunoprecipitation analysis. A number of 3 IGF1R-aAb positive sera and a negative control serum were analyzed by precipitation of the complex formed with the full length IGF1R-luciferase fusion. In addition, immunoprecipitations were conducted with the 4 IGF1R domain epitopes separately fused to luciferase. Using the full length (FL) IGF1R, a clearly positive signal for IGF1R-aAb with at least 2.5- to more than 8-fold higher signal than control was shown for IGF1R-aAb positive sera 1-3 compared to serum control (Figure 5.30). When binding of IGF1R-aAb from sera 1 and 2 was tested with one of the four IGF1R-epitopes, no considerable divergence became visible. All samples showed slightly increased signals compared to control, but binding was not nearly as good as with

the full length receptor. A similar result was obtained, when IGF1R-aAb positive serum 3 was used. However, this serum showed some reaction to epitopes 3 and 4, but still not nearly comparable to the full length receptor. Using different epitopes for precipitating control serum, no differences appeared compared to the use of the full length receptor.
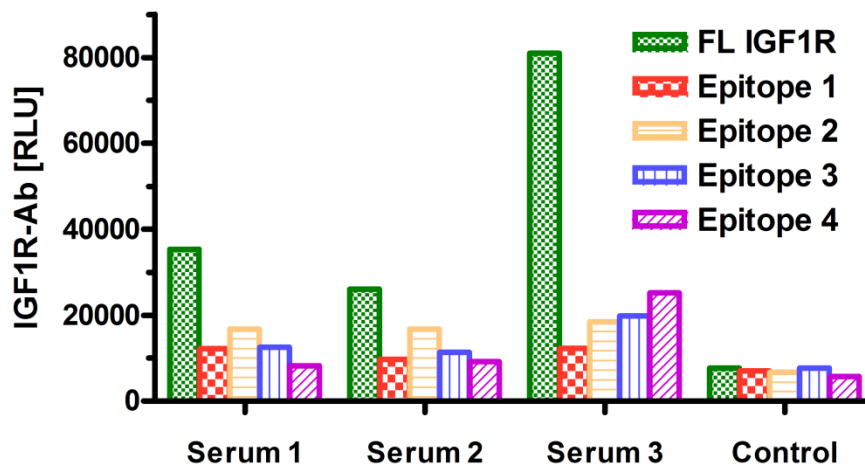
Figure 5.30: *Epitope analysis. Interaction of autoantibodies from human sera with the full-length (FL) IGF1R and with different domains of the extracellular part of the IGF1R (epitopes 1-4). Three positive sera (Serum 1-3) and one negative serum (Control) were analyzed for IGF1R autoantibody concentrations by measuring IGF1R-Luc activity in the immunoprecipitates. Each value represents the mean of duplicate measurements. Comparable results were obtained in several additional independently performed experiments.*

5.4.6 Bridging experiments with monoclonal antibodies against the IGF1R

As previously described, the generated antibodies versus IGF1R were able to bind its antigen specifically (see 5.3.5; Figure 5.24). To test, if both variable chain regions of the monoclonal antibodies bind IGF1R simultaneously, IGF1R was presented as the donor molecule immobilized to a 2B5-antibody-coated tube using the 2B5-peptide tag fused C-terminal to IGF1R. After applying the monoclonal antibodies (100 µg/ml) and exhaustive washing procedures, an IGF1R-Luc fusion protein was added and luciferase activity was determined following washing. Monoclonal TSHR-antibody (TRAK1) and monoclonal antibody against FABP (FABP1) served in the same concentration as negative, non-binding antibody controls, PBS as buffer control (Figure 5.31). Monoclonal antibody AK2045/01 showed a 15-times higher RLU and AK2046/01 showed an 11-times higher RLU than the negative controls. AK2047/01 and AK2048/01 gave results similar to the negative control samples, AK2049/01B yielded an around 3.5-times higher signal than control. These results are in line with the preliminary experiments using human serum (section 5.2.1, Figure 5.15) and support the notion that the IGF1R-Ab are capable of binding two molecules of their antigen with both existing variable regions simultaneously. This simultaneous binding of two antigen molecules constitutes the molecular basis for

our construction of a bridge-assay test format for the routine and fast determination of IGF1R-aAb concentrations.
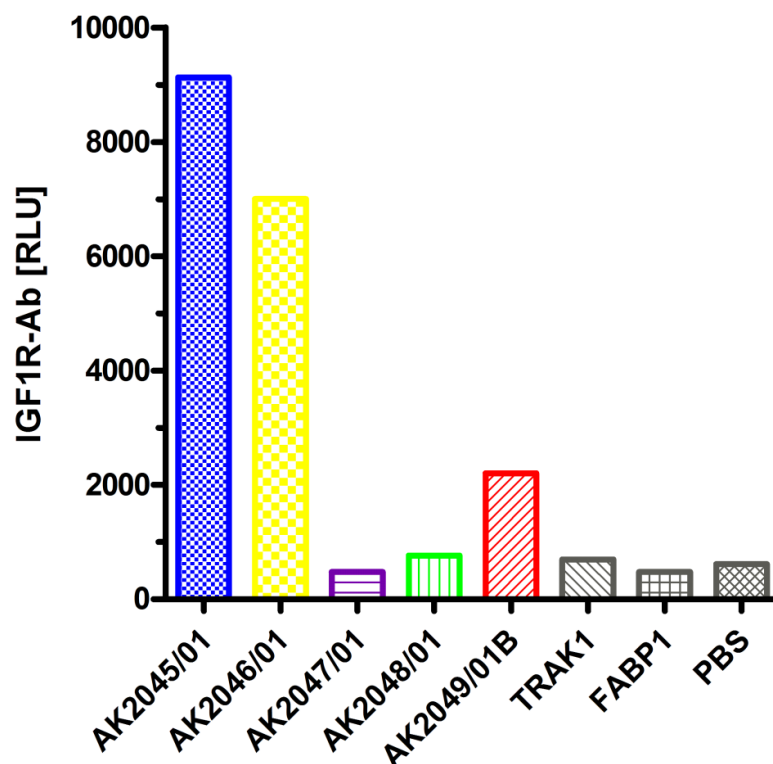
Figure 5.31: *Binding of two IGF1R molecules by monoclonal antibodies.* *IGF1R was immobilized to a 2B5-antibody-coated tube using the 2B5-peptide tag fused C-terminal to IGF1R. After adding the newly generated monoclonal antibodies (100 µg/ml) and exhaustive washing, an IGF1R-Luc fusion protein was added and luciferase activity was determined following washing. Monoclonal TSHR-antibody (TRAK1) and monoclonal antibody against FABP (FABP1) served in the same concentration as negative, non-binding antibody control, PBS as buffer control. Columns represent mean of double determinations, the experiment was replicated once with similar results.*

5.4.7   Cross binding of IGF1R-Ab to the IR

This led directly to the question, if on one hand two antibodies exist in those sera, whereas one represents an autoantibody reactive with the IGF1R and the other with the IR. On the other hand, an individual autoantibody species may bind both, the IGF1R and IR, due to their high sequence and structural similarity of around 60% [174, 175]. Consequently, previously identified sera positive for IGF1R- and IR-aAb (section 5.6) were subjected to a bridge assay in which the cross linking of IGF1R with IR through the aAb was tested (hetero-bridge assay). The experimental setup was adopted from the previously described homo-bridge assay (section 5.2) with the exception that the same antigen was not used twice for binding every Fab-region of the antibody, but the IGF1R and the IR were applied in parallel. In the first step, the IR, fused to a 2B5 peptide tag, was immobilized to 2B5-antibody coated tubes to catch the aAb. In a second step, an

IGF1R-Luc protein was bound by the second Fab-region of the IR-bound antibody and a successful hetero-bridge was detected by luciferase substrate turnover (Table 5.13, main column 2). Relative antibody titers were recorded in RLU for one sample without serum, a sample with both IGF1R-Ab and IR-Ab negative serum, and three sera positive for IGF1R-Ab and IR-Ab, respectively. Values were normalized to the highest value of the individual set and presented in an additional column. In the IR – IGF1R hetero-bridge assay, all three double positive sera showed 7 to 8 times higher RLU values than the negative serum, which represented only 13 % of the maximum signal value. Values for the three double positive sera obtained were closely together between 36.6 and 42.2 thousand RLU ranging from 87 to 100% of maximum value, respectively. The same experiment was performed vice versa, catching sera antibodies with immobilized IGF1R-2B5 antigen and detecting bound antibodies by binding to the IR-Luc fusion protein (Table 5.13, main column 3). Herein, the IGF1R-Ab and IR-Ab negative serum represented a value of 15% compared to the maximum, values for the three double positive sera obtained were between 4.8 and 17.9 thousand RLU, i.e., ranging from 27 to 100% of maximum value, respectively. The sample without serum yielded 5% of the maximum value in both assay variants. Double positive sera 2 and 3 showed very similar results in both assay variants, independent from the antigen position. For positive serum 1, the maximum value was obtained in the IR – IGF1R hetero-bridge assay, but a value of 27% of the maximum value in the IGF1R – IR hetero-bridge assay.

A potential cross-reactivity of the five monoclonal antibodies newly generated against the IGF1R were analyzed in a homo-bridge assay for the binding of two IGF1R molecules (Section 5.4.6 and Figure 5.31, represented in Table 5.14, column 2), in which 3 of 5 monoclonal antibodies showed high to moderate capability of binding both antigens simultaneously. The normalized binding of these antibodies scored values of 100, 77 and 24%. Two remaining monoclonal antibodies to the IGF1R and to unrelated antigens and PBS, which served as assay controls, scored beneath 8% of the maximum value. A hetero-bridge assay for binding of IGF1R and IR at once was performed using the same samples. The relative positions of the IGF1R and the IR as antigen were changed by exchanging the catching and the detection antigens from one assay to the other (Table 5.14, column 3 and 4). In both tested hetero-bridge assay formats AK2045/01 yielded the highest detectable value of RLU, while AK2046/01 showed around 55% of its rate in both hetero-bridge assays, in comparison to 77% in the IGF1R-IGF1R homo-bridge assay. Considering the IR-IGF1R assay, the other analyzed monoclonal antibodies as well as controls showed results near and beneath 10% of the maximal value. Regarding the complementary IGF1R-IR assay, the obtained RLU were in general clearly lower than in the previously described ones, and the range smaller and even the control samples

showed scores of around 20%. However, obvious binding of both antigens was obtained with AK2045/01, AK2046/01 and AK2049/01B.

Table 5.13: *Cross-reactivity of autoantibodies in sera determined positive for IGF1R- and IR-aAb. Serum samples, determined previously positive in IGF1R-Ab or IR-Ab precipitation assays, were subjected to a hetero-bridge assay in two variants (main column 2 or 3). The immobilized antigen as 2B5-peptide fusion protein is indicated in row 2, the luciferase-fusion protein used in row 3. Relative antibody titers are presented in both assay setups in RLU for one sample without serum, an IGF1R-Ab and IR-Ab negative serum, and 3 IGF1R-Ab and IR-Ab positive sera. Values are normalized to the highest value of the individual set in an additional column.*

	IR – IGF1R		IGF1R – IR	
immobilized	IR-2B5		IGF1R-2B5	
detection by	IGF1R-Luc		IR-Luc	
serum	[RLU]	[% of max.]	[RLU]	[% of max.]
without	2135	5	947	5
negative	5348	13	2616	15
positive 1	42240	100	4814	27
positive 2	39341	93	17961	100
positive 3	36646	87	12839	71

Table 5.14: *Cross-reactivity of monoclonal antibodies against IGF1R to the IR. Five monoclonal antibodies created against the IGF1R as antigen were analyzed in a homo-bridge assay for binding of two IGF1R molecules and in a hetero-bridge assay for binding to one IGF1R and one IR. The presentation of the different antigens was subject to change. The catching and detection antigens used are indicated in the appropriate row for every experimental setup. Monoclonal antibodies to unrelated antigens and PBS served as assay controls. Results are presented in RLU and normalized to the highest value of the individual set.*

	IGF1R – IGF1R		IR – IGF1R		IGF1R – IR	
immobilized	IGF1R-2B5		IR-2B5		IGF1R-2B5	
detection by	IGF1R-Luc		IGF1R-Luc		IR-Luc	
sample	[RLU]	[% of max.]	[RLU]	[% of max.]	[RLU]	[% of max.]
AK2045/01	9130	100	7458	100	1558	100
AK2046/01	7002	77	4025	54	880	56
AK2047/01	474	5	518	7	324	21
AK2048/01	764	8	624	8	355	23
AK2049/01B	2204	24	859	12	1050	67
TRAK1	697	8	336	5	283	18
FABP1	477	5	295	4	329	21
PBS	613	7	449	6	373	24

5.5 Prevalence of IGF1R-aAb in different patient populations

The IGF1R autoantibody precipitation assay was designed for analysis of mid-sized clinically relevant cohorts, which means a sample number of up to 500 serum samples. The precipitation assay has a volume requirement of 10 µl or less, but manual processing and treatment of every single sample is a labor-intensive process due to precipitation and incubation steps during the procedure. Total assay procedure required three days and all samples of one cohort had to be treated the same, which was more difficult when sample number increased. When sample collectives were very large, the analyses have been split in several individual assay sets, otherwise an identical treatment of all samples was not ensured.

5.5.1 Graves' Orbitopathy

As described above, the IGF1R is considered to be of high importance in Graves' Orbitopathy (GO). This led to the hypothesis, that antibodies, speculatively stimulating antibodies, directed against the IGF1R were involved in GO development [43, 44]. Thus, the IGF1R-Luc precipitation assay was the ideal method for detecting IGF1R-Ab in serum samples of diseased and healthy individuals. A sample collective of serum samples, originating from 584 patients suffering from GO, was analyzed using the IGF1R-autoantigen specific precipitation assay compared to 92 control sera from healthy individuals. Serum samples were kindly provided from Dr. Anja Eckstein (Department of Ophthalmology at the University Hospital Essen, Germany). Both, GO and control samples included around 90% of female patients in an age range of 20 to 65 years. The cutoff values of the analyzed sample collective was calculated after excluding the upper and lower 5% of values, SD was determined and values above MV+2SD were classified as slightly positive, values above MV+3SD as clearly positive. The key data for the IGF1R-Ab originating from both, sera of the control group and sera of GO patients, are presented in (Table 5.15, A) in raw data and relative values, when MV was set to 1.0, as well. Threshold values were also aligned to the MV. The result of relative IGF1R-Ab titers in both inspected sample collectives were plot in a diagram next to each other (Figure 5.32). A Y-axis in logarithmic scale was chosen in order to improve the arrangement of all included data. Tested sera showed wide spread results again, while the main population of samples did not cross a relative IGF1R-Ab titer of 3.0. A constantly numerously shrinking set of samples was obtained in rising relative titers up to values of at least 30. A few sera spike to higher relative titers, one at around 50 in the control group, and four up to 80 in the patient group. Distribution of samples over the whole plotting area seemed comparable in control samples and serum samples of patients with GO. In the control cohort, values above a relative titer of 4.35 (MV+2SD) were classified as slightly positive

and values above 6.03 (MV+3SD) as clearly positive. For the samples from GO patients, values above a relative titer of 3.45 (MV+2SD) were classified as slightly positive and values above 4.67 (MV+3SD) as a clearly positive criterion for positivity. After analysis of the data, for the control group 8 sera were obtained, matching the criterion for strong positivity, but no additional as slightly positive (Table 5.15, B). This led to a prevalence of IGF1R-Ab in the control group of 8.7% for both point of views, because values representing distinct positive samples were included in the Threshold for slightly positive samples. In the cohort of GO patients, 59 sera showed a positive relative titer for IGF1R-Ab, leading to a prevalence of 10.1%. 45 out of these 59 positive serum samples did also match the criterion for a high relative IGF1R-Ab titer, representing 7.8% of the samples.

Table 5.15: *Prevalence of aAb to the IGF1R in serum samples of patients with Graves' disease.* (A) Key data of IGF1R-Ab assay for 92 control samples and 584 serum samples from patients with Graves' Orbitopathy (GO). Both the direct RLU values and the calculated ratios with respect to the mean value (MV), which was determined after excluding the upper and lower 5% of total values, were given with threshold values for 2 or 3SD. (B) Prevalence of aAb to IGF1R in these serum samples. Both the absolute number and percentage of aAb positive samples were indicated.

A

Assay	Control sera		Patient sera	
Unit	RLU	MV = 1.0	RLU	MV = 1.0
MV	2211	1.00	1742	1.00
SD	3708	1.68	2131	1.22
MV+2SD	9627	4.35	6004	3.45
MV +3SD	13335	6.03	8136	4.67

B

Assay	Control sera (n = 92)		Patient sera (n = 584)	
Positive sera	IGF1R-aAb [n]	Prevalence [%]	IGF1R-aAb [n]	Prevalence [%]
> MV+2SD	8	8.7	59	10.1
> MV+3SD	8	8.7	45	7.7
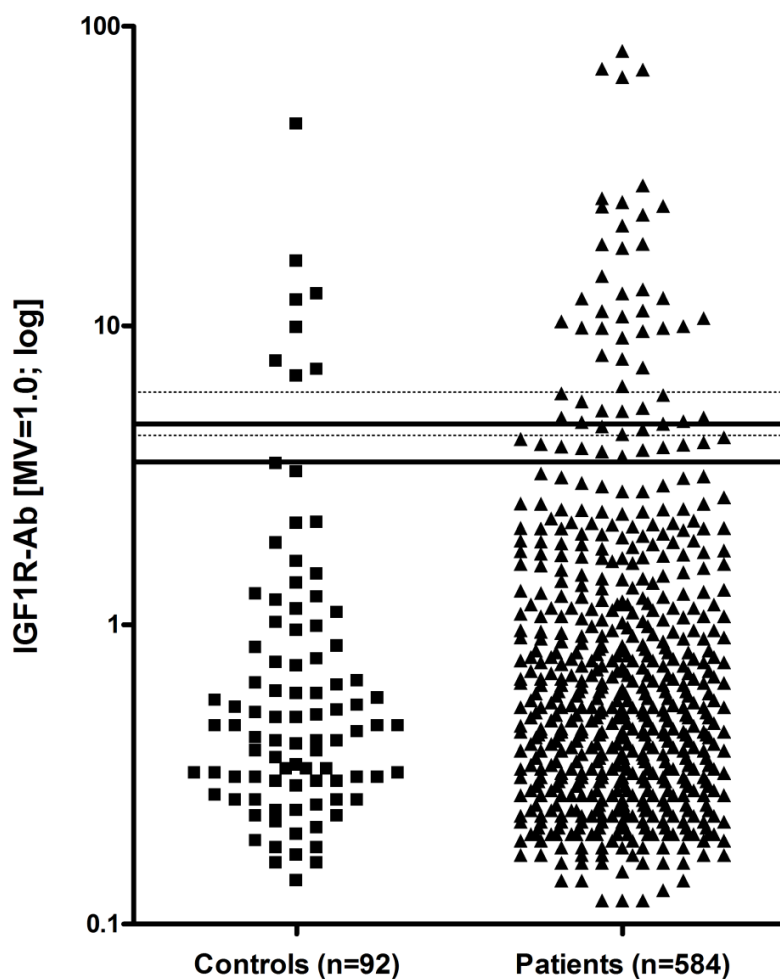
Figure 5.32: *Prevalence of aAb to the IGF1R in serum samples of patients with Graves' disease.* Determination of IGF1R-aAb in 584 serum samples from patients with Graves' Orbitopathy (GO) and in 92 control samples, using the IGF1R-Ab precipitation assay. Mean value (MV) and SD were calculated after excluding the upper and lower 5% of values for each cohort. MV was set to 1.0. Applied relative aAb values of all serum samples were plotted in the graph. Threshold values for positivity were calculated, while values above MV+2SD (lower line) were classified as slightly positive, values above MV+3SD (superior line) as clearly positive (dotted lines – control samples; solid lines – GD samples). Y-axis in logarithmic scale in order to improve arrangement of data.

5.5.2 Diabetes mellitus

A sample cohort of 401 serum samples originating from diabetes mellitus patients was investigated blinded to the phenotype for the presence of IGF1R-aAb. The general description of the disease "diabetes mellitus" in the sample collective was not specified in more detail. For this reason, it was considered that a mixed population of diabetes subtypes is represented in this cohort. For analyzing this large number of samples, the cohort was split into 2 comparable sets in size, which have been tested one after the other. It was attempted to conduct all experimental steps in an identical way at two consecutive dates. Experimental set 1 contained serum samples 1 to 207, experimental set 2 contained serum samples 208 to 401. Results are presented as RLU as classification for IGF1R-aAb for every set individually (Figure 5.33, (A) Set 1, (B) Set 2). For determination of positivity, the mean signal value (MV) of the sample set was calculated after excluding the upper and lower 5% of values to ensure availability of normal or near to normal serum samples for calculation of the mean, on which positivity ranking was based. Standard deviations (SD) were calculated with the described values, while values above MV+2SD were classified as slightly positive, values above MV+3SD as clearly positive. Key data for the IGF1R-Ab assays are presented for each assay set individually below (Table 5.16, A). The mean value differed between both assay sets from ~12.6 thousand RLU in set 1 and ~21.8 thousand RLU in set 2. Thus, also different SD values were calculated. The signals of most of the samples were located in a bulk representing a cloud between 8 thousand and 15 thousand RLU for set 1 or 15 thousand and 27 thousand RLU for set 2, respectively. A smaller subpopulation existed below this cloud, and a larger number of samples were observed clearly above the cloud. This image was obtained similarly for both assay sets. In both sets one value spiked to very high RLU values above 114 thousand RLU and 150 thousand RLU, respectively. Considering criteria for positivity, 10 serum samples appeared strongly positive with values above MV+3SD, 8 samples were obtained in between the values for MV+2SD and MV+3SD, as a result 18 values represented positive samples for IGF1R-Ab (Table 5.16, B). The prevalence for IGF1R-Ab in assay set 1 was calculated to 4.9% for strongly positive samples, and to 8.7% for all positive serum samples. Prevalence in set 1 was referred to 206 serum samples, although 207 serum samples were analyzed, because one serum turned out to be wrongfully labeled as diabetes serum, the patient was truly suffering from pancreatitis. For this particular serum, an IGF1R-Ab value of 11012 was determined, which fits perfectly to the calculated MV and was clearly negative. In assay set 2, 12 serum samples appeared strongly positive with values above MV+3SD, 7 samples were obtained in between the values for MV+2SD and MV+3SD, as a result 19 values represented positive samples for IGF1R-Ab. The prevalence for IGF1R-Ab in assay set 2

was determined to 6.2% for strongly positive samples and to 9.8% for all positive serum samples.
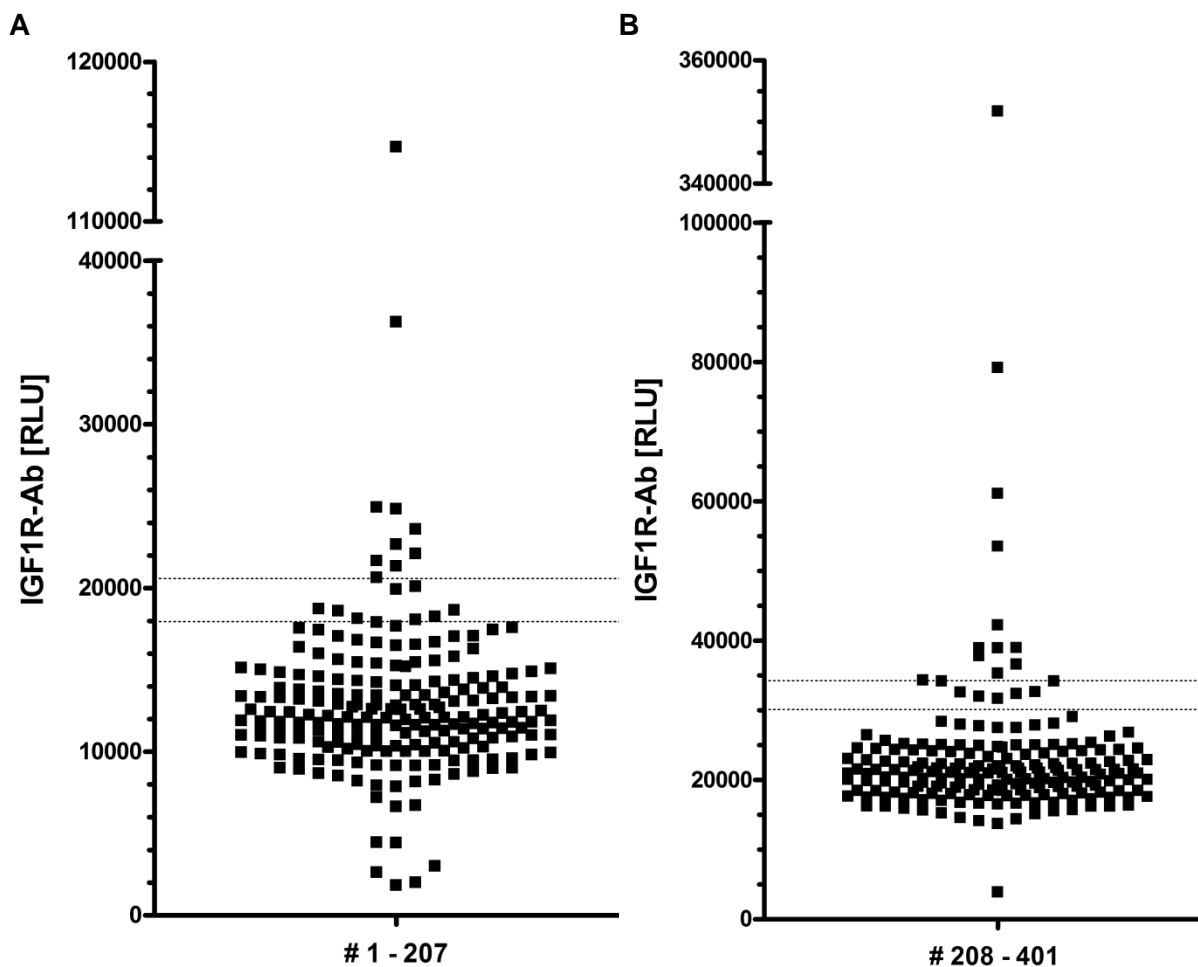
Figure 5.33: *Prevalence of aAb to the IGF1R in a cohort of diabetes mellitus patients.*
Determination of IGF1R-aAb in samples with consecutively labeled numbers 1 to 207 (A) and in
samples with consecutively labeled numbers 208 to 401 (B) in the IGF1R-Ab precipitation assay.
Both assays were prepared independently at different dates due to practicability reasons to ensure
proper and highly similar experimental conditions within one sample set. Mean value (MV) and SD
were calculated after excluding the upper and lower 5% of values. Values above MV+2SD (lower
dotted line) were classified as slightly positive, values above MV+3SD (superior dotted line) as
clearly positive.

Table 5.16: *Prevalence of aAb to the IGF1R in a serum collective of diabetes mellitus*
patients. (A) Key data of IGF1R-Ab assay for 401 serum samples split into two assay sets. Both
the direct RLU values and the calculated ratios with respect to the mean value (MV), which was
determined after excluding the upper and lower 5% of total values, are given with threshold values
for 2SD or 3SD. (B) Prevalence of aAb to IGF1R in these serum samples. Both the absolute
number and percentage of aAb positive samples are indicated. Consecutively listed blinded sample
numbers were labeled by an # in front of the accordant digit. Asterisk label (*): Sample number
#148 was wrongfully labeled as diabetes serum, patient was truly suffering from pancreatitis.

Prevalence calculations were performed for n = 206 in sample set 1 and n = 400 for the total cohort.

A

Assay	Set 1: # 1-207 (n = 206) *		Set 2: # 208-401 (n = 194)	
Unit	RLU	MV = 1.0	RLU	MV = 1.0
MV	12630	1.00	21810	1.00
SD	2653	0.21	4160	0.19
MV+2SD	17936	1.42	30130	1.38
MV +3SD	20589	1.63	34290	1.57

B

Assay	Set 1: # 1-207 (n = 206) *		Set 2: # 208-401 (n = 194)	
Positive sera	IGF1R-aAb [n]	Prevalence [%]	IGF1R-aAb [n]	Prevalence [%]
> MV+2SD	18	8.7	19	9.8
> MV+3SD	10	4.9	12	6.2
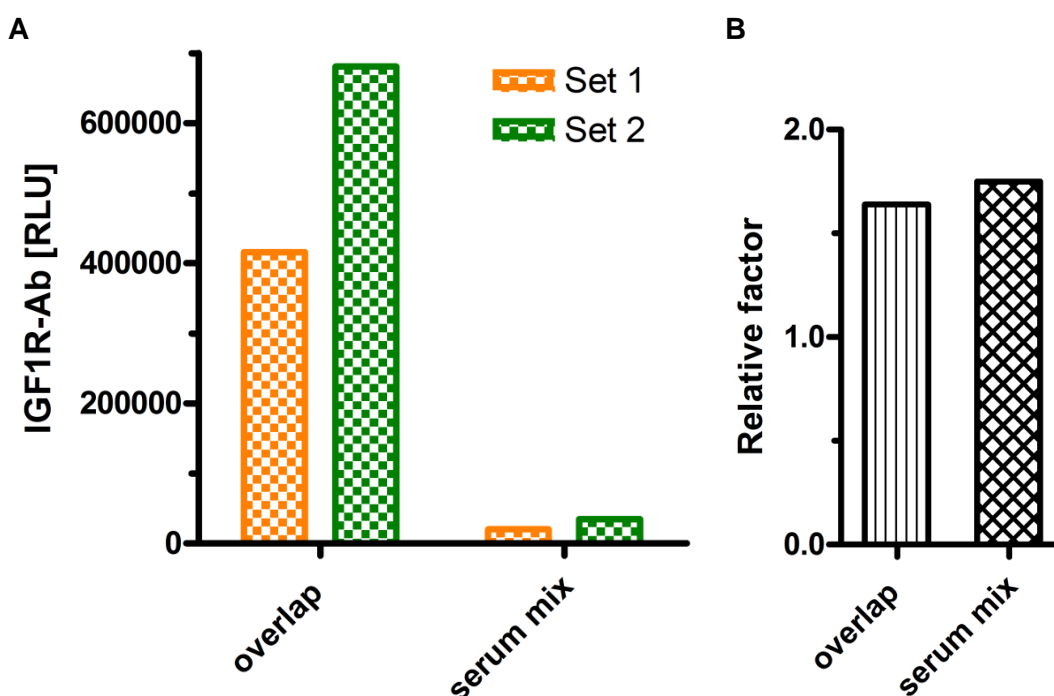
Figure 5.34: *Control experiments proceeded in both assay sets.* *(A) 17 serum samples of the present study were analyzed in both assay sets individually, indicated as "overlap" samples. Their RLU values were added, the same was done for a measurement of 4 identical serum samples, originating from a standard-serum mixture. (B) A relative factor between both assay sets was determined from summed up RLU values of the overlap samples and standard sera.*

Controls have been performed in parallel in both assay sets. A number of 17 identical serum samples from assay set 1 were additionally measured in assay set 2, same was a standard-serum-mix in quadruplicates. RLU values of these samples were summed up in both sets individually (Figure 5.34, A). An increase of RLU was clearly visible in assay set 2 in both groups of control samples, compared to assay set 1. This was also observed

previously by looking at the central distribution of values in both assay sets (Figure 5.33) and the calculated means (Table 5.16, A), which were evidently higher in assay set 2. A relative factor between both assay sets was determined from summed up RLU values of each control-sample group. The result showed a factor of 1.64 for assay set 1 and a nearby factor of 1.75 for assay set 2 (Figure 5.34, B). Overlapping serum samples, which have been analyzed in both sets, were examined in more detail (Table 5.17). One out of 17 samples was positive for IGF1R-Ab in assay set 1, 10 were highly positive and 6 were negative. All negative samples remained negative in assay set 2. Seven highly positive samples were same classified in set 2, two of those were degraded to positive samples and one changed to negative, but was extremely close to the threshold value. The positive sample remained positive in assay set 2. Collectively, no large differences inside one assay set and between both assay sets occurred, considering systematical approaches and direct comparison.

Table 5.17: *Overlap samples measured in assay set 1 and set 2. A number of 17 identical serum samples from the present study were analyzed in both assay sets. Samples rated positive (MV+2SD) were indicated in light green, samples determined strongly positive (MV+3SD) were highlighted in dark green. Key data from both assays are transferred from Table 5.16 for comparison of obtained data in both sets. Summed up RLU values of these 17 overlap samples are presented in Figure 5.34, A.*

Overlap samples #	Set 1 [RLU]	Set 2 [RLU]
14	20080	32933
15	22096	31829
16	20628	35699
23	24814	55846
26	21319	29688
28	21650	32832
37	36237	51361
42	22645	46323
54	114655	130552
142	23593	50105
201	10390	20506
202	11794	27875
203	11604	27587
204	10892	25369
205	10022	20676
206	24918	42409
207	8660	19165
Sum	415997	680755
Key data assay sets		
MV	12630	21810
MV+2SD	17936	30130
MV+3SD	20589	34290

Based on data presented above (Table 5.16), mean values of the individual assay sets were set to 1.0 yielding relative sample values for every assay. Obtained data of both sets (n=401) were plotted as relative IGF1R-Ab titer in one graph, while criteria for positivity were averaged for graphical presentation therein (Figure 5.35). Values above a relative titer of 1.40 (MV+2SD) were classified as slightly positive, values above 1.60 (MV+3SD) as clearly positive. Consequently, a similar distribution of sample values for IGF1R-Ab appeared as previously described for individual analysis of the assay sets (compare to Figure 5.33, A and B). The mean population of samples was again located in a bulk representing a cloud between a relative titer of 0.6 and 1.3. A subpopulation existed below this cloud and a larger number of samples was obtained above. Two samples spiked over the bulk at relative titers of around 9 and 16, as detected before, one in every assay set.

In total consideration of the total of 400 serum samples originating from diabetes mellitus patients, 37 samples were obtained positive for IGF1R-Ab, which led to a prevalence of 9.3%. Strongly positive tested for IGF1R-Ab were 22 serum samples, resulting in a prevalence of 5.5% (Table 5.18).
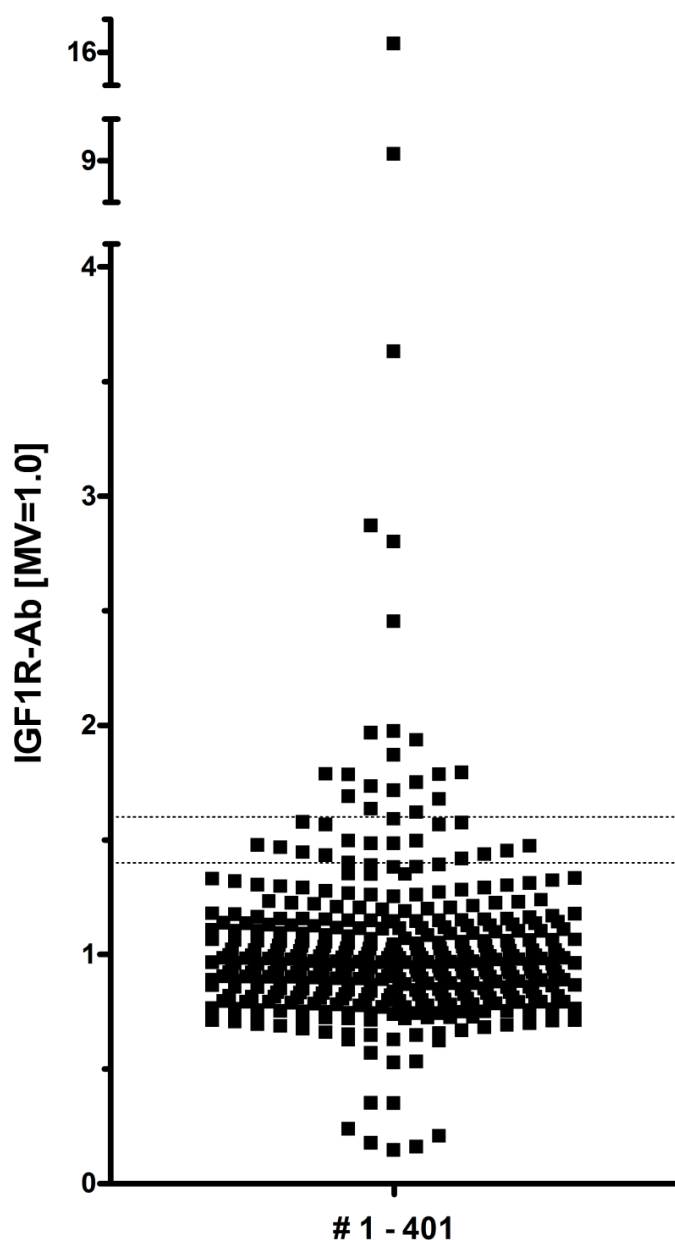
Figure 5.35: *Prevalence of aAb to the IGF1R in the cohort of diabetes mellitus patients.* Determination of IGF1R-aAb in 401 serum samples from patients with diabetes mellitus in the IGF1R-Ab precipitation assay. The sample collective was split into two assays prepared independently at different experiment dates due to practicability reasons to ensure proper and identical experimental conditions and handling within one sample set. Mean value (MV) and SD were calculated after excluding the upper and lower 5% of values, MV was set to 1.0 for each set, applied relative values of all serum samples were plotted in the graph. Values above MV+2SD (lower dotted line) were classified as slightly positive, values above MV+3SD (superior dotted line) as clearly positive.

Table 5.18: *Summary of IGF1R-aAb prevalence in a cohort of diabetes mellitus patients.* Results were evaluated by considering each set on its own as described above (Table 5.16). Positive sera of both sets were added, obtained prevalence was averaged. Asterisk label (*): One sample was labeled incorrectly as diabetes serum, thus the serum was excluded from analysis.

Assay	Set 1 and 2: # 1-401 (n = 400) *	
Positive sera	IGF1R-aAb [n]	Prevalence [%]
> MV+2SD	37	9.3
> MV+3SD	22	5.5

5.5.3 Growth deficient children

Serum samples from growth-deficient children were obtained from cooperation partners at the Charité Berlin (Dr. Susanna Wiegand and Dr. Peter Kühnen, Institute for Experimental Pediatric Endocrinology, Charité Berlin, Germany). A total of 628 serum samples consecutively labeled as #1 to #726 were analyzed blinded to the clinical phenotype in the IGF1R-Ab assay. A total of 98 serum samples were empty or missing within this cohort. For the analysis, the sample collective was again split into two assay sets of approximately 300 serum samples each, which were prepared independently by two operators.

Evaluation of IGF1R-Ab positive samples was performed for each assay set individually as described before and key data were calculated based on the cohort's raw data. An additional evaluation was made considering the total number of samples (Table 5.19). This was done regardless of set affiliation, as control samples including the standard-serum mixture yielded nearly identical results in both sets when measured in quadruplicates (Figure 5.36). For that reason, presentation of the results had been possible as IGF1R-Ab-levels in RLU in a single graph. For better highlighting the correlation inside the data set, the results are also presented relative to the total mean value (Figure 5.37). A bulk of serum samples was located below a relative IGF1R-Ab titer of 2.0, which did also represent the first threshold value for positivity (MV+2SD). Above this value, the number of samples declined gradually, and only few passed the threshold value for strong positivity at 2.49 (MV+3SD). Some serum samples reached relative IGF1R-Ab titers of up to 20. The two strongest positive samples spiked even to a titer of 105. In total numbers, 60 out of 628 sera appeared positive on IGF1R-Ab, which represented a prevalence of 9.6%. Out of those sera, 44 were obtained strongly positive, representing a prevalence of 7.0%. Prevalence differed slightly, when evaluating both sets separately, followed by averaging the data obtained, compared to data evaluated of the total cohort (Table 5.20).

Table 5.19: *Key data of IGF1R-Ab assay with serum samples of growth deficient children.* *A total number of 628 serum samples were distributed into two assay sets (column 2 and 3). Thresholds values based on the raw data are illustrated, including MV of the correspondent sample set, which was determined after excluding the upper and lower 5% of total values, and threshold values for MV+2SD and MV+3SD. Additionally calculations were made for the whole data set, independent from the sets the assay was performed in (last column). Relative values for MV = 1.0 were added in this evaluation. Asterisk label (*): 98 samples throughout the cohort were empty or missing, resulting in a reduced sample number compared to sample labels.*

Serum samples	# 1-325	# 326-726		total # 1-726	
n *	300	328		628	
Unit	RLU	RLU		RLU	MV = 1.0
MV	3086	2714		2892	1.00
SD	1360	1476		1432	0.50
MV+2SD	5805	5667		5756	1.99
MV+3SD	7165	7143		7188	2.49
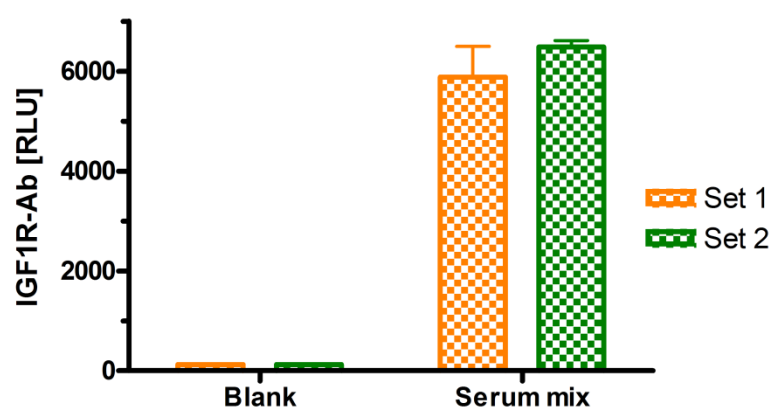
Figure 5.36: *Control experiments included in both assay sets.* *Four identical serum samples, originating from a standard-serum mixture, were analyzed in both assay sets individually. Samples were measured in quadruplicates, bars represent mean +/- SD. No significant difference was determined when Serum mix from set 1 and set 2 were compared (p = 0.323).*
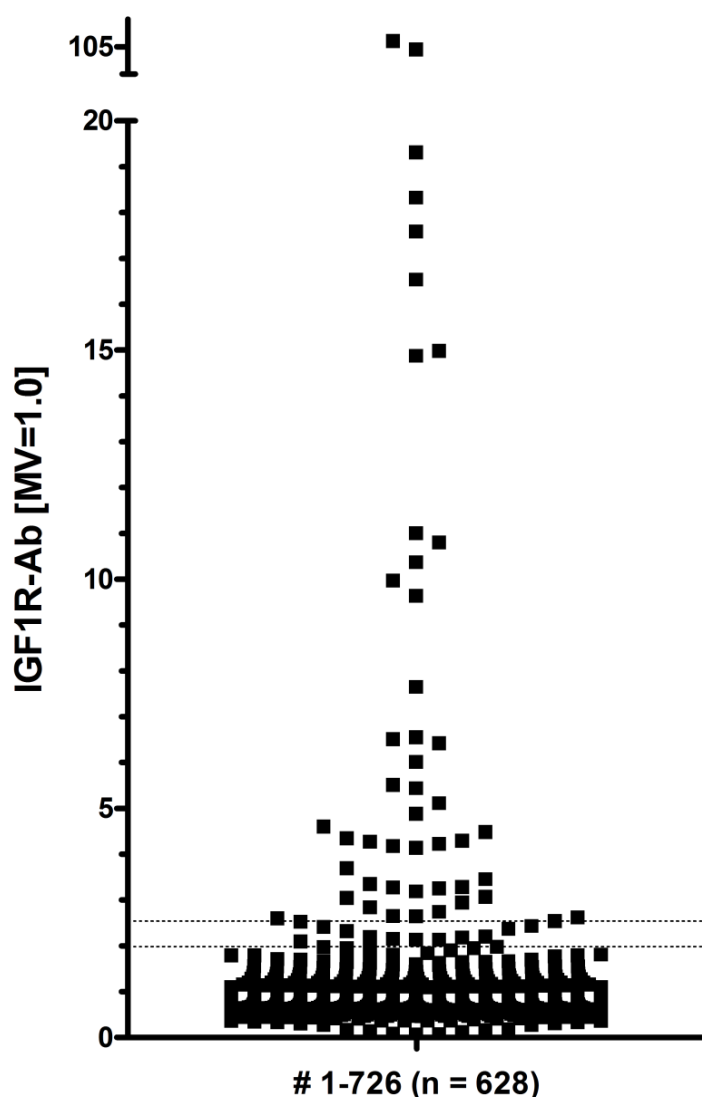
Figure 5.37: *Prevalence of aAb to the IGF1R with serum samples of growth deficient children.* A total of 628 serum samples, numbered # 1 to # 726, were analyzed in the IGF1R-Ab precipitation assay, considering that 98 serum samples were missing within the cohort (consecutively listed blinded sample numbers, labeled internally by an # in front of the accordant digit). The sample collective was split into two assays prepared independently by two operators at one experimental date each due to practicability reason to ensure proper and identical experimental conditions within one sample set. Mean value (MV) and SD were calculated after excluding the upper and lower 5% of values, MV was set to 1.0 for each set and relative values of all serum samples were plotted in the graph. Values above MV+2SD (value: 1.99; lower dotted line) were classified as slightly positive, values above MV+3SD (value: 2.49; superior dotted line) as clearly positive.

Table 5.20: *Prevalence of aAb to IGF1R in serum samples of growth deficient children.* The absolute number of IGF1R-aAb positive serum samples was determined for each of the two sample sets and percentage of aAb positive samples was indicated (column 2 and 3). Prevalence calculations were performed with respect to true analyzed sample numbers. Sum of number of positive sera and averaged prevalence of the two sample sets was presented in column 4. An additional evaluation was made for the whole data set, independent from sets the assay was performed in (last column).

Serum samples	# 1-325	# 326-726	# 1-726		total # 1-726
n	300	328	628		628
Positive sera [n]			Sum		
> MV+2SD	28	32	60		60
> MV+3SD	21	24	45		44
Prevalence [%]			Average		
> MV+2SD	9.3	9.8	9.6		9.6
> MV+3SD	7.0	7.3	7.2		7.0

5.6 Characterization of cross-reacting aAb to the IGF1R and IR

Autoantibody prevalence in the sample collective with DM-patients (section 5.5.2) was not only determined for the IGF1R as autoantigen, prevalence was determined to the IR as well (unpublished data, in cooperation with C. Schwiebert, IEE, Charité Berlin). The IR-luciferase precipitation assay is similar in its format and methodology to the IGF1R-luciferase precipitation assay. Thus an IR-Luc fusion was engineered, recombinantly expressed and recombinant cell extracts were used for binding IR-aAb from human sera. When viewing at data for each receptor-aAb independently from previously mentioned sample collective, a similar distribution pattern of autoantibody titers in both assays occurred (Figure 5.38). Relevant raw data for prevalence analysis are presented in Table 5.21, A. Considering the high positive values (>MV+3SD), aAb were detected with a prevalence of approximately 5% each. When looking at all positive samples (>MV+2SD), a prevalence of nearly 9% for IGF1R-aAb and of 11% for IR-aAb was calculated (Table 5.21, B).

Looking at positive sera from the sample collective for IGF1R- and IR-aAb more closely, a comparable number of sera turned out to be simultaneously positive for IGF1R-aAb and IR-aAb, respectively. Considering all positive samples (>MV+2SD), 10 out of the 18 positive samples for IGF1R-aAb were only positive for IGF1R-aAb, but the other 8 of these 18 samples were simultaneously positive for IR-aAb (Figure 5.39, A). 15 out of the 23 positive samples for IR-aAb were only positive for IR-aAb, but 8 of these 23 samples were simultaneously positive for IGF1R-aAb. When looking at the strong positive samples (>MV+3SD), 5 out of the 10 strong positive samples for IGF1R-aAb were only positive for IGF1R-aAb, but the other 5 were simultaneously positive for IR-aAb (Figure 5.39, B). 7 out of the 12 strong positive samples for IR-aAb were positive for IR-aAb only, but the remaining 5 were simultaneously positive for IGF1R-aAb. The correlation of samples being simultaneous positive to IGF1R- and IR-aAb in the analyzed sample collective was calculated up to 50% regarding the strong positive samples (Table 5.22). Giving consideration to all positive samples, the correlation of samples positive to both aAb was between 35% and 45%. Thus a numerous fraction of positive samples turned out to react with both the IGF1R and the IR.
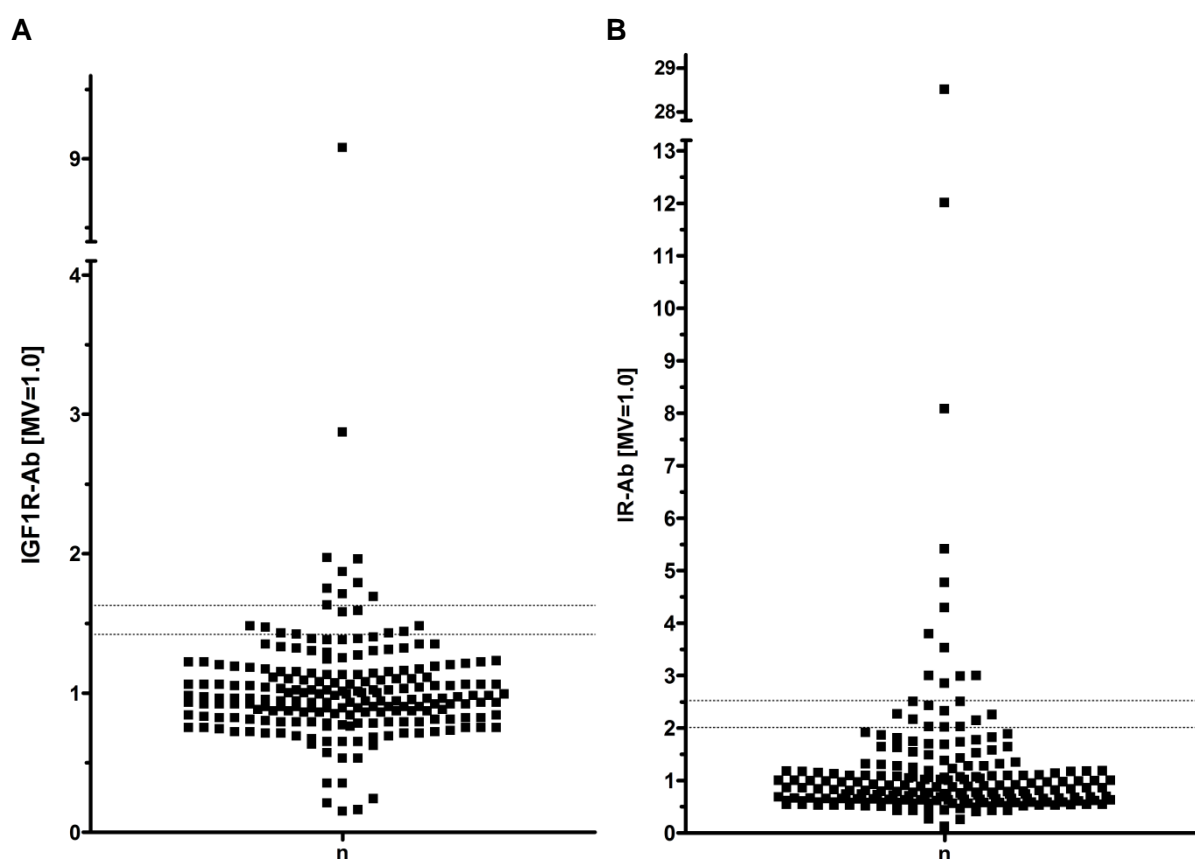
Figure 5.38: *Prevalence of aAb to the IGF1R and IR in the identical sample collective.* *Determination of IGF1R-Ab (A) and IR-Ab (B) in 207 serum samples using the IGF1R- or the IR-Ab precipitation assay. Mean value (MV) and SD were calculated after excluding the upper and lower 5% of values. To calculate relative concentrations the MV was set to 1.0. Values above MV+2SD (lower dotted line) were classified as slightly positive, values above MV+3SD (superior dotted line) as clearly positive.*

Table 5.21: *Prevalence of aAb to the IGF1R and IR in the same sample collective.* *(A) Key data of IGF1R- and IR-Ab assay for 207 serum samples. Both the direct RLU values and the calculated ratios with respect to the mean value (MV) are given with threshold values for 2SD or 3SD. (B) Prevalence of aAb to IGF1R and IR in these serum samples. Both the absolute number and percentage of aAb positive samples are indicated.*

A

Assay	IGF1R-aAb		IR-aAb	
Unit	RLU	MV = 1.0	RLU	MV = 1.0
MV	12630	1.00	4680	1.00
SD	2653	0.21	2366	0.51
MV+2SD	17936	1.42	9412	2.01
MV +3SD	20589	1.63	11779	2.52

B

Positive sera	IGF1R-aAb [n]	Prevalence [%]	IR-aAb [n]	Prevalence [%]
> MV+2SD	18	8.7	23	11.1
> MV+3SD	10	4.8	12	5.8

A

positive sera [n] > MV+2SD

B

positive sera [n] > MV+3SD
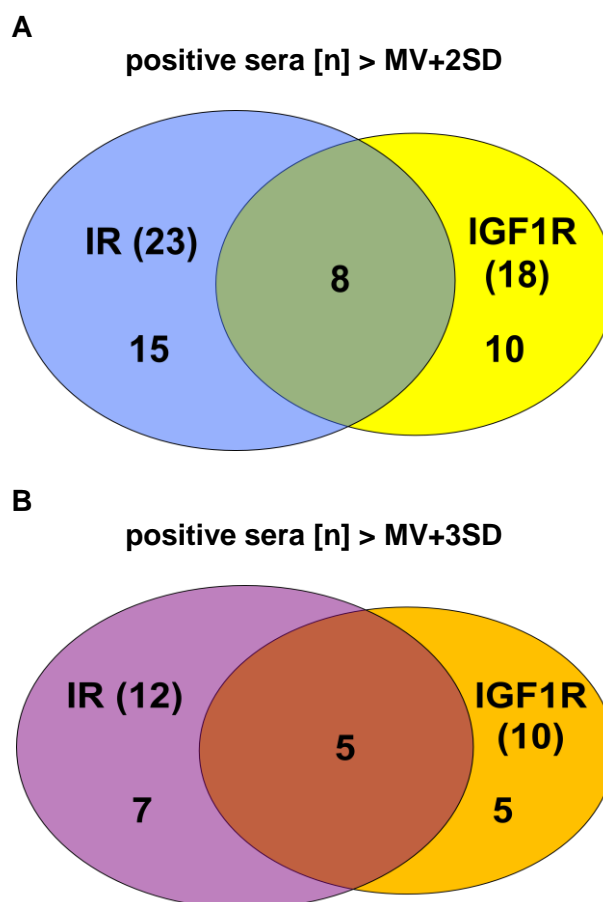
Figure 5.39: *Correlation of samples being simultaneously positive for IGF1R- and IR-autoimmunity.* (A) Correlation in samples defined as aAb-positive by a less stringent (MV+2SD) and (B) stringent (MV+3SD) criterion for aAb-positivity.

Table 5.22: *Correlation of positive samples to IGF1R- and IR-aAb in the same sample collective.* Percentages indicate the number of sera being positive for both aAb tested.

Criteria for positivity	IGF1R-aAb		IR-aAb	
	> MV+2SD	> MV+3SD	> MV+2SD	> MV+3SD
Correlation	45%	50%	35%	42%

5.7 Test of cross-reaction to the IGF2R

Analyses of patient collectives showed very interesting and surprising data with respect to presence of autoantigens in the insulin and IGF1 system. Thus an adaption of the receptor precipitation assay was performed to test for the insulin-like growth factor 2 receptor (IGF2R) as autoantigen. The proven method described for IGF1R was adapted to the IGF2R from the cloning and recombinant expression of the receptor as C-terminal luciferase fusion to its purification and extract preparation for analysis.

Prevalence of IGF2R-aAb were analyzed in samples preliminary determined negative or positive for IGF1R-aAb using the IGF2R-Ab luciferase precipitation assay. The assay was built up and performed as known for the IGF1R-Ab luciferase precipitation assay. Serum samples were obtained from preliminary analyzed patient sera. From the collective of children with growth deficiency ("Pedendo") (section 5.5.3) 25 negative and 56 sera positive to IGF1R-aAb were chosen. Out of the "DM" collective (section 5.5.2) 25 sera negative and 46 sera positive to IGF1R-aAb were selected for further analysis. Results were plotted for every of these single sample sets (Figure 5.40), while the solid line in each cluster representing the mean of this sample set. Mean value and SD were calculated after excluding the upper and lower 5% of values for sample set "Pedendo" (indicated blue) and "DM" (indicated orange) individually, making no difference between preliminary determined positive or negative samples for IGF1R-aAb. Values above MV+2SD (lower dotted line) were classified as slightly positive, values above MV+3SD (superior dotted line) as clearly positive. In the "Pedendo" collective 6 out of 81 sera were determined positive to IGF2R-aAb, while 5 of those were clearly positive with values higher than MV+3SD. 5 of these 6 positive sera were also positive for IGF1R-aAb. In the "DM" collective 5 of 71 were determined positive to IGF2R-aAb, while 3 of those were clearly positive with values higher MV+3SD. 3 of these 5 sera were also positive for IGF1R-aAb. Interestingly the large majority of IGF1R-aAb positive sera showed no elevated prevalence in IGF2R-aAb neither in "Pedendo" samples (5 positive out of 56) nor in "DM" samples (3 positive out of 46).

Table 5.23: *Characteristics of analyzed samples for autoantibodies versus IGF2R using the IGF2R-Ab luciferase precipitation assay. Serum samples were obtained from preliminary analyzed patient sera on IGF1R-aAb from collective "Pedendo" and "DM".*

	"Pedendo"	"DM"
samples [n]	81	71
IGF2R-aAb pos./neg. [n]	6 / 75	5 / 66
IGF1R-aAb pos. [n]	56	46
of these IGF2R-aAb pos./neg. [n]	5 / 51	3 / 43
IGF1R-aAb neg. [n]	25	25
of these IGF2R-aAb pos./neg. [n]	1 / 24	2 / 23
	[RLU]	[RLU]
MV	2136	4661
SD	965	2278
3 SD	2895	6835
2 SD	1930	4557
MV + 3 SD	5031	11496
MV + 2 SD	4066	9218
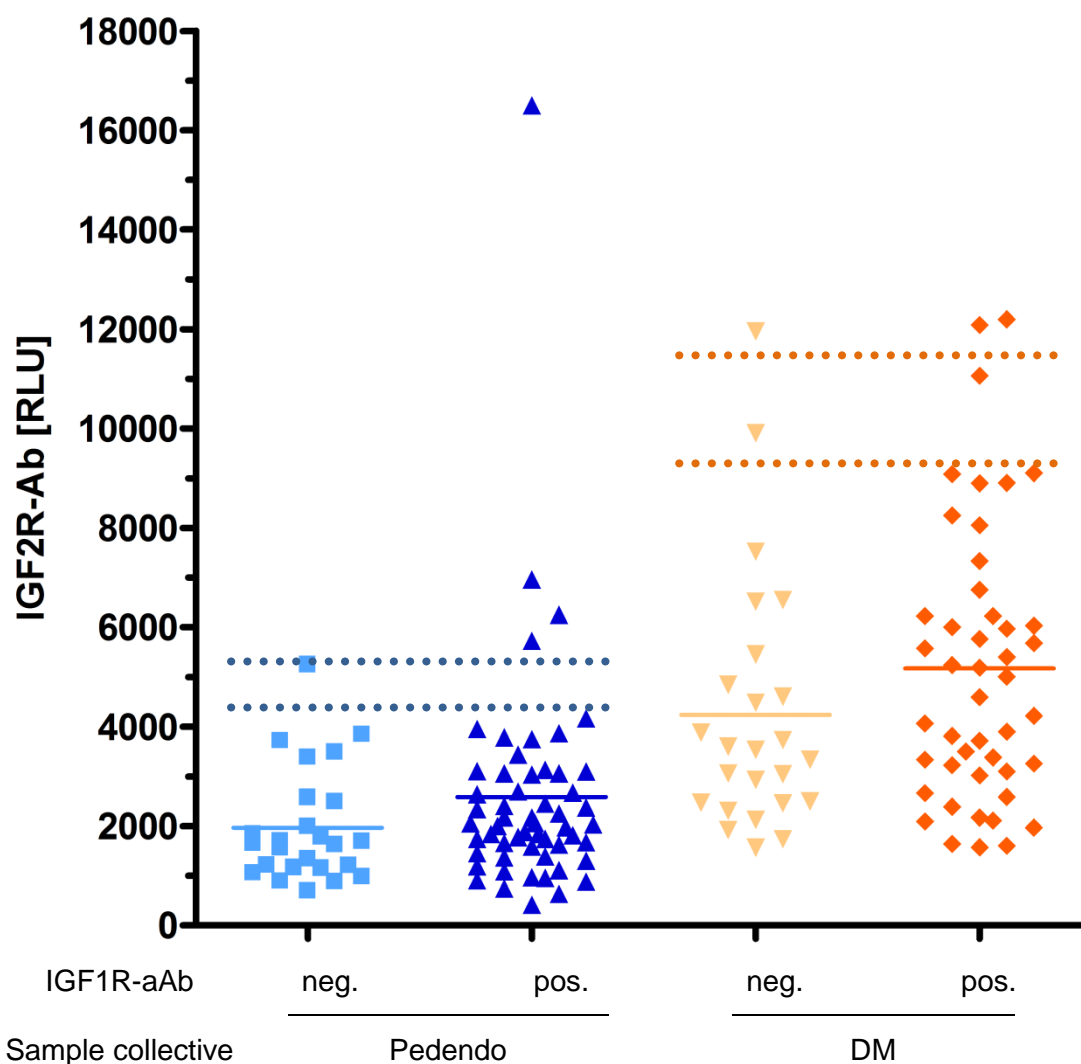
Figure 5.40: *Prevalence of IGF2R-aAb in samples preliminary determined negative or positive for IGF1R-aAb.* *The IGF1R-Ab luciferase precipitation assay was adapted to the IGF2R as autoantigen. The assay was built up and performed according for the IGF1R-Ab luciferase precipitation assay. Serum samples were obtained from preliminary analyzed patient sera. 25 negative and 56 sera positive to IGF1R-aAb from "Pedendo" collective and 25 sera negative and 46 sera positive to IGF1R-aAb of the "DM" collective were chosen. Mean value (MV) and SD were calculated after excluding the upper and lower 5% of values. Values above MV+2SD (lower dotted line) were classified as slightly positive, values above MV+3SD (superior dotted line) as clearly positive. Classification was calculated for sample set "Pedendo" and "DM" individually. Solid line in each cluster represents the mean of the sample set.*

Collectively, these data indicate that autoantibodies to both the IGF1R and IGF2R exist in children with growth deficiency and patients with diabetes mellitus, and that some subjects contain autoantibodies to both receptors. In how far these autoantibodies affect disease susceptibility, course and severity remains to be established in future studies.

6 Discussion

6.1 Expression of recombinant proteins

Production process

During the process of assay establishment, the antigen, which is needed in the assay for specific antibody detection, is the first critical resource making the assay reliable. Hence, the quality of the recombinant protein is of central importance for establishing a reliable assay suitable of measuring autoreactive IgG. This is the reason, why it was essential to express full-length biologically active recombinant receptor molecules instead of soluble IGF1R-fragments or isolated domains. After establishing the stable HEK293 cell lines, which expressed the genetically engineered recombinant fusion proteins used in this study, comparisons between different culture systems were made. Stably transfected cell lines were mostly based on adherent cells. Consequently, first expansion of cell culture and generation of an increasing amount of cell mass, including the desired recombinant proteins, was performed with adherent cultivated stable cell lines. To use an alternative system with higher potential for upscaling the production process, adherent cultivated cells were adapted to serum free suspension culture conditions.

As described in material and methods, adaption of adherent cultivated cells is associated with a relatively delicate and heavy workload, up to the point, at which the superspinner system could be inoculated with cell suspension. A direct comparison of both cultivation systems was performed, including culturing of IGF1R-Luc cells in 6 tissue culture flasks, with a surface of 150 cm^2 each, and culturing these cells in a superspinner with 1 L culture volume, which were supposed to include a similar operating effort. The obtained cell pellet net weights of 1.2 g (adherent) and 3.0 g (suspension), respectively, underline that suspension cultivated cells in a spinner system grow up to a considerably higher cell density than in tissue culture flask and are thus the better production system for high-volume assay development. This might be caused on the one side due to limited space on the surface in flasks, and on the other side due to better stirring and improved distribution of nutrients and gas entry into the spinner system. As a considerable hurdle, primarily adherent cultivated cell lines, like in this case HEK293, tend to aggregation and cluster formation in suspension culture, whereby a few cells suffer intense nutrient limitations. This could negatively influence the quality of the recombinant protein.

However, the cell extracts prepared during this study showed a high specific luciferase activity in general, originating from the fusion protein, generated in adherent and suspension culture. The slightly reduced amount of specific activity of cell extracts originating from suspension-cultivated cells, compared to adherent cultures, might be

caused by the previously described nutrient limitation. Thus, cultivation of suspension-adapted cells in the superspinner system ensures an effective and reliable method to produce a high cell mass in a short period of time. The total workflow includes less final effort and results in a similar high quality of recombinant protein, compared to adherent culture. Beside these advantages, the superspinner system promises the option for an efficient upscaling of protein production, producing a large amount of cell mass over the time. During one production process, 10 to 20 percent of culture volume could be kept in the spinner at the time of the harvest and culture could directly proceed for further production. Depending on performance of viability and cell growth, the spinner could be harvested twice a week, which will result in a suitable high yield of high quality recombinant protein expressing cells over weeks. Additionally, the superspinner system could serve as the first platform to an industrial upscaling of the culture to bioreactor size. The monitored recloning-process of stable protein expressing cell clones indicates similar results in producibility of 2 reclones compared to the original clone. Thus, a long term integration of the gene already occurred in the original expression clone and recloning was not compellable necessary to ensure a consistent product quality and yield of recombinant protein, when selection pressure remained maintained. This case might be analyzed for each clone individually.

Correct functional expression

Multiple experiments performed on various methodical approaches indicated a correct functionality of the expressed antigen. Correct functional expression of the luciferase protein was verified by luciferase-substrate turnover measurements of IGF1R-Luc cell extracts, which is in line with the observation of the luciferase reporter protein as a reliable reporter system. Correct functionality of the hormone binding domain of the IGF1R was demonstrated in *in vivo* hormone-binding experiments with recombinantly expressed receptor, immobilized on tubes, proving a prominent hormone binding capacity. The acridiunium labeled IGF1 was able to be competed against by unlabeled hormone, underlining the biological cause of the binding effect. These results were reproduced when reclones were analyzed and further supported by cell culture experiments, in which the receptor is in any case present in the natural condition. In this case, unspecific effects based on receptor extraction or immobilization were excluded. The IGF1 hormone binding study on stably transfected IGF1R-HEK293 cells was intended to show correct and functional integration of recombinantly expressed IGF1R in the plasma membrane of the cell. Primarily the experiment had been confirmed at 37°C only. But the method performed, including acridinium labeled hormone binding on the cell surface of living cells, was not questioned in detail. In consequence, it was possible that free label or a fragment

of the labeled IGF1 was internalized by the HEK cells and might give rise to the detected signal. Thus, a control experiment on low temperature conditions proved that the label was retained on the outer surface of the cell membrane and the surface binding was in fact accomplished.

Membrane fractions

The immunoprecipitation assay was performed with whole cell lysates. Thus precipitation might appear with both, correctly membrane inserted IGF1R-Luc fusion protein and fusion protein not inserted into the plasma membrane. This could impact, whether anti-IGF1R-Ab recognize epitopes on the fusion protein, since the conformation may change during posttranslational modification processes and membrane insertion. Subcellular fractionation prepared from either HEK293 cells stably expressing IGF1R-Luc or HEK293 wild type cells showed a distribution of expressed IGF1R-Luc fusion protein located approximately 71% in the plasma membrane and 29% inside the cell. The fraction of IGF1R-Luc, existing unincorporated in the membrane, might eventually represent a biologically irrelevant fraction, which could at most contribute to background noise of the Luc-signal when immunoprecipitated in the assay. Alternatively, it might represent recombinant protein on its way to the final plasma membrane localization. The experimental results regarding discrimination of positive from negative IGF1R-Ab did not support these concerns, since a very prudent cutoff line between negative and positive sera of MV plus at least 3 SD also contributes to high specificity. By this, sera with low-affinity antibodies may have been excluded from the positives in the design of this assay method. But for speed, costs and reproducibility issues, the assay design was constructed as simple as possible by reducing the number of preparation steps necessary for assay set up to a minimum.

6.2 Assay buildup and characterization

Characterization experiments of the interaction of serum antibodies with the recombinantly expressed IGF1R as autoantigen were performed to ensure highly reliable and reproducible results, which included analysis of patient sera to determine IGF1R-Ab titers, as well as experiments for the verification of biological effects.

Because free IGF1 is necessarily present in human serum, the IGF1R-Ab precipitation assay was tested for interference by the IGF1 hormone. The signal of several IGF1R-aAb positive sera was even recovered in the presence of IGF1 in concentrations of up to 10 mg/L, which represent a far and unphysiological high excess of hormone. Matrix effects were excluded and appropriate characteristics of dilution and linearity were investigated by suitable experiments. A cutoff criterion for positivity was reached at 15 ng IgG/ml of a commercially available monoclonal antibody. A detection limit for IGF1R-Ab in human

sera might show a different result, but the determined value demonstrates a highly precise assay system. The stability of the autoantigen was tested under assay condition and could be guaranteed for at least 10 days at room temperature. This experiment represented unexpectedly rough conditions for the antigen, but a high antigen-stability might be necessary due to shipping, storage or handling of the antigen in commercial use and should have reached the best possible rate.

Further, it could be verified that the IGF1R-Ab assay does specifically identify antibodies against the IGF1R, because only the Ig preparations from positive sera, compared to control sera, gave positive results. Accordingly, sera and isolated Ig were able to immunoprecipitate the IGF1R with a clear correlation to their relative aAb titers with a similar efficiency. These results indicate that both test matrices, i.e., crude sera and isolated Ig, are similarly well-suited to detect and quantify IGF1R-aAb. The usage of patient sera instead of Ig preparations was defined as critical point for suitability of the assay for a broad range of applications and at the commercial level. Thus, for reasons of comfort, speed, and costs, it appears consequently unnecessary to isolate Ig prior to analysis in the IGF1R-Ab assay. With respect to the important parameter and final point of the methodical characterization of the IGF1R-Luc precipitation assay, coefficients of variation were determined. The inter assay CV was calculated to be 13.6% and the intra assay CV to 9.9%. These scores do reflect the performance of the assay in the hands of the particular users. Experimental results with higher intra assay CVs often reflect poor pipetting technique on the part of the operator. In addition, mishandling due to sample preparation, like a different number of freeze-thaw cycles, vortexing or centrifugation steps, would lead to divergent results. Thus a standard operation procedure, compulsory for all users, including material calibration instructions, e.g. for pipettes and output device, will help improving the CVs. However, in the field of immunoassay-research inter assay CVs <15% and intra assay CVs <10% are considered to define a reproducible and reliable assay [176].

6.3 Biological effects and molecular actions of IGF1R-Ab

Previously determined IGF1R-aAb positive samples efficiently recognized and immunoprecipitated the IGF1R as antigen. This was chosen as a basis for future experiments intending to come closer to the understanding of IGF1R-aAb biological effects and molecular actions. The experiments described here proved that the positive sera were capable of inhibiting the autophosphorylation of the receptor when it was stimulated *in vitro* by its endogenous ligand IGF1. In contrast, the experimental setup for the study of activating IGF1R-aAb, Ig from IGF1R-aAb positive serum samples were not stimulating IGF1R activity and no consistent effects of the Ig on IGF1R

autophosphorylation were observed, indicating that IGF1R-aAb are not stimulating in nature. In the setup for detection of inhibiting activity of IGF1R-aAb, IGF1-induced autophosphorylation of the IGF1R was efficiently abrogated by IGF1R-aAb positive sera in HEK cells. IGF1R-dependent signaling, represented by IGF1-dependent effects on cell growth, was competently impaired in MCF7 cell culture by adding isolated Ig from IGF1R-aAb positive sera, which affected IGF1-dependent cell proliferation, apoptosis, or both.

These results suggest that IGF1R-aAb bind the receptor and negatively affect the IGF1 signaling cascade. Thus, the molecular procedural method of binding was interesting to be characterized in more detail. A first preliminary epitope analysis with IGF1R domains showed that the IGF1R autoantibodies interacted with different parts of the IGF1R, even though the complete signal intensity with the full-length receptor could not be recovered with the fragments. This is referring to the conclusion, that IGF1R-aAb recognize a number of „conformational" epitopes of the IGF1R. They do not interact with only one special part or peptide sequence of the IGF1R. This led to the assumption that IGF1R-aAb may be conformational Ab's as already described for TSHR [177, 178].

The most suitable and appropriate mechanism for the previously proven prevention of receptor signal transduction by serum antibodies is blocking of hormone binding, preferably by blocking the hormone binding site at the receptor. However, the observation of competition of hormone binding by antibodies from IGF1R-aAb positive determined sera was not successful in this study. Similar results, where binding of IGF1R-aAb at the receptor by potential blocking was suggested, were already obtained in the past, but only reported for very few of the positive sera. In one of these first publications, in which a 125-iodine labeled placental IGF1R was used for IGF1R-Ab determination, two populations of autoantibodies were suggested [45]. The authors hypothesized the presence of two species of antibodies against the IGF1R, while the wide majority of positive sera contained IgG autoantibodies that bound to the IGF1R at a locus different from the IGF1 binding site and did not inhibit IGF1 binding. The additional positive sera contained antibodies that bound to the IGF1R at or near the IGF1 binding site, inhibited hormone binding, and probably caused IGF1 resistance. In the same line, Shimoyama and colleagues found anti-IR autoantibodies in 10 of 104 human diabetes sera, but only one of these positive sera inhibited insulin binding [46].

IGF1R-Ab bind two molecules of IGF1R

The newly generated monoclonal antibodies to the IGF1R were used to address important aspects for further biological characterization of IGF1R autoantibodies, the assay system and their mode of binding to their antigen. The monoclonal antibodies were subjected to the IGF1R bridge assay, in which two molecules of the antigen IGF1R were presented

one after another. In 3 of 5 monoclonal antibodies analyzed, both variable chain regions were able to bind their antigen simultaneously. More clearly, one antibody bound two receptors via its two variable chain regions. As a continuative very important result, IGF1R-Ab present in human serum sample was also capable of binding IGF1R at both variable chain regions. Methodically, this opens the opportunity to develop an additional variant of the IGF1R-Ab diagnostic assay to be prepared at stationary phase. The capability of IGF1R-Ab binding two antigens (IGF1R) at the same time widens the options about the molecular details of how the antibody interacts with the IGF1R. On the one hand, the binding capability is enhanced by factor two, which might lead to a higher efficiency rate in the antibodies original function. On the other hand, the recruitment of receptors in steric proximity might affect their signal transduction activities.

Cross reactivity of the IGF1R- with IR-aAb positive sera

One of the first very promising studies conducted in this work, using the IGF1R-Ab precipitation assay, was the determination of IGF1R-Ab levels in samples of DM-patients. Analyses of a second autoantigen – the IR – demonstrated a prevalence of around 5% for highly positive aAb to IGF1R and 5% positive sera to the IR in the analyzed samples. Further reflection showed an unexpected high correlation of samples being simultaneously positive for IGF1R-aAb and IR-aAb. This relatively high number of positive samples reacting with both the IGF1R and the IR, either indicates the presence of multiple specific-aAb isoforms or of one type of cross-reacting aAb in a given human serum sample. These findings may be of significant clinical relevance for the current diabetes epidemic, but further analyzes are needed to test this hypothesis.

These surprising results do also designate a new application for the IGF1R bridge assay, by adding not a homologous autoantigen, but a second one, like the IR, whereby a heterologous bridge assay will be generated. This would give a new exciting opportunity to study antibody-antigen interactions on the molecular level regarding insulin- and IGF1-related metabolism deficiencies by which new links might be found.

Summary of the biological effects of IGF1R-Ab

The present study verifies the existence of autoantibodies to the IGF1R in humans. The Ig isolated from IGF1R-aAb positive individuals bind the IGF1R and interfere with IGF1-dependent receptor activation, IGF1R-dependent signaling and IGF1-dependent effects on cell growth. However, the biological characterization indicates that these antibodies are of antagonistic activity as compared to the natural ligand IGF1 and inhibit IGF1-dependent signaling by binding conformational epitopes of IGF1R. Most antibodies recognize a conformational epitope of their antigen, which has a specific three-dimensional shape and a distinct protein structure, which is further typically necessary for functionality [179].

Further interesting questions were, if IGF1R-aAb's were polyclonal or monoclonal. Or whether Fab fragments may contribute to biological effects, which may affect physiological responses, like effects on proliferation or blocking IGF1 induced IGF1R phosphorylation, as a consequence of interactions with Fc receptors. This clearly needs to be determined in future studies.

Experiments using the IGF1R-Ab as bridge in between two IGF1R molecules verified that IGF1R-Ab are capable of binding two of their antigens simultaneously by both variable chain regions. Surprisingly, human individuals exist, in whose sera both IGF1R-Ab and IR-Ab are detectable at a significant level. By this, a new sight in the interplay of autoimmunity regarding IGF1R and IR as autoantigen should be considered and the molecular action and potential biological effects need to be further investigated.

Up to the authors' knowledge, the herein performed *in vitro* experiments were the first using novel methods based on recombinantly expressed fully functional IGF1R, in combination with clinical sera containing IGF1R-Ab, to address their biological effects *in vitro*.

6.4 Relevance of IGF1R autoimmune diagnostics

The newly established IGF1R-Ab luciferase precipitation assay does specifically detect and quantify IGF1R-Ab in human serum samples. The main findings do underline the systematic correctness of the detection method and are supported by various points. A specific immunoprecipitation of the recombinant IGF1R as autoantigen, which originated from HEK293 cells, was only possible by IGF1R-Ab positive but not by negative sera. The comparison of crude sera and purified antibody preparations showed very similar results in the different detection systems, confirming that the antibodies were responsible for the obtained RLU signals.

The physiological relevance and biological importance of the assay system were shown by the fact that only the positive but not the control sera were able to inhibit the IGF1-induced autophosphorylation of IGF1R in HEK cells in culture. Further, IGF1-induced growth of MCF7 cells was specifically inhibited by the IGF1R-aAb positive sera but not by negative sera.

The results on the prevalence of IGF1R-aAb positive sera in patients with Graves' disease, Diabetes mellitus, growth deficiency and healthy controls led to the conclusion that the IGF1R represents a typical autoantigen, similar to many other endogenous proteins, raising specific autoreactive IgG in both, healthy subjects and patients. However, all positive sera tested on biological effects at the IGF1R so far, were binding it, but without activation. Even an inhibitory effect on IGF1R-mediated signalling was observed in Western blot analysis. Up to now there is no evidence, in literature and this study as well,

that humans with IGF1R-stimulating autoantibodies existed. For the investigation of the clinical aspects in IGF1R autoimmunity, more clinical studies and experiments using additional and complementary systems or methods with the purpose of a better characterization of IGF1R-aAb and clarify their pathophysiological significance are needed. Nevertheless, the relatively high prevalence and the potent *in vitro* activities of the IGF1R-aAb observed in this study clearly justify further research into this direction.

Detection of IGF1R-Ab in pathogenic and normal serum samples

One of the most interesting and controversially discussed ideas in the endocrine field of Graves' disease researchers and clinicians is the existence of high-affinity stimulating IGF1R-Ab, circulating in the blood of patients, which cause the exophthalmus and could serve as an additional clinical parameter in GO diagnosis and treatment. In respect to the aims of this study, the development of an assay system, which permits a fast and direct identification of IGF1R-Ab in human serum samples, was required. Accordingly, a novel and verified assay for detection and quantification of IGF1R-Ab using recombinant full-length IGF1R as autoantigen was successfully established. The assay showed to be effective in practical application for identification of IGF1R-aAb positive individuals, with a prudent criterion for positivity of IGF1R-Ab by a very strict and conservatively chosen threshold value of more than two or three standard deviations from the mean signals. For appearance reliable testing of clinical sample cohorts, in which autoimmunity to the IGF1R should be determined, a corresponding sample set of healthy controls should serve as donor for establishing a suitable threshold value as criterion of positivity. In this work, not every analyzed sample cohort met this requirement because of sample limitation in the present stage of basic research in assay development. However, in overall context, a very good discrimination between human serum samples in slight positivity for IGF1R-Ab and clear positivity for IGF1R-Ab, compared to negative for IGF1R-Ab was possible and appeared as a meaningful distinction of IGF1R-Ab concentrations.

A potential limitation of the assay system needs to be discussed at this point. Some reports showed pathogenic antibodies binding with low affinity to their antigen, which was described for SLE [180] or glomerulonephritis [181]. It is questionable in how far low-affinity IGF1R-aAb would be detected by our novel assay. If those additional low affinity binding antibodies existed in GO, they might have been missed in our analyses, supposedly due to the robust protein-A mediated precipitation step. An existence of a small fraction of undetected low affinity binding IGF1R-aAb, which additionally may have a blocking or stimulating character, might need to be identified with an assay obtaining no immunoprecipitation step. Nevertheless, the IGF1R-Ab precipitation assay was applied to several selections of samples, numbered up to 600 human serum samples in total. The

proof of principle by performance of the assay in this scale shows that IGF1R-Ab determination is not only available for exclusively selected patients, but will also be a very interesting tool for screening large clinical, intervention or epidemiological studies.

IGF1R-Ab in GO

Analyzing the present cohort of GO-patients, it came to us as a surprise to find 9% in the corresponding control group of healthy individuals as being IGF1R-Ab positive, compared to also nearby 10% being IGF1R-Ab positive of the GO sera. This finding indicates the same prevalence of IGF1R-aAb in GO patients and apparently healthy controls. If stimulating IGF1R-aAb were directly involved in disease incidence, one would expect to find a higher prevalence of these aAb in the GO patients as the disease does not severely affect mortality. As this was not the case, it can be concluded that the IGF1R-aAb are not related to GO disease incidence and course. This notion is even further supported by the finding that the autoantibodies identified even proved as being of antagonistic nature in comparison to the growth-stimulating hormone IGF1.

These findings are in contrast to a number of earlier reports suggesting a likely significant contribution of IGF1R-aAb to GO, leading to the hypothesis that patients with Graves' disease were suffering from a worsening of the disease, when both TS-Ab and IGF1R-aAb were simultaneously present [43, 182, 183]. Up to now, a suitable method for direct determination of IGF1R-Ab levels in patient sera was not available and nearly all supporting evidence were gained in an indirect way. Thus, in a small cohort of patients it was demonstrated that IgG from patients with GO could displace 125-Iodine labelled IGF1 from binding sites on fibroblasts [35]. As a conclusion, 50% of GD patients were found to be IGF1R-aAb positive, but it appeared to be independent from GO. The technique used was very different from the one used in this study, as described later in this section, and additionally, the cut-off criteria for "IGF1R-Ab positivity" was seemingly less stringent. If the criterion of only 1 SD or 2 SD above average was chosen in this study, it would also end up with a higher proportion of positive sera.

Another research group found evidence for the competition of radiolabeled IGF1 by Graves' patients IgG preparations when binding to cell membranes [43]. In line with this, IgG from GO-patients could elicit a cellular response in orbital fibroblasts donated from patients with ophthalmopathy, to be precise in the production of cytokines, but the response was not detected in orbital fibroblasts from healthy donors [184]. However, despite today's given availability of human IGF1R cDNA and recombinant IGF1R protein, these results have not been verified with the appropriate control experiments, e.g. specific over expression or knock-down of the IGF1R to prove the specificity. Thus, a specific interaction of analyzed IgG preparations with biologically functional IGF1R molecules was

not definitely shown [35], or IGF1R activation was again shown in an indirect way by demonstrating rising FRAP/mTOR/p70s6k pathway activity, which was initially not traced down to activation of the IGF1R [184]. Another crucial clinical aspect in the hypothesis about presumptive stimulating IGF1R-aAb in GO is also still open: Why do other acromegaly-like medical findings, like effects on stature, bones and cartilage, growth, glucose metabolism or neoplasia, do not come up significantly more often in GO-positive patients than in patients without GO, given the well-known wide-spread expression of IGF1R on human cells. If indeed stimulating IGF1R-aAb existed in the GO patients, some signs of acromegaly would have been observed and reported in the patients. This has never been the case. Accordingly, no indications are present indicating that an activated IGF1 axis by stimulating IGF1R-aAb supports GO disease incidence and course. A comparable prevalence of IGF1R-aAb showed up in patients and controls. This is in line with an obvious lack of correlation between IGF1R-Ab levels and the CAS- or NOSPECS-status [185], which represent a "Clinical Activity Score" or a "Clinical Severity Score" for GD and GO determination and diagnosis [186].

IGF1R-Ab in DM and growth deficient children

Prevalence of IGF1R-Ab was determined in a sample collective of 400 patients with diabetes mellitus type 1 or type 2, which was blinded and not further specified. Determination was performed in two samples sets, which conformed each other clearly with a IGF1R-aAb prevalence of approximately 9% and 10%, respectively, for slightly positive results and around 5% and 6%, respectively, for clearly positive IGF1R-aAb serum samples. Results obtained in both assay sets were compared by the determination of IGF1R-aAb titers in a set of overlapping samples. The results were reproduced perfectly with one exception in 17 samples, indicating a good reproducibility of the measurements. In consideration of the total of 400 serum samples originating from diabetes mellitus patients, an overall prevalence of 9.3% was obtained, while 5.5% of serum samples were tested strongly positive for IGF1R-Ab. These are considerable numbers that warrant further clinical evaluation of their pathogenic role in this disease.

The prevalence of IGF1R-aAb in serum samples of growth deficient children was determined to 5 to 10 percent, dependent on the grade of positivity. This result indicates a potential contribution of IGF1R-aAb to pathophysiology of a significant number of patients. Even though the clinical phenotype of IGF1R-aAb prevalence in the observed sample collective of growth deficient children is apparent, it had been important to show an obvious correlation of IGF1R-aAb and clinical phenotype for further support and promotion of the relevance of IGF1R autoimmunity. These IGF1R-aAb positivity – phenotype correlations are currently considered and clinically analyzed in the lab of the collaborators

at the Institute for Experimental Pediatric Endocrinology, Charité - Universitätsmedizin Berlin.

Assay development and routine testing

Several experiments in this study were chosen in respect to establish a diagnostic assay which can easily be developed to highest analytical standards and brought to market in the near future. The combination of stringent criteria on quality on one hand, and on practicability on the other, needs the combination of several factors. Determination of detection limit, exclusion of matrix effects, reproducibility of results and coefficients of variations were confirmed. These experiments indicated that the precipitation assay meets high requirements at the level of methodically robustness and qualitative and quantitative autoantibody binding as well.

The further developed antigen-antibody bridging assay methodically opens the opportunity to develop an additional variant of the IGF1R-Ab diagnostic assay to be prepared at stationary phase. This chance is also facilitated by the fact that a lyophilization of the tagged receptor to a tube via a tag specific antibody is possible and the receptor retains its functionality. In one line with this, miniaturization of the bridge assay to 96-well plate format also showed very promising results, although no final tests using a sample collective have been performed so far. A miniaturization of the precipitation assay to 96-well format will be more complex to master and to suite in the field of routine clinical diagnostics. A down-scale of the precipitation assay for basic research-demands was already practicable at preliminary experiments (data not shown).

In this study it was demonstrated that a large number of human serum samples of a diagnostic cohort can be applied to aAb determination by the IGF1R-Ab precipitation assay. The largest amount of human serum samples in which IGF1R-Ab titers have been determined was the cohort of GO patients with nearly six hundred serum samples. This is at present unparalleled in the medical literature.

Monoclonal antibodies to the IGF1R were also successfully developed. Generation and cultivation of hybridoma producing recombinant antibody as well as purification is a standard process. Because these steps worked commendable with our cooperation partners, this process will not be discussed in detail. The immunization method might be noteworthy, because immunization was performed genetically by injecting the cDNA on an expression vector as described in Costagliola and co-workers [165]. This method differs from the routine method by injecting a polypeptide. In this case, the genetic immunization appeared as the only practical solution for obtaining antibodies against the full-length receptor. Recombinant expression of the receptor and then its immunization would not

have been possible as the transmembrane protein can hardly be purified to high purity as required for antibody-generation.

A further, maybe not directly obvious but very important result, was the performance of the applied screening method for monoclonal hybridoma clones for IGF1R-Ab production. Reproducible data were collected in the screening rounds and verified the assay method, by which an IGF1R – antibody binding takes place. By this a recurrent verification of antibodies to the receptor and vice versa was proven. This is very important for further development of an assay detecting antibodies to the IGF1R. The produced monoclonal antibodies may be used as a standard marker in the assay for calibration purposes. Additionally, further characteristics of antibody receptor binding can be characterized more easily, when a larger and homogenous amount of antibody is available. Even though, monoclonal antibodies cannot put directly to the same functional level of pathologically active IGF1R-aAb in human serum. Before doing so, a more detailed characterization of both, the monoclonal antibody and serum autoantibodies has to be performed carefully. But extend of this work might fill a new study.

During development of the assay a proof of principle was necessary, in which the assay scheme does also work for another target. Thus, a structural and functional very different target apart from the IGF1R was chosen; the IGF2R, representing a single membrane spanning domain-containing type I transmembrane protein, but fitting thematically perfect into this study because of thematic proximity, waiting for the same ligands, and last but not least out of interest due to the poorly known receptor function. As shown in this study, the IGF2R-Ab precipitation assay works on the same principle as the IGF1R-Ab precipitation assay. Additionally, co-workers impressively demonstrated an IR-Ab precipitation assay with comparable prevalence to IGF1R-aAb during diagnostic determination of IR-aAb titers (unpublished results). In summary, these results indicate that both, the described assay scheme and experimental method, work excellent for various autoantigens. In the described method of the innovative bridge assay, a specific combination of autoantigens in one assay reaction is possible. Thus, the thesis of co-binding of IGF1R and IR by one autoantibody could be explained (compared to section 5.6, and correspondent discussion), when both antigens are presented one after another. Such a proof had not been shown so far, but by the bridge assay technology a platform was developed, which could enable the proof of this concept.

Contribution of IGF1R-Ab

The relevance of establishing a direct assay for IGF1R-Ab was shown during this study in a field, where the role of IGF1R-Ab function was widely accepted without ever having being proven beyond doubt; in the pathophysiology of GO. Further, the existence of

autoimmunity against the IGF1R was demonstrated in IGF1R-signaling dependent pathophysiology, namely in growth deficiency and diabetes. By that, the general need for an assay format for autoimmune diagnostic was becoming obvious. The determination of IGF1R autoimmunity may further be applied in the differential diagnosis in diseases like GO, diabetes mellitus and growth-abnormality related diseases, if the autoantibody-disease symptoms correlations yield new and meaningful insights. This is currently attempted by the clinical colleagues. In case the IGF1R-Ab could be established as a diagnostic marker, the potential treatment options need to be discussed and tested. Again, not only for diagnosis, but also for treatment success verification, the novel assays presented here will prove as essential prerequisites for these developments.

Considering all the performed clinical analysis, it was shown, that identification and relative quantification of endogenous IGF1R-Ab in humans can successfully be accomplished by these novel assays, and that the basic principle of the assays is methodically adaptable to further targets, as shown in this study for the IGF2R.

A further undisputed fact is that IGF1R mediates key features of malignancy, leading to a promising development of therapeutic Ab's against cancer targeting the IGF1R, which is discussed beneath in more detail. Trying to draw a conclusion out of this fact regarding IGF1R-aAb, an interesting question rises up: Do autoantibodies against IGF1R protect from cancer? The question cannot be answered directly, but might be in the near future, when bringing together the proven knowledge about the IGF1R as autoantigen and the IGF1R as a target in the treatment of cancer. Studying this opportunity, a publication came into view, leading to support the courageous hypothesis: An ethnic group of Ecuadorians was decreased in height, but developed hardly any neoplasias at all [187]. Mutations in their growth hormone receptor gene were identified in the subjects, leading to severe growth hormone receptor (GHR) and IGF1 deficiencies. The individuals with GHR deficiency exhibited only one non-lethal malignancy and no cases of diabetes, in contrast to 17% cancer and 5% diabetes prevalence in the control group. The authors discussed that mice as well as humans with reduced activity of the GH/IGF1-axis are protected from cancer and diabetes mellitus. These reported cases support the hypothesis that autoimmunity to a GH/IGF1-axis relevant receptor, e.g. serum autoantibodies to the IGF1R, may lead to growth deficiency, but are at the same time potentially involved in protecting from cancer. This hypothesis might also be supported by the fact that growth hormone deficiency is associated with both, a major reduction in pro-aging signaling and reduction in cancer prevalence, as reviewed in [188].

IGF1R-Ab as anti-cancer drug

One hot topic, not being part of this thesis, but currently in highly expertise research focus, is the usage of IGF1R-Ab as anti-cancer drugs. On the molecular level it was observed that IGF1R overexpression induces tumor formation and metastasis [122, 123]. Later, targeting non-small cell lung cancer cells by dual inhibition of the insulin receptor and the insulin-like growth factor-1 receptor was successfully reducing tumorigenesis [189]. Insulin resistance, type 2 diabetes and obesity are widely known as major risk factors for different types of malignancies [190-192]. Another key component in Insulin / IGF1R signalling is PI3K/Akt, which is known for its role modulating several substrate functions that regulate cell cycle progression, cell survival and cellular growth [193, 194]. In clinical trials the treatment with IGF1R directed monoclonal antibodies seems to be relatively well-tolerated. As main side effects, hyperglycemia, fatigue, and thrombocytopenia have been described [195-197]. Clinical activity has been observed in a broad range of tumor types, including Ewing sarcoma, rhabdomyosarcoma, osteosarcoma, non–small-cell lung cancer, neuroendocrine tumors, and prostate cancer. With respect to gastrointestinal tumors, activity has been reported in colorectal cancer and pancreatic cancer, as reviewed in [198]. Especially the IgG1 antibody AMG 479 ("Ganitumab", Amgen; Thousand Oaks, USA) has shown promising clinical activity in a randomized phase II trial in the treatment of pancreatic cancer when combined with gemxitabine ("Gemzar", Lilly; Indianapolis, USA). The combination therapy resulted in improved median progression-free and overall survival compared with single-agent gemcitabine [199]. But there also exist critical results in anti-IGF1R antibody therapy. Surprisingly, termination of a Ganitumab phase 3 study was stopped for futility in metastatic pancreatic cancer in 2012 (Amgen; Thousand Oaks, CA, USA; News Release: Aug. 8, 2012). In summary, the IGF-1R signaling pathway represents a rational target for cancer therapy, with evidence for clinical activity in several gastrointestinal cancers. Moving forward, the success of the drug development program in identifying clinically active inhibitor compounds will depend on the incorporation of biomarker-guided patient selection, on development of certain key pharmacodynamic biomarkers, and on careful evaluation of combination therapies [200]. Accordingly, the identification of subjects with endogenous IGF1R-aAb may prove of high clinical and therapeutic relevance in oncology, as these subjects may respond differently to novel cancer treatment regimen, and may potentially not develop these fast-growing tumors as observed in IGF1R-aAb negative patients. However, these hypotheses need of course to be tested experimentally in the future.

7 References

1. Wiener, A.S., E.B. Gordon, and C. Gallop, *Studies on autoantibodies in human sera.* J Immunol, 1953. **71**(2): p. 58-65.
2. Burnet, F.M., *The immunological significance of the thymus: an extension of the clonal selection theory of immunity.* Australas Ann Med, 1962. **11**: p. 79-91.
3. Boyden, S.V., *Natural antibodies and the immune response.* Adv Immunol, 1966. **5**: p. 1-28.
4. Avrameas, S., *Natural autoantibodies: from 'horror autotoxicus' to 'gnothi seauton'.* Immunol Today, 1991. **12**(5): p. 154-9.
5. Wassermann A., N.A., Bruck C., *Eine serodiagnostische Reaktion bei Syphilis.* Deutsche Medizinische Wochenschrift, 1906. **32**(19): p. 745-746.
6. Pangborn, M.C., *Cardiolipin and its application in a chemically purified antigen for the serodiagnosis of syphilis.* Proc N Y State Assoc Public Health Lab, 1946. **26**(1): p. 26-9.
7. Rose, N.R., *Autoantibodies*, ed. G.M.E. Shoenfeld Y., Meroni P. L. . Vol. 2. 2007: Elsevier Inc. 872.
8. Harvey, A.M., *Auto-immune disease and the chronic biologic false-positive test for syphilis.* JAMA, 1962. **182**: p. 513-8.
9. Friou, G.J., S.C. Finch, and K.D. Detre, *Interaction of nuclei and globulin from lupus erythematosis serum demonstrated with fluorescent antibody.* J Immunol, 1958. **80**(4): p. 324-9.
10. Holborow, E.J., D.M. Weir, and G.D. Johnson, *A serum factor in lupus erythematosus with affinity for tissue nuclei.* Br Med J, 1957. **2**(5047): p. 732-4.
11. Suh, C.H. and H.A. Kim, *Cytokines and their receptors as biomarkers of systemic lupus erythematosus.* Expert Rev Mol Diagn, 2008. **8**(2): p. 189-98.
12. Bailey, T., K. Rowley, and A. Bernknopf, *A review of systemic lupus erythematosus and current treatment options.* Formulary, 2011. **46**: p. 178–194.
13. Burek, C.L., W.H. Hoffman, and N.R. Rose, *The presence of thyroid autoantibodies in children and adolescents with autoimmune thyroid disease and in their siblings and parents.* Clin Immunol Immunopathol, 1982. **25**(3): p. 395-404.
14. Nielen, M.M., et al., *Simultaneous development of acute phase response and autoantibodies in preclinical rheumatoid arthritis.* Ann Rheum Dis, 2006. **65**(4): p. 535-7.
15. Blank, M., et al., *Bacterial induction of autoantibodies to beta2-glycoprotein-I accounts for the infectious etiology of antiphospholipid syndrome.* J Clin Invest, 2002. **109**(6): p. 797-804.
16. Zinkernagel, R.M., et al., *Virus-induced autoantibody response to a transgenic viral antigen.* Nature, 1990. **345**(6270): p. 68-71.
17. Ziem, G. and J. McTamney, *Profile of patients with chemical injury and sensitivity.* Environ Health Perspect, 1997. **105 Suppl 2**: p. 417-36.
18. Wesche, B., et al., *Induction of autoantibodies to the adrenal cortex and pancreatic islet cells by interferon alpha therapy for chronic hepatitis C.* Gut, 2001. **48**(3): p. 378-83.
19. Tanriverdi, F., et al., *Antipituitary antibodies after traumatic brain injury: is head trauma-induced pituitary dysfunction associated with autoimmunity?* Eur J Endocrinol, 2008. **159**(1): p. 7-13.
20. Pollard, K.M. and D.H. Kono, *Requirements for innate immune pathways in environmentally induced autoimmunity.* BMC Med, 2013. **11**: p. 100.
21. Schott, M., W.A. Scherbaum, and N.G. Morgenthaler, *Thyrotropin receptor autoantibodies in Graves' disease.* Trends Endocrinol Metab, 2005. **16**(5): p. 243-8.
22. Endo, K., et al., *Detection and properties of TSH-binding inhibitor immunoglobulins in patients with Graves' disease and Hashimoto's thyroiditis.* J Clin Endocrinol Metab, 1978. **46**(5): p. 734-9.
23. Chiovato, L., et al., *Incidence of antibodies blocking thyrotropin effect in vitro in patients with euthyroid or hypothyroid autoimmune thyroiditis.* J Clin Endocrinol Metab, 1990. **71**(1): p. 40-5.
24. Cornelis, S., et al., *Purification and characterization of a soluble bioactive amino-terminal extracellular domain of the human thyrotropin receptor.* Biochemistry, 2001. **40**(33): p. 9860-9.

25. Rapoport, B., et al., *The thyrotropin (TSH) receptor: interaction with TSH and autoantibodies.* Endocr Rev, 1998. **19**(6): p. 673-716.

26. Hollowell, J.G., et al., *Serum TSH, T(4), and thyroid antibodies in the United States population (1988 to 1994): National Health and Nutrition Examination Survey (NHANES III).* J Clin Endocrinol Metab, 2002. **87**(2): p. 489-99.

27. Rees Smith, B., S.M. McLachlan, and J. Furmaniak, *Autoantibodies to the thyrotropin receptor.* Endocr Rev, 1988. **9**(1): p. 106-21.

28. Prabhakar, B.S., R.S. Bahn, and T.J. Smith, *Current perspective on the pathogenesis of Graves' disease and ophthalmopathy.* Endocr Rev, 2003. **24**(6): p. 802-35.

29. Sapin, R., et al., *Increased sensitivity of a new assay for anti-thyroglobulin antibody detection in patients with autoimmune thyroid disease.* Clin Biochem, 2003. **36**(8): p. 611-6.

30. McLachlan, S.M. and B. Rapoport, *The molecular biology of thyroid peroxidase: cloning, expression and role as autoantigen in autoimmune thyroid disease.* Endocr Rev, 1992. **13**(2): p. 192-206.

31. Shulman, L.E. and A.M. Harvey, *Hashimoto's Thyroiditis in False-Positive Reactors to the Tests for Syphilis.* Am J Med, 1964. **36**: p. 174-87.

32. Bahn, R.S., *Graves' ophthalmopathy.* N Engl J Med, 2010. **362**(8): p. 726-38.

33. van Steensel, L., et al., *Orbit-infiltrating mast cells, monocytes, and macrophages produce PDGF isoforms that orchestrate orbital fibroblast activation in Graves' ophthalmopathy.* J Clin Endocrinol Metab, 2012. **97**(3): p. E400-8.

34. Tsui, S., et al., *Evidence for an association between thyroid-stimulating hormone and insulin-like growth factor 1 receptors: a tale of two antigens implicated in Graves' disease.* J Immunol, 2008. **181**(6): p. 4397-405.

35. Weightman, D.R., et al., *Autoantibodies to IGF-1 binding sites in thyroid associated ophthalmopathy.* Autoimmunity, 1993. **16**(4): p. 251-7.

36. Hsiao, P.J. and J.H. Tsai, *Increased insulin-like growth factor-1 receptors in thyroid tissues of Graves' disease.* J Formos Med Assoc, 1994. **93**(11-12): p. 925-32.

37. Smith, T.J., *The putative role of fibroblasts in the pathogenesis of Graves' disease: evidence for the involvement of the insulin-like growth factor-1 receptor in fibroblast activation.* Autoimmunity, 2003. **36**(6-7): p. 409-15.

38. Imai, Y., et al., *Effect of growth factors on hyaluronan and proteoglycan synthesis by retroocular tissue fibroblasts of Graves' ophthalmopathy in culture.* Acta Endocrinol (Copenh), 1992. **126**(6): p. 541-52.

39. Douglas, R.S., et al., *Divergent frequencies of IGF-I receptor-expressing blood lymphocytes in monozygotic twin pairs discordant for Graves' disease: evidence for a phenotypic signature ascribable to nongenetic factors.* J Clin Endocrinol Metab, 2009. **94**(5): p. 1797-802.

40. Brix, T.H., et al., *A population-based study of Graves' disease in Danish twins.* Clin Endocrinol (Oxf), 1998. **48**(4): p. 397-400.

41. Smith, T.J. and N. Hoa, *Immunoglobulins from patients with Graves' disease induce hyaluronan synthesis in their orbital fibroblasts through the self-antigen, insulin-like growth factor-I receptor.* J Clin Endocrinol Metab, 2004. **89**(10): p. 5076-80.

42. Pritchard, J., et al., *Synovial fibroblasts from patients with rheumatoid arthritis, like fibroblasts from Graves' disease, express high levels of IL-16 when treated with Igs against insulin-like growth factor-1 receptor.* J Immunol, 2004. **173**(5): p. 3564-9.

43. Pritchard, J., et al., *Immunoglobulin activation of T cell chemoattractant expression in fibroblasts from patients with Graves' disease is mediated through the insulin-like growth factor I receptor pathway.* J Immunol, 2003. **170**(12): p. 6348-54.

44. Smith, T.J., *Insulin-like growth factor-I regulation of immune function: a potential therapeutic target in autoimmune diseases?* Pharmacol Rev, 2010. **62**(2): p. 199-236.

45. Tappy, L., et al., *Antibodies to insulin-like growth factor I receptors in diabetes and other disorders.* Diabetes, 1988. **37**(12): p. 1708-14.

46. Shimoyama, R., Y. Fujita-Yamaguchi, and G. Boden, *Anti-insulin receptor antibodies in human diabetes.* Diabetes Res Clin Pract, 1989. **7 Suppl 1**: p. S59-66.

47. Zhou, P., et al., *Insulin receptor autoimmunity and insulin resistance.* J Pediatr Endocrinol Metab, 2008. **21**(4): p. 369-75.

48. Maruyama, T., et al., *Anti-insulin-like growth factor-1 autoantibodies in type 1 diabetes.* Ann N Y Acad Sci, 2002. **958**: p. 267-70.

49. Rinderknecht, E. and R.E. Humbel, *The amino acid sequence of human insulin-like growth factor I and its structural homology with proinsulin.* J Biol Chem, 1978. **253**(8): p. 2769-76.

50. Bergerot, I., et al., *Insulin-like growth factor-1 (IGF-1) protects NOD mice from insulitis and diabetes.* Clin Exp Immunol, 1995. **102**(2): p. 335-40.

51. Rosenfeld, R.G., et al., *Simultaneous inhibition of insulin and somatomedin-C binding to cultured IM-9 lymphocytes by naturally occurring antireceptor antibodies.* Diabetes, 1981. **30**(11): p. 979-82.

52. LeRoith, D. and C.T. Roberts, Jr., *The insulin-like growth factor system and cancer.* Cancer Lett, 2003. **195**(2): p. 127-37.

53. Samani, A.A., et al., *The role of the IGF system in cancer growth and metastasis: overview and recent insights.* Endocr Rev, 2007. **28**(1): p. 20-47.

54. Coutinho, M.F., M.J. Prata, and S. Alves, *A shortcut to the lysosome: the mannose-6-phosphate-independent pathway.* Mol Genet Metab, 2012. **107**(3): p. 257-66.

55. Bergman, D., et al., *Insulin-like growth factor 2 in development and disease: a mini-review.* Gerontology, 2013. **59**(3): p. 240-9.

56. Li, X., A.G. Garrity, and H. Xu, *Regulation of membrane trafficking by signalling on endosomal and lysosomal membranes.* J Physiol, 2013. **591**(Pt 18): p. 4389-401.

57. Scharf, J.G., F. Dombrowski, and G. Ramadori, *The IGF axis and hepatocarcinogenesis.* Mol Pathol, 2001. **54**(3): p. 138-44.

58. Coolican, S.A., et al., *The mitogenic and myogenic actions of insulin-like growth factors utilize distinct signaling pathways.* J Biol Chem, 1997. **272**(10): p. 6653-62.

59. Johnson, S.E. and R.E. Allen, *The effects of bFGF, IGF-I, and TGF-beta on RMo skeletal muscle cell proliferation and differentiation.* Exp Cell Res, 1990. **187**(2): p. 250-4.

60. Leloup, L., et al., *Involvement of calpains in growth factor-mediated migration.* Int J Biochem Cell Biol, 2006. **38**(12): p. 2049-63.

61. Johnson, G.L. and R. Lapadat, *Mitogen-activated protein kinase pathways mediated by ERK, JNK, and p38 protein kinases.* Science, 2002. **298**(5600): p. 1911-2.

62. Manning, B.D. and L.C. Cantley, *AKT/PKB signaling: navigating downstream.* Cell, 2007. **129**(7): p. 1261-74.

63. Ghosh, P., N.M. Dahms, and S. Kornfeld, *Mannose 6-phosphate receptors: new twists in the tale.* Nat Rev Mol Cell Biol, 2003. **4**(3): p. 202-12.

64. Treadway, J.L., et al., *Assembly of insulin/insulin-like growth factor-1 hybrid receptors in vitro.* J Biol Chem, 1989. **264**(36): p. 21450-3.

65. Soos, M.A., et al., *Receptors for insulin and insulin-like growth factor-I can form hybrid dimers. Characterisation of hybrid receptors in transfected cells.* Biochem J, 1990. **270**(2): p. 383-90.

66. Jones, J.I. and D.R. Clemmons, *Insulin-like growth factors and their binding proteins: biological actions.* Endocr Rev, 1995. **16**(1): p. 3-34.

67. Blat, C., J. Villaudy, and M. Binoux, *In vivo proteolysis of serum insulin-like growth factor (IGF) binding protein-3 results in increased availability of IGF to target cells.* J Clin Invest, 1994. **93**(5): p. 2286-90.

68. Manes, S., et al., *The matrix metalloproteinase-9 regulates the insulin-like growth factor-triggered autocrine response in DU-145 carcinoma cells.* J Biol Chem, 1999. **274**(11): p. 6935-45.

69. Holly, J. and C. Perks, *The role of insulin-like growth factor binding proteins.* Neuroendocrinology, 2006. **83**(3-4): p. 154-60.

70. Salmon, W.D., Jr. and W.H. Daughaday, *A hormonally controlled serum factor which stimulates sulfate incorporation by cartilage in vitro.* J Lab Clin Med, 1957. **49**(6): p. 825-36.

71. Froesch, E.R., et al., *Antibody-Suppressible and Nonsuppressible Insulin-Like Activities in Human Serum and Their Physiologic Significance. An Insulin Assay with Adipose Tissue of Increased Precision and Specificity.* J Clin Invest, 1963. **42**: p. 1816-34.

72. Daughaday, W.H., et al., *Somatomedin: proposed designation for sulphation factor.* Nature, 1972. **235**(5333): p. 107.

73. Rinderknecht, E. and R.E. Humbel, *Polypeptides with nonsuppressible insulin-like and cell-growth promoting activities in human serum: isolation, chemical characterization, and some biological properties of forms I and II.* Proc Natl Acad Sci U S A, 1976. **73**(7): p. 2365-9.

74. Laron, Z., *Somatomedin-1 (recombinant insulin-like growth factor-1): clinical pharmacology and potential treatment of endocrine and metabolic disorders.* BioDrugs, 1999. **11**(1): p. 55-70.

75. Pollak, M., *Insulin and insulin-like growth factor signalling in neoplasia.* Nat Rev Cancer, 2008. **8**(12): p. 915-28.

76. Slattery, M.L., et al., *Genetic variation in IGF1, IGFBP3, IRS1, IRS2 and risk of breast cancer in women living in Southwestern United States.* Breast Cancer Res Treat, 2007. **104**(2): p. 197-209.

77. Hartmann, W., et al., *Insulin-like growth factor II is involved in the proliferation control of medulloblastoma and its cerebellar precursor cells.* Am J Pathol, 2005. **166**(4): p. 1153-62.

78. Kalla Singh, S., et al., *Differential insulin-like growth factor II (IGF-II) expression: A potential role for breast cancer survival disparity.* Growth Horm IGF Res, 2010. **20**(2): p. 162-70.

79. Baker, J., et al., *Role of insulin-like growth factors in embryonic and postnatal growth.* Cell, 1993. **75**(1): p. 73-82.

80. Furstenberger, G. and H.J. Senn, *Insulin-like growth factors and cancer.* Lancet Oncol, 2002. **3**(5): p. 298-302.

81. Miura, Y., H. Kato, and T. Noguchi, *Effect of dietary proteins on insulin-like growth factor-1 (IGF-1) messenger ribonucleic acid content in rat liver.* Br J Nutr, 1992. **67**(2): p. 257-65.

82. Daughaday, W.H. and P. Rotwein, *Insulin-like growth factors I and II. Peptide, messenger ribonucleic acid and gene structures, serum, and tissue concentrations.* Endocr Rev, 1989. **10**(1): p. 68-91.

83. Firth, S.M. and R.C. Baxter, *Cellular actions of the insulin-like growth factor binding proteins.* Endocr Rev, 2002. **23**(6): p. 824-54.

84. Oh, Y., et al., *Synthesis and characterization of insulin-like growth factor-binding protein (IGFBP)-7. Recombinant human mac25 protein specifically binds IGF-I and -II.* J Biol Chem, 1996. **271**(48): p. 30322-5.

85. Shimasaki, S. and N. Ling, *Identification and molecular characterization of insulin-like growth factor binding proteins (IGFBP-1, -2, -3, -4, -5 and -6).* Prog Growth Factor Res, 1991. **3**(4): p. 243-66.

86. Baxter, R.C., *IGF binding protein-3 and the acid-labile subunit: formation of the ternary complex in vitro and in vivo.* Adv Exp Med Biol, 1993. **343**: p. 237-44.

87. Twigg, S.M. and R.C. Baxter, *Insulin-like growth factor (IGF)-binding protein 5 forms an alternative ternary complex with IGFs and the acid-labile subunit.* J Biol Chem, 1998. **273**(11): p. 6074-9.

88. Kalluri, H.S. and R.J. Dempsey, *IGFBP-3 inhibits the proliferation of neural progenitor cells.* Neurochem Res, 2011. **36**(3): p. 406-11.

89. Ricort, J.M. and M. Binoux, *Insulin-like growth factor (IGF) binding protein-3 inhibits type 1 IGF receptor activation independently of its IGF binding affinity.* Endocrinology, 2001. **142**(1): p. 108-13.

90. Megyesi, K., et al., *The NSILA-s receptor in liver plasma membranes. Characterization and comparison with the insulin receptor.* J Biol Chem, 1975. **250**(23): p. 8990-6.

91. Bondy, C.A., et al., *Cellular pattern of insulin-like growth factor-I (IGF-I) and type I IGF receptor gene expression in early organogenesis: comparison with IGF-II gene expression.* Mol Endocrinol, 1990. **4**(9): p. 1386-98.

92. Ullrich, A., et al., *Insulin-like growth factor I receptor primary structure: comparison with insulin receptor suggests structural determinants that define functional specificity.* EMBO J, 1986. **5**(10): p. 2503-12.

93. Ward, C.W., P.A. Hoyne, and R.H. Flegg, *Insulin and epidermal growth factor receptors contain the cysteine repeat motif found in the tumor necrosis factor receptor.* Proteins, 1995. **22**(2): p. 141-53.

94. Marino-Buslje, C., et al., *A third fibronectin type III domain in the extracellular region of the insulin receptor family.* FEBS Lett, 1998. **441**(2): p. 331-6.

95. Trombetta, E.S. and A. Helenius, *Lectins as chaperones in glycoprotein folding.* Curr Opin Struct Biol, 1998. **8**(5): p. 587-92.

96. Garrett, T.P., et al., *Crystal structure of the first three domains of the type-1 insulin-like growth factor receptor.* Nature, 1998. **394**(6691): p. 395-9.

97. Kato, H., et al., *Essential role of tyrosine residues 1131, 1135, and 1136 of the insulin-like growth factor-I (IGF-I) receptor in IGF-I action.* Mol Endocrinol, 1994. **8**(1): p. 40-50.

98. Rechler, M.M. and S.P. Nissley, *The nature and regulation of the receptors for insulin-like growth factors.* Annu Rev Physiol, 1985. **47**: p. 425-42.

99.   Chernausek, S.D., S. Jacobs, and J.J. Van Wyk, *Structural similarities between human receptors for somatomedin C and insulin: analysis by affinity labeling.* Biochemistry, 1981. **20**(26): p. 7345-50.

100.   Kornfeld, S., *Structure and function of the mannose 6-phosphate/insulinlike growth factor II receptors.* Annu Rev Biochem, 1992. **61**: p. 307-30.

101.   Hassan, A.B., *Keys to the hidden treasures of the mannose 6-phosphate/insulin-like growth factor 2 receptor.* Am J Pathol, 2003. **162**(1): p. 3-6.

102.   Lobel, P., N.M. Dahms, and S. Kornfeld, *Cloning and sequence analysis of the cation-independent mannose 6-phosphate receptor.* J Biol Chem, 1988. **263**(5): p. 2563-70.

103.   Hancock, M.K., et al., *Identification of residues essential for carbohydrate recognition by the insulin-like growth factor II/mannose 6-phosphate receptor.* J Biol Chem, 2002. **277**(13): p. 11255-64.

104.   Schmidt, B., et al., *Localization of the insulin-like growth factor II binding site to amino acids 1508-1566 in repeat 11 of the mannose 6-phosphate/insulin-like growth factor II receptor.* J Biol Chem, 1995. **270**(25): p. 14975-82.

105.   Byrd, J.C. and R.G. MacDonald, *Mechanisms for high affinity mannose 6-phosphate ligand binding to the insulin-like growth factor II/mannose 6-phosphate receptor.* J Biol Chem, 2000. **275**(25): p. 18638-46.

106.   Byrd, J.C., et al., *Dimerization of the insulin-like growth factor II/mannose 6-phosphate receptor.* J Biol Chem, 2000. **275**(25): p. 18647-56.

107.   Braulke, T., *Type-2 IGF receptor: a multi-ligand binding protein.* Horm Metab Res, 1999. **31**(2-3): p. 242-6.

108.   De Souza, A.T., et al., *M6P/IGF2R gene is mutated in human hepatocellular carcinomas with loss of heterozygosity.* Nat Genet, 1995. **11**(4): p. 447-9.

109.   Pollak, M.N., E.S. Schernhammer, and S.E. Hankinson, *Insulin-like growth factors and neoplasia.* Nat Rev Cancer, 2004. **4**(7): p. 505-18.

110.   Rother, K.I. and D. Accili, *Role of insulin receptors and IGF receptors in growth and development.* Pediatr Nephrol, 2000. **14**(7): p. 558-61.

111.   Wu, J. and A.X. Zhu, *Targeting insulin-like growth factor axis in hepatocellular carcinoma.* J Hematol Oncol, 2011. **4**: p. 30.

112.   Favelyukis, S., et al., *Structure and autoregulation of the insulin-like growth factor 1 receptor kinase.* Nat Struct Biol, 2001. **8**(12): p. 1058-63.

113.   Baserga, R., F. Peruzzi, and K. Reiss, *The IGF-1 receptor in cancer biology.* Int J Cancer, 2003. **107**(6): p. 873-7.

114.   Byron, S.A., et al., *Insulin receptor substrates mediate distinct biological responses to insulin-like growth factor receptor activation in breast cancer cells.* Br J Cancer, 2006. **95**(9): p. 1220-8.

115.   Guertin, D.A. and D.M. Sabatini, *An expanding role for mTOR in cancer.* Trends Mol Med, 2005. **11**(8): p. 353-61.

116.   Datta, S.R., A. Brunet, and M.E. Greenberg, *Cellular survival: a play in three Akts.* Genes Dev, 1999. **13**(22): p. 2905-27.

117.   Efeyan, A. and D.M. Sabatini, *Nutrients and growth factors in mTORC1 activation.* Biochem Soc Trans, 2013. **41**(4): p. 902-5.

118.   Liu, J.P., et al., *Mice carrying null mutations of the genes encoding insulin-like growth factor I (Igf-1) and type 1 IGF receptor (Igf1r).* Cell, 1993. **75**(1): p. 59-72.

119.   Ouban, A., et al., *Expression and distribution of insulin-like growth factor-1 receptor in human carcinomas.* Hum Pathol, 2003. **34**(8): p. 803-8.

120.   Chitnis, M.M., et al., *The type 1 insulin-like growth factor receptor pathway.* Clin Cancer Res, 2008. **14**(20): p. 6364-70.

121.   Sell, C., et al., *Effect of a null mutation of the insulin-like growth factor I receptor gene on growth and transformation of mouse embryo fibroblasts.* Mol Cell Biol, 1994. **14**(6): p. 3604-12.

122.   Lopez, T. and D. Hanahan, *Elevated levels of IGF-1 receptor convey invasive and metastatic capability in a mouse model of pancreatic islet tumorigenesis.* Cancer Cell, 2002. **1**(4): p. 339-53.

123.   Jones, R.A., et al., *Transgenic overexpression of IGF-IR disrupts mammary ductal morphogenesis and induces tumor formation.* Oncogene, 2007. **26**(11): p. 1636-44.

124.   Wu, Y., et al., *Reduced circulating insulin-like growth factor I levels delay the onset of chemically and genetically induced mammary tumors.* Cancer Res, 2003. **63**(15): p. 4384-8.

125. Arteaga, C.L., et al., *Blockade of the type I somatomedin receptor inhibits growth of human breast cancer cells in athymic mice.* J Clin Invest, 1989. **84**(5): p. 1418-23.

126. Yee, D., *Insulin-like growth factor receptor inhibitors: baby or the bathwater?* J Natl Cancer Inst, 2012. **104**(13): p. 975-81.

127. Robertson, J.F., et al., *Ganitumab with either exemestane or fulvestrant for postmenopausal women with advanced, hormone-receptor-positive breast cancer: a randomised, controlled, double-blind, phase 2 trial.* Lancet Oncol, 2013. **14**(3): p. 228-35.

128. Jassem, J., et al. *Randomized, open label, phase III trial of figitumumab in combination with paclitaxel and carboplatin versus paclitaxel and carboplatin in patients with non-small cell lung cancer (NSCLC).* in *ASCO Annual Meeting.* 2010. Proc Am Soc Clin Oncol 28:15s (suppl; abstr. 7500).

129. Pappo, A.S., et al., *R1507, a monoclonal antibody to the insulin-like growth factor 1 receptor, in patients with recurrent or refractory Ewing sarcoma family of tumors: results of a phase II Sarcoma Alliance for Research through Collaboration study.* J Clin Oncol, 2011. **29**(34): p. 4541-7.

130. Wilson, S. and S.K. Chia, *IGF-1R inhibition: right direction, wrong pathway?* Lancet Oncol, 2013. **14**(3): p. 182-3.

131. Pietrzkowski, Z., et al., *Inhibition of growth of prostatic cancer cell lines by peptide analogues of insulin-like growth factor 1.* Cancer Res, 1993. **53**(5): p. 1102-6.

132. Girnita, A., et al., *Cyclolignans as inhibitors of the insulin-like growth factor-1 receptor and malignant cell growth.* Cancer Res, 2004. **64**(1): p. 236-42.

133. LeRoith, D. and L. Helman, *The new kid on the block(ade) of the IGF-1 receptor.* Cancer Cell, 2004. **5**(3): p. 201-2.

134. Gombos, A., et al., *Clinical development of insulin-like growth factor receptor--1 (IGF-1R) inhibitors: at the crossroad?* Invest New Drugs, 2012. **30**(6): p. 2433-42.

135. Zha, J. and M.R. Lackner, *Targeting the insulin-like growth factor receptor-1R pathway for cancer therapy.* Clin Cancer Res, 2010. **16**(9): p. 2512-7.

136. Tramontano, D., et al., *Insulin-like growth factor-I stimulates the growth of rat thyroid cells in culture and synergizes the stimulation of DNA synthesis induced by TSH and Graves'-IgG.* Endocrinology, 1986. **119**(2): p. 940-2.

137. Tramontano, D., A.C. Moses, and S.H. Ingbar, *The role of adenosine 3',5'-monophosphate in the regulation of receptors for thyrotropin and insulin-like growth factor I in the FRTL5 rat thyroid follicular cell.* Endocrinology, 1988. **122**(1): p. 133-6.

138. Tramontano, D., et al., *Adenosine 3',5'-monophosphate mediates both the mitogenic effect of thyrotropin and its ability to amplify the response to insulin-like growth factor I in FRTL5 cells.* Endocrinology, 1988. **122**(1): p. 127-32.

139. Clement, S., et al., *Low TSH requirement and goiter in transgenic mice overexpressing IGF-I and IGF-Ir receptor in the thyroid gland.* Endocrinology, 2001. **142**(12): p. 5131-9.

140. Park, Y.J., et al., *p66Shc expression in proliferating thyroid cells is regulated by thyrotropin receptor signaling.* Endocrinology, 2005. **146**(5): p. 2473-80.

141. Cass, L.A. and J.L. Meinkoth, *Differential effects of cyclic adenosine 3',5'-monophosphate on p70 ribosomal S6 kinase.* Endocrinology, 1998. **139**(4): p. 1991-8.

142. Verschure, P.J., et al., *Histochemical analysis of insulin-like growth factor-1 binding sites in mouse normal and experimentally induced arthritic articular cartilage.* Histochem J, 1996. **28**(1): p. 13-23.

143. Slonim, A.E., et al., *A preliminary study of growth hormone therapy for Crohn's disease.* N Engl J Med, 2000. **342**(22): p. 1633-7.

144. Eisenbarth, G.S., A.G. Ziegler, and P.A. Colman, *Pathogenesis of insulin-dependent (type I) diabetes mellitus* in *Joslin's Diabetes Mellitus*, C.E. Kahn and G.C. Weir, Editors. 1994, Lea and Febiger: Philadelphia. p. 216-239.

145. Xuan, S., et al., *Defective insulin secretion in pancreatic beta cells lacking type 1 IGF receptor.* J Clin Invest, 2002. **110**(7): p. 1011-9.

146. Calderari, S., et al., *Defective IGF2 and IGF1R protein production in embryonic pancreas precedes beta cell mass anomaly in the Goto-Kakizaki rat model of type 2 diabetes.* Diabetologia, 2007. **50**(7): p. 1463-71.

147. Van Schravendijk, C.F., et al., *Evidence for the presence of type I insulin-like growth factor receptors on rat pancreatic A and B cells.* Endocrinology, 1987. **121**(5): p. 1784-8.

148. Zhang, Q., et al., *Insulin-like growth factor II signaling through the insulin-like growth factor II/mannose-6-phosphate receptor promotes exocytosis in insulin-secreting cells.* Proc Natl Acad Sci U S A, 1997. **94**(12): p. 6232-7.

149. Bonner-Weir, S. and F.E. Smith, *Islet cell growth and the growth factors involved.* Trends Endocrinol Metab, 1994. **5**(2): p. 60-4.

150. George, M., et al., *Beta cell expression of IGF-I leads to recovery from type 1 diabetes.* J Clin Invest, 2002. **109**(9): p. 1153-63.

151. Kulkarni, R.N., et al., *beta-cell-specific deletion of the Igf1 receptor leads to hyperinsulinemia and glucose intolerance but does not alter beta-cell mass.* Nat Genet, 2002. **31**(1): p. 111-5.

152. Giannoukakis, N., et al., *Prevention of beta cell dysfunction and apoptosis activation in human islets by adenoviral gene transfer of the insulin-like growth factor I.* Gene Ther, 2000. **7**(23): p. 2015-22.

153. Clemmons, D.R., et al., *Rh/IGF-I/rhIGFBP-3 administration to patients with type 2 diabetes mellitus reduces insulin requirements while also lowering fasting glucose.* Growth Horm IGF Res, 2005. **15**(4): p. 265-74.

154. Caliebe, J., et al., *IGF1, IGF1R and SHOX mutation analysis in short children born small for gestational age and short children with normal birth size (idiopathic short stature).* Horm Res Paediatr, 2012. **77**(4): p. 250-60.

155. Ester, W.A., et al., *Two short children born small for gestational age with insulin-like growth factor 1 receptor haploinsufficiency illustrate the heterogeneity of its phenotype.* J Clin Endocrinol Metab, 2009. **94**(12): p. 4717-27.

156. Hoopes, B.C., et al., *The insulin-like growth factor 1 receptor (IGF1R) contributes to reduced size in dogs.* Mamm Genome, 2012. **23**(11-12): p. 780-90.

157. Schultheiss, O.C. and S.J. Stanton, *Assessment of salivary hormones*, in *Methods in Social Neuroscience* E.B. Harmon-Jones, J.S., Editor 2009, Guilford Press: New York.

158. Hollenbach, B., et al., *New assay for the measurement of selenoprotein P as a sepsis biomarker from serum.* J Trace Elem Med Biol, 2008. **22**(1): p. 24-32.

159. Mullis, K., et al., *Specific enzymatic amplification of DNA in vitro: the polymerase chain reaction.* Cold Spring Harb Symp Quant Biol, 1986. **51 Pt 1**: p. 263-73.

160. Laemmli, U.K., *Cleavage of structural proteins during the assembly of the head of bacteriophage T4.* Nature, 1970. **227**(5259): p. 680-5.

161. Strober, W., *Trypan blue exclusion test of cell viability.* Curr Protoc Immunol, 2001. **Appendix 3**: p. Appendix 3B.

162. Rees, S., et al., *Bicistronic vector for the creation of stable mammalian cell lines that predisposes all antibiotic-resistant cells to express recombinant protein.* Biotechniques, 1996. **20**(1): p. 102-4, 106, 108-10.

163. Tang, D.C., M. DeVit, and S.A. Johnston, *Genetic immunization is a simple method for eliciting an immune response.* Nature, 1992. **356**(6365): p. 152-4.

164. Davis, H.L., M.L. Michel, and R.G. Whalen, *DNA-based immunization induces continuous secretion of hepatitis B surface antigen and high levels of circulating antibody.* Hum Mol Genet, 1993. **2**(11): p. 1847-51.

165. Costagliola, S., et al., *Genetic immunization against the human thyrotropin receptor causes thyroiditis and allows production of monoclonal antibodies recognizing the native receptor.* J Immunol, 1998. **160**(3): p. 1458-65.

166. *World Medical Association Declaration of Helsinki: ethical principles for medical research involving human subjects.* JAMA, 2013. **310**(20): p. 2191-4.

167. Juul, A., et al., *Free insulin-like growth factor I serum levels in 1430 healthy children and adults, and its diagnostic value in patients suspected of growth hormone deficiency.* J Clin Endocrinol Metab, 1997. **82**(8): p. 2497-502.

168. Friedrich, N., et al., *Reference ranges of serum IGF-1 and IGFBP-3 levels in a general adult population: results of the Study of Health in Pomerania (SHIP).* Growth Horm IGF Res, 2008. **18**(3): p. 228-37.

169. Contreras-Gomez, A., et al., *Protein production using the baculovirus-insect cell expression system.* Biotechnol Prog, 2014. **30**(1): p. 1-18.

170. Smith, G.E., M.D. Summers, and M.J. Fraser, *Production of human beta interferon in insect cells infected with a baculovirus expression vector.* Mol Cell Biol, 1983. **3**(12): p. 2156-65.

171. Rychlowska, M., et al., *Application of baculovirus-insect cell expression system for human therapy.* Curr Pharm Biotechnol, 2011. **12**(11): p. 1840-9.

172. Mena, J.A. and A.A. Kamen, *Insect cell technology is a versatile and robust vaccine manufacturing platform.* Expert Rev Vaccines, 2011. **10**(7): p. 1063-81.

173. Minich, W.B. and U. Loos, *Detection of functionally different types of pathological autoantibodies against thyrotropin receptor in Graves' patients sera by luminescent immunoprecipitation analysis.* Exp Clin Endocrinol Diabetes, 2000. **108**(2): p. 110-9.

174. Adams, T.E., et al., *Structure and function of the type 1 insulin-like growth factor receptor.* Cell Mol Life Sci, 2000. **57**(7): p. 1050-93.

175. De Meyts, P. and J. Whittaker, *Structural biology of insulin and IGF1 receptors: implications for drug design.* Nat Rev Drug Discov, 2002. **1**(10): p. 769-83.

176. Grotjan, H.E. and A.K. Brooks, *Data interpretation and quality control* in *Immunoassay* E.P. Diamandis and T.K. Christopoulos, Editors. 1996, Academic Press, Inc. : San Diego, USA. p. 51 - 94.

177. Michalek, K., et al., *TSH receptor autoantibodies.* Autoimmun Rev, 2009. **9**(2): p. 113-6.

178. Ando, T., et al., *Dissecting linear and conformational epitopes on the native thyrotropin receptor.* Endocrinology, 2004. **145**(11): p. 5185-93.

179. Goldsby, R.A., *Immunology. "Antigens (Chapter 3)"* 5ed2003, New York: W. H. Freeman.

180. van Es, J.H., et al., *Somatic mutations in the variable regions of a human IgG anti-double-stranded DNA autoantibody suggest a role for antigen in the induction of systemic lupus erythematosus.* J Exp Med, 1991. **173**(2): p. 461-70.

181. Doi, T., et al., *Analysis of IgG immune complexes in sera from patients with membranous nephropathy: role of IgG4 subclass and low-avidity antibodies.* Nephron, 1991. **57**(2): p. 131-6.

182. Wiersinga, W.M., *Autoimmunity in Graves' ophthalmopathy: the result of an unfortunate marriage between TSH receptors and IGF-1 receptors?* J Clin Endocrinol Metab, 2011. **96**(8): p. 2386-94.

183. Smith, T.J., *Insulin-like growth factor-I regulation of immune function: a potential therapeutic target in autoimmune diseases?* Pharmacol Rev, 2011. **62**(2): p. 199-236.

184. Pritchard, J., et al., *Igs from patients with Graves' disease induce the expression of T cell chemoattractants in their fibroblasts.* J Immunol, 2002. **168**(2): p. 942-50.

185. Minich, W.B., et al., *Autoantibodies to the IGF1 receptor in Graves' orbitopathy.* J Clin Endocrinol Metab, 2013. **98**(2): p. 752-60.

186. Eckstein, A.K., et al., *Thyrotropin receptor autoantibodies are independent risk factors for Graves' ophthalmopathy and help to predict severity and outcome of the disease.* J Clin Endocrinol Metab, 2006. **91**(9): p. 3464-70.

187. Guevara-Aguirre, J., et al., *Growth hormone receptor deficiency is associated with a major reduction in pro-aging signaling, cancer, and diabetes in humans.* Sci Transl Med, 2011. **3**(70): p. 70ra13.

188. Junnila, R.K., et al., *The GH/IGF-1 axis in ageing and longevity.* Nat Rev Endocrinol, 2013. **9**(6): p. 366-76.

189. Vincent, E.E., et al., *Targeting non-small cell lung cancer cells by dual inhibition of the insulin receptor and the insulin-like growth factor-1 receptor.* PLoS One, 2013. **8**(6): p. e66963.

190. Coughlin, S.S., et al., *Diabetes mellitus as a predictor of cancer mortality in a large cohort of US adults.* Am J Epidemiol, 2004. **159**(12): p. 1160-7.

191. Vigneri, P., et al., *Obesity and cancer.* Nutr Metab Cardiovasc Dis, 2006. **16**(1): p. 1-7.

192. Fair, A.M., et al., *Energy balance, insulin resistance biomarkers, and breast cancer risk.* Cancer Detect Prev, 2007. **31**(3): p. 214-9.

193. Erejuwa, O.O., S.A. Sulaiman, and M.S. Wahab, *Effects of honey and its mechanisms of action on the development and progression of cancer.* Molecules, 2014. **19**(2): p. 2497-522.

194. Carnero, A., et al., *The PTEN/PI3K/AKT signalling pathway in cancer, therapeutic implications.* Curr Cancer Drug Targets, 2008. **8**(3): p. 187-98.

195. Zhang, H. and D. Yee, *The therapeutic potential of agents targeting the type I insulin-like growth factor receptor.* Expert Opin Investig Drugs, 2004. **13**(12): p. 1569-77.

196. Lopez-Calderero, I., E. Sanchez Chavez, and R. Garcia-Carbonero, *The insulin-like growth factor pathway as a target for cancer therapy.* Clin Transl Oncol, 2010. **12**(5): p. 326-38.

197. Rodon, J., et al., *Early drug development of inhibitors of the insulin-like growth factor-I receptor pathway: lessons from the first clinical trials.* Mol Cancer Ther, 2008. **7**(9): p. 2575-88.

198. Golan, T. and M. Javle, *Targeting the insulin growth factor pathway in gastrointestinal cancers.* Oncology (Williston Park), 2011. **25**(6): p. 518-26, 529.

199.   Kindler, H.L., et al., *A randomized, placebo-controlled phase 2 study of ganitumab (AMG 479) or conatumumab (AMG 655) in combination with gemcitabine in patients with metastatic pancreatic cancer.* Ann Oncol, 2012. **23**(11): p. 2834-42.
200.   Chu, E., *The IGF-1R pathway as a therapeutic target.* Oncology (Williston Park), 2011. **25**(6): p. 538-9, 543.
201.   Magrane, M. and U. Consortium, *UniProt Knowledgebase: a hub of integrated protein data.* Database (Oxford), 2011. **2011**: p. bar009.

8   Supplementary material

Amino acid sequence of IGF1R

Wild type protein sequence of the human IGF1R (Uniprot [201], Acc.no. P08069) with a length of 1367 amino acids:

```
   1 MKSGSGGGSP TSLWGLLFLS AALSLWPTSG EICGPGIDIR NDYQQLKRLE
  51 NCTVIEGYLH ILLISKAEDY RSYRFPKLTV ITEYLLLFRV AGLESLGDLF
 101 PNLTVIRGWK LFYNYALVIF EMTNLKDIGL YNLRNITRGA IRIEKNADLC
 151 YLSTVDWSLI LDAVSNNYIV GNKPPKECGD LCPGTMEEKP MCEKTTINNE
 201 YNYRCWTTNR CQKMCPSTCG KRACTENNEC CHPECLGSCS APDNDTACVA
 251 CRHYYYAGVC VPACPPNTYR FEGWRCVDRD FCANILSAES SDSEGFVIHD
 301 GECMQECPSG FIRNGSQSMY CIPCEGPCPK VCEEEKKTKT IDSVTSAQML
 351 QGCTIFKGNL LINIRRGNNI ASELENFMGL IEVVTGYVKI RHSHALVSLS
 401 FLKNLRLILG EEQLEGNYSF YVLDNQNLQQ LWDWDHRNLT IKAGKMYFAF
 451 NPKLCVSEIY RMEEVTGTKG RQSKGDINTR NNGERASCES DVLHFTSTTT
 501 SKNRIIITWH RYRPPDYRDL ISFTVYYKEA PFKNVTEYDG QDACGSNSWN
 551 MVDVDLPPNK DVEPGILLHG LKPWTQYAVY VKAVTLTMVE NDHIRGAKSE
 601 ILYIRTNASV PSIPLDVLSA SNSSSQLIVK WNPPSLPNGN LSYYIVRWQR
 651 QPQDGYLYRH NYCSKDKIPI RKYADGTIDI EEVTENPKTE VCGGEKGPCC
 701 ACPKTEAEKQ AEKEEAEYRK VFENFLHNSI FVPRPERKRR DVMQVANTTM
 751 SSRSRNTTAA DTYNITDPEE LETEYPFFES RVDNKERTVI SNLRPFTLYR
 801 IDIHSCNHEA EKLGCSASNF VFARTMPAEG ADDIPGPVTW EPRPENSIFL
 851 KWPEPENPNG LILMYEIKYG SQVEDQRECV SRQEYRKYGG AKLNRLNPGN
 901 YTARIQATSL SGNGSWTDPV FFYVQAKTGY ENFIHLIIAL PVAVLLIVGG
 951 LVIMLYVFHR KRNNSRLGNG VLYASVNPEY FSAADVYVPD EWEVAREKIT
1001 MSRELGQGSF GMVYEGVAKG VVKDEPETRV AIKTVNEAAS MRERIEFLNE
1051 ASVMKEFNCH HVVRLLGVVS QGQPTLVIME LMTRGDLKSY LRSLRPEMEN
1101 NPVLAPPSLS KMIQMAGEIA DGMAYLNANK FVHRDLAARN CMVAEDFTVK
1151 IGDFGMTRDI YETDYYRKGG KGLLPVRWMS PESLKDGVFT TYSDVWSFGV
1201 VLWEIATLAE QPYQGLSNEQ VLRFVMEGGL LDKPDNCPDM LFELMRMCWQ
1251 YNPKMRPSFL EIISSIKEEM EPGFREVSFY YSEENKLPEP EELDLEPENM
1301 ESVPLDPSAS SSSLPLPDRH SGHKAENGPG PGVLVLRASF DERQPYAHMN
1351 GGRKNERALP LPQSSTC
```

Figure 8.1: ***Protein sequence of wild type IGF1R.*** *Amino acid sequence of wild type IGF1R according to Uniprot accession number P08069. Amino acid indications at descriptions of modifications of the receptor used in this study refer to the denoted sequence.*

Modifications of the wild type receptor used in this study are described in detail in "material and methods" (section 4). Indication of amino acid numbers for the description of used receptor-variants refer to the previously presented scheme.

9 Index of publications

The following publication was prepared during this thesis:

<u>Title</u>

Autoantibodies to the IGF1 Receptor in Graves' Orbitopathy

<u>Authors</u>

Waldemar B. Minich, Nora Dehina, Tim Welsink, Christian Schwiebert, Nils G. Morgenthaler, Josef Köhrle, Anja Eckstein, and Lutz Schomburg

<u>Journal</u>

The Journal of Clinical Endocrinology & Metabolism, 2013 Feb;98(2):752-60. doi: 10.1210/jc.2012-1771. PMID: 23264397. Copyright © 2013 by The Endocrine Society.

<u>Publication date</u>

First Published Online December 21, 2012

10 Abbreviation index

Abbreviation	Description
35S	radioactive isotope of sulfur
aa	amino acid
aAb	autoantibody
Ab	antibody
AKT	protein kinase B
approx.	approximately
ATP	Adenosintriphosphat
BAD	Bcl-2-associated death promoter
BCL	B-cell lymphoma
BCL-XL	B-cell lymphoma-extra large
BSA	bovine serum albumin
cAMP	cyclic adenosine monophosphate
CAS	clinical activity score
CCP	cyclic citrullinated peptide
cDNA	coding deoxyribonucleic acid
CGE	capillary gel electrophoresis
CV	coefficient of variation
CVol	column volume
Da	Dalton
DM	diabetes mellitus
DMF	dimethylformamid
DMSO	dimethylsulfoxid
DNA	deoxyribonucleic acid
DTT	dithiothreitol
E.coli	*Escherichia coli*
EDTA	ethylenediaminetetraacetic acid
EGTA	ethylene glycol tetraacetic acid
ELISA	enzyme-linked immunosorbent assay
EO	endocrine orbitopathy
ERK	extracellular-signal-regulated kinase
FABP	fatty acid binding protein
FBS	fetal bovine serum
FCS	fetal calf serum
FL	full-length
GD	Graves' disease
GH	growth hormone
GHR	growth hormone receptor

GO	Graves' orbitopathy
GSK-3β	glycogen synthase kinase 3 beta
HEK	human embryonic kidney
HEPES	4-(2-hydroxyethyl)-1-piperazineethanesulfonic acid
HPLC	high pressure liquid chromatography
HRP	horse radish peroxidase
ICI	immunochemical intelligence GmbH
IEE	Institute for Experimental Endocrinology
Ig	Immunoglobulins
IGF	insulin-like growth factor
IGF1	insulin-like growth factor 1
IGF1R	insulin-like growth factor 1 receptor
IGF2	insulin-like growth factor 2
IGF2R	insulin-like growth factor 2 receptor
IGFBP	insulin-like growth factor binding protein
IPTG	isopropyl β-D-1-thiogalactopyranoside
IR	insulin receptor
IRS	insulin resistance syndrome
IRS-1	insulin receptor substrate 1
IRS-2	insulin receptor substrate 2
LA	lupus-anticoagulans
lacZ	β-Galactosidase
LB	Lennox broth
Luc	luciferase
M6P	mannose-6-phosphate
mAb	monoclonal antibody
MAP	mitogen-activated protein
MAPK	mitogen-activated protein kinase
MCS	multiple cloning site
MPR	mannose-6-phosphate receptor
mTOR	mammalian target of rapamycin
mTORC1	mammalian target of rapamycin complex 1
mTORC2	mammalian target of rapamycin complex 2
MV	mean value
NF-κB	nuclear factor kappa-B
NOD	non-obese diabetic
NOSPECS	Werner-Classification of endocrine orbitopathy
NPT II	neomycin phosphotransferase II
NSILA	non-suppressable insulin-like activity
p27	cyclin-dependent kinase inhibitor 1B

PA	protein-A matrix
PAGE	polyacrylamide gel electrophoresis
PBS	phosphate buffered saline
PCR	polymerase chain reaction
PDK1	pyruvate dehydrogenase kinase isozyme 1
PI3K	phosphoinositol 3-kinase
PIP3	phosphatidylinositol 3,4,5-triphosphat
PVDF	polyvinylidenfluorid
QC	quality control
RAF	rapidly accelerated fibrosarcoma kinase
RAS	rat sarcoma (G-protein)
RLU	relative light units
RT	room temperature
SD	standard deviation
SDS	sodium dodecyl sulfate
SHC	Src homology domain-containing protein
SLB	sample loading buffer
SLE	systemic lupus erythematosus
SOB	super optimal broth
SOC	super optimal broth with catabolite repression
SS	superspinner system
TAE	Tris-acetate-EDTA-buffer
TAO	thyroid-associated ophthalmopathy
TBAb	thyroid blocking antibody
TBST	Tris-buffered saline and Tween 20
TCF	tissue culture flask
Tg	thyroglobulin
TPO	thyroid peroxidase
TRAK	monoclonal thyroid stimulating hormone receptor antibody
TSAb	thyroid stimulating antibody
TSH	thyroid stimulating hormone
TSHR	thyroid stimulating hormone receptor
WT	wild type
X-gal	5-Brom-4-chlor-3-indoxyl-β-D-galactopyranosid

Not listed are units used according to the IUPAC (International Union of Pure and Applied Chemistry) unit definition system.

11 Acknowledgements

I would like to take this opportunity to thank a number of people who offered support and friendship by which this work was only possible.

First of all, I would like to thank Professor Dr. Lutz Schomburg for his dedicative encouragement and for providing an admirable scientific environment at the Institute for Experimental Endocrinology at Charité - Universitätsmedizin Berlin. He provided me with many great points and ideas to include. Further I would like to thank Prof. Dr. Josef Köhrle for his constant support.

I would like to thank ICI – immunochemical intelligence GmbH, especially Siegmund Karasch, and InVivo Biotech Services GmbH, in particularly Dr. Wolfgang Weglöhner, for all of the support and funding they were able to provide to me in order to make this thesis possible.

I am indebted to Professor Dr. Markus Wahl of the Institute for Chemistry and Biochemistry at Freie Universität Berlin for accepting the role of a second referee.

I would like to thank Prof. Dr. Anja Eckstein from Essen University and Dr. Susanna Wiegand and Dr. Peter Kühnen from the Institute for Experimental Pediatric Endocrinology at Charité - Universitätsmedizin Berlin for providing human serum samples and fruitful cooperation. Also I would like to thank the team from Unicus Karlsburg OHG and their expertise in monoclonal antibody development.

I would also like to thank Dr. Waldemar B. Minich, who gave me advice whenever it was required, and for being an encouraged and patient advisor in the lab. Further I would like to thank my colleague Christian Schwiebert for productive collaboration and fruitful discussions.

I would like to thank all members from the labs of the Institute for Experimental Endocrinology at Charité, to the colleagues from ICI laboratory, as well as the wonderful team of InVivo. Thank you very much for your support, technical advices, and all the help and friendship.

I am deeply grateful to my Mum and my Dad, who always supported me enormously throughout my entire education. Further I would like to thank for all the care I got from my sisters, my entire family and from a lot of close friends as well.

My wonderful wife Julia - I cannot find the words to express my gratitude and faithfulness – I would like to thank for all her patient help and support. You were there for me in so many ways. Thank you and our adorable daughter Klara for all the good and happiness that both of you bring to my life.

12 Curriculum vitae

The CV was excluded from published thesis for reasons of privacy.